Renormalization of the NN interaction with a chiral two-pion-exchange potential: Central phases and the deuteron

M. Pavón Valderrama* and E. Ruiz Arriola†
Departamento de Física Atómica, Molecular y Nuclear, Universidad de Granada, E-18071 Granada, Spain.
(Received 6 July 2005; published 8 November 2006)

We analyze the renormalization of the NN interaction at low energies and the deuteron bound state through the chiral two-pion-exchange potential assumed to be valid from zero to infinity. The short distance van der Waals singularity structure of the potential as well as the requirement of orthogonality conditions on the wave functions determine that after renormalization, in the ${}^1S_0$ singlet channel and in the ${}^3S_1$–${}^3D_1$ triplet channel, one can use the deuteron binding energy, the asymptotic D/S ratio, and the S-wave scattering lengths as well as the chiral potential parameters as independent variables. We use then the asymptotic wave function normalization A_S of the deuteron and the singlet and triplet effective ranges to determine the chiral constants yielding c_1, c_3, and c_4. The role of finite cutoff corrections, the loss of predictive power due to uncertainties in the input data, and the connection to one-pion-exchange distorted wave perturbative approaches is also discussed.

DOI: 10.1103/PhysRevC.74.054001 PACS number(s): 21.30.Fe, 11.10.Gh, 13.75.Cs, 21.45.+v

I. INTRODUCTION

The possibility suggested by Weinberg [1] and pioneered by Ray, Ordoñez, and Van Kolck [2–4] of making model-independent predictions for NN scattering using effective field theory (EFT) methods and, more specifically, chiral perturbation theory (ChPT) has triggered a lot of activity in recent years (for a review, see, e.g., Ref. [5]). In addition to the previous works, most subsequent calculations dealing with the specific consequences of ChPT have been focused on making predictions for NN scattering phase shifts and deuteron properties based on the genuine two-pion-exchange (TPE) chiral potentials [6–27], although some incipient work has also recently been started implementing three-pion-exchange effects [14,15,18,28,29]. In a given partial wave (coupled) channel with good total angular momentum, the reduced NN renormalized potential [$U(r) = MV(r)$] in configuration space can schematically be written in local and energy-independent form [7,11,12] (see Refs. [2–4] for an energy-dependent representation) for any distances larger than a finite short distance radial regulator r_c,

$$U(r) = \frac{Mm^3}{f^2} W_{\rm LO}(mr, g) + \frac{Mm^5}{f^4} W_{\rm NLO}(mr, g, \bar{d}) + \frac{m^6}{f^4} W_{\rm NNLO}(mr, g, \bar{c}_1, \bar{c}_3, \bar{c}_4) + \cdots, \quad (1)$$

where the potential is written as a low energy expansion, in which LO means the Leading Order contribution, NLO the Next-to-Leading Order, NNLO the Next-to-Next-to-Leading order, and so on. Here, $W(x)$ are known dimensionless functions which are everywhere finite except for the origin where they exhibit power law divergencies, which demand the use of some regularization. In writing the previous expression, we have disregarded distributional contact terms (deltas and derivatives of deltas) localized at the origin which strengths are scheme dependent but do not contribute for $r \geqslant r_c > 0$. The renormalized potential is completely specified by the pion mass m, the pion weak decay constant f, the nucleon mass M, the axial coupling constant g, the Goldberger-Treimann discrepancy $\bar{d}_{18}$, and three additional low energy constants $\bar{c}_1 = c_1 M$, $\bar{c}_3 = c_3 M$, and $\bar{c}_4 = c_4 M$ which can be deduced directly from the analysis of low energy πN scattering within ChPT [30–33]. Given this information, one can then solve the single or coupled channel Schrödinger equation imposing a regularity condition of the wave function at the origin for each separate channel. In this paper, we will work under the assumption that the long-range pieces of the potential should be iterated to all orders, but some perturbative analysis will also be done. Our motivation is to describe long-range correlations between observables in the NN problem in a model-independent way. As we will see below, some additional physical information is still required in the form of either counterterms or short distance boundary conditions to make the problem well posed if one indeed wants to remove the regularization. They depend exclusively on the short distance behavior of the renormalized potential through phases of the wave function. The number of phases depends crucially on the repulsive or attractive character of the potential close to the origin. In this sense, the power counting for the short distance interactions cannot be regarded as independent of the power counting of the singular chiral potentials. Nonperturbatively, this materializes, after renormalization, in noninteger power counting for physical observables. This imposes severe limitations on the admissible structure of counterterms and the corresponding renormalization conditions of the quantum mechanical problem. We must emphasize that *our approach is not the conventional EFT one* of allowing all possible short distance counterterms consistent with the symmetry, and to a certain extent, our viewpoints are admittedly heterodox within the conventional EFT framework. However, based on the physical requirement of having small wave functions in the short-range unknown region, the basic

*Electronic address: mpavon@ugr.es
†Electronic address: earriola@ugr.es

and orthodox quantum mechanical requirements of completeness and orthogonality of states are deduced, providing a justification for the additional restrictions. We recall here the series of works by Phillips and Cohen [34,35] (see also Ref. [36]), where restrictions on zero-range interactions were deduced for nonsingular potentials based on the Wigner causality conditions. Here, we extend their results also to the singular NN interactions of Eq. (1).

The theorem underlying the EFT developments is that if chiral symmetry is spontaneously broken down in QCD, the true NN potential at long distances is embedded in the parameter envelope of the general chiral NN potential, Eq. (1), and the chiral expansion provides a reliable hierarchy at those long distances. The hope is that compatible and perhaps accurate determinations of both πN and NN low energy data, bound states, and resonances can be achieved with the same sets of parameters. The problem is that in order to make truly model-independent predictions, short distance ambiguities should be under control and their size smaller than the experimental data uncertainties used as input to the calculation. Only then can the renormalization program be carried out satisfactorily as it was done in the OPE case [37–42], although, as recognized by Nogga, Timmermans, and van Kolck, this may be done at the expense of modifying the power counting [42] of the counterterms in favor of renormalizability (see also Ref. [41] for a complementary formulation in terms of boundary conditions). The present work analyzes this problem extending our previous OPE renormalized calculations to NNLO TPE and its implication in the values of the chiral constants.

The determination of the chiral constants c_1, c_3, and c_4 (in units of GeV^{-1} from now on) from πN scattering has been undertaken in several works and shows significant systematic discrepancies depending on the details of the analysis. In heavy baryon ChPT for low energy πN scattering [30], the values $c_1 = -1.23 \pm 0.16$, $c_3 = -5.94 \pm 0.09$, and $c_4 = 3.47 \pm 0.05$ were deduced with a σ term of $\sigma(0) = 70$ MeV. In Ref. [31], the analysis of low energy πN scattering inside the Mandelstam triangle yields $c_1 = -0.81 \pm 0.15$, $c_3 = -4.69 \pm 1.34$, and $c_4 = 3.40 \pm 0.04$ with, however, a bit too low σ term $\sigma(0) = 40$ MeV as compared to ChPT. Unitarization methods reproducing the phase shifts [32,33] from threshold to the Δ resonance region conclude $c_1 = -0.43 \pm 0.04$, $c_3 = -3.10 \pm 0.05$, and $c_4 = 1.51 \pm 0.04$.

The values of the chiral constants c_1, c_3, and c_4 also depend on regularization details of the NN chiral interaction. The πN values from Ref. [31] were taken in the nucleon-nucleon NNLO calculation of Ref. [10] with sharp and Gaussian cutoffs $\Lambda = 0.6$–0.8 GeV in momentum space, and momentum-dependent counterterms were supplemented and determined from a fit to the NN database relying on the partial wave analysis (PWA) of Ref. [43,44]. Likewise, Ref. [19] constructs a NNLO chiral potential where channel-dependent Gaussian momentum space cutoffs in the range $\Lambda = 0.4$–0.5 GeV were used to fit the NN database [45]. The N^{3}LO extension of this work [28] uses only one common cutoff and fixing $c_1 = -0.81$ produces $c_3 = -3.20$ and $c_4 = 5.40$. In Ref. [11], the NNLO calculation was done in configuration space with a short distance cutoff at $r = 1.4$ fm, where an energy- and channel-dependent boundary condition was imposed, and the fixed value $c_1 = -0.76 \pm 0.07$ was used to make a PWA to pp data yielding $c_3 = -5.08 \pm 0.24$ and $c_4 = 4.70 \pm 0.70$. An update of this calculation also including np data [21] generates $c_3 = -4.78 \pm 0.10$ and $c_4 = 3.96 \pm 0.22$. The calculations of Ref. [22,23] improve the cutoff dependence of the potential in momentum space by using spectral regularization, and taking again Gaussian cutoffs and fixing $c_1 = -0.81$ yields, after fitting the counterterms to the NN PWA [43,44], the values $c_3 = -3.40$ and $c_4 = 3.40$. The extension of this work to N^{3}LO has been done in Ref. [29] keeping the same values for c_3 and c_4 and readjusting the counterterms.

In a renormalized theory, results should be insensitive to the auxiliary regularization method if the regulator is removed at the end. If a fit to the database proves successful, then the resulting parameters should be cutoff independent or at least the systematic uncertainty induced by the regularization should be smaller than the statistical errors induced by experimental data. Otherwise, the cutoff becomes a physical parameter. The first indication that finite cutoff effects are sizable in the present calculations has to do with the variety of values that have been used in the literature for the low energy constants c_1, c_3, and c_4 to adjust NN partial waves and deuteron properties [10,11,21–23,28] (see also the comment in Ref. [24]). Obviously, we do not expect the values of c to agree exactly, but the discrepancies should be at the level of the difference in the approximation.[1] Since the database is the same but the regularization schemes are different, one unavoidably suspects that these determinations of the low energy constants may perhaps be regularization and hence cutoff dependent.

To get a proper perspective on the issue of renormalization, let us consider the size of the contributions of the (renormalized) chiral potential in configuration space at different distances. For instance, at $r = 1.4$ fm in the $^1S_0$ channel, each order in the expansion is about an order of magnitude smaller than the preceding one. At short distances, however, the situation is exactly the opposite: higher orders dominate over the lower orders. In the previous example of the $^1S_0$ channel, LO and NLO become comparable at $r \sim 0.9$ fm, and NLO and NNLO become comparable at distances at which the value $r \sim 0.1$–0.4 fm depends strongly on the particular choice of low energy constants c_3 and c_4. Actually, a general feature of the chiral NN potentials at NNLO relates to their short distance behavior; they develop an attractive van der Waals singularity $U \sim -\mathrm{MC}_6/r^6$ similar to the one found for neutral atomic systems. In such a situation, the standard regularity condition at the origin only specifies the wave function uniquely if the potential is repulsive, but some additional information is required if the potential is attractive [46] (for a comprehensive review in the one channel case see, e.g., Ref. [47]). Within the EFT framework, the problem has been revisited in Ref. [48]. The net result is that the regularity condition at the origin

[1] For instance, pion loops at NLO modify the contribution to c_3 by $\sim 3g_A^2 m^2/(64\pi f^2) \sim 0.4/\mathrm{GeV}$. This contribution must be taken into account when comparing numbers between [11,21,31], and the present approach. Only the extractions using the N^{3}LO NN potential in Ref. [28] are made at the same order as those from [31].

tames the singularity [41] and, in fact, more singular potentials become less important at low energies.

In this work, we reanalyze the NN chiral potential including TPE potential at NNLO. We carry out the analysis entirely in coordinate space following the ideas developed in our previous work [41] for the OPE potential. In configuration space, the (renormalized) potential is finite except at the origin, a point which should be carefully handled, requiring a delicate numerical limiting procedure. Unlike previous works on the TPE potential, ours tries to remove the cutoff completely, taking the consequences seriously. This does not mean that finite cutoff calculations are necessarily incorrect or not entitled to describing all or part of the data, but there are also good reasons for removing the cutoff and looking at the physical consequences. First, the limit exists in a strict mathematical sense under well-defined conditions, as the analysis below shows. This is a nontrivial fact, because calculations done in momentum space can only address this question numerically by adding counterterms suggested by an *a priori* power counting on the short distance potential. As shown in Ref. [42], this does not always work, and calculations may require some trial and error. Second, as far as we know, this is the only way to remove short distance ambiguities, thereby making the calculations truly model independent. Third, the study of peripheral waves has proven to be successful by using perturbative renormalized amplitudes corresponding to irreducible TPE and iterated OPE where the cutoff has been removed in the intermediate state [7,20]. Peripheral waves mainly probe large distances in the Born approximation, but they also see some of the short distance interaction due to rescattering effects. Fourth, the advantage of renormalization is that one should obtain the same results provided one uses as input the same physical information, regardless whether the calculation is done in coordinate or momentum space, and also regardless of the particular regularization. Finally, a reliable estimate of the errors and convergence rate of the chiral expansion can be done, without any spurious cutoff contamination. In principle, the higher the order in the chiral expansion the better, provided there is perfect errorless data to fit the increasing number of low energy constants appearing at any order. However, the chiral expansion may reach a limited predictive power because of finite experimental accuracy in the low energy constants used as input. The output inherits a propagated error which may eventually become larger than the experimental uncertainty.[2] Finite cutoff uncertainties are not a substitute for propagating input experimental errors to the predictions of the theory, and they can be regarded at best as a lower bound on systematic errors. In this paper, we regard this possible cutoff dependence as purely numerical inaccuracies of the calculation and not as a measure of the uncertainty in the predictions of the theory, so we make any effort to minimize these cutoff-induced systematic errors.

In the process of eliminating the cutoff , we find some surprises, and effects not explored up to now become manifest. Even for low energy scattering parameters and deuteron properties, for which the description should be more reliable and robust, we find systematic discrepancies in our calculation with values quoted in the literature, and we conclusively identify these discrepancies as finite cutoff effects. This might provide a natural explanation for why calculations with different cutoff methods fitting the NN phase shifts [43–45] obtain different results for the chiral constants c_1, c_3, and c_4 or why different values of the constants yield good fits to the data. According to our study, for the lowest phases the reason can partly be related to the dominance of short distance van der Waals singularities for a system with unnaturally large scattering lengths or a weakly bound state, as it is the case for the $^1S_0$ and $^3S_1$–$^3D_1$ channels. In some cases, the effect may be as high as 30%, as in the effective range of the triplet $^3S_1$ channel. The size of the effect depends on the value of the low energy πN constants c_1, c_3, and c_4. Given the significant sensitivity of low energy NN properties and deuteron properties on these low energy πN constants, we try to make a fit to some low energy properties for which uncertainties are reliably known and where we expect the chiral theory to be most reliable. At this point, we depart from the standard large-scale fits to all phase shifts or partial wave analyses where the low energy threshold parameters are determined *a posteriori*. The assignment of statistical errors on the fitting parameters c_1, c_3, and c_4 is often not addressed (see, however, Refs. [11,21]) because the NN databases used to fit the phase shifts [43–45] are treated as errorless. We also try to improve on this point within our framework.

The paper is organized as follows. In Sec. II we discuss the basic assumption of the smallness of the wave function in the short-range unknown region and its consequences. We also analyze the constraints based on causality and analyticity of the S matrix. In Sec. III, we introduce the classification of boundary conditions which will be used in the paper to effectively renormalize the amplitudes in both the one-channel and the coupled-channel cases. We will also review the orthogonality constraints for singular potentials already used in our previous work [41] for the OPE potential. Section IV deals with the description of the singlet $^1S_0$ channel. From the superposition principle of boundary conditions, we show how a universal form of a low energy theorem arises for the threshold parameters as well as for the phase shift. In Sec. V, we discuss the interesting triplet $^3S_1$–$^3D_1$ channel for both the deuteron bound state and the corresponding scattering states, where full use of the orthogonality constraints as well as the superposition principle of boundary conditions generate interesting analytical relations connecting deuteron and scattering properties. In Sec. VI, a careful discussion of errors for our cutoff-independent results is given. Also, a determination of the chiral constants based on low energy data and deuteron properties is made. In Sec. VII, we present a simplified study on the significance of the chiral van der Waals forces and the striking similarities with the full calculations for the S waves. In Sec. VIII, we show some puzzling results for the NLO calculation in the deuteron channel. We also comment on the relation to finite cutoff calculations and the conflict between Weinberg counting and nonperturbative renormalization at NLO. We also outline possible solutions to

[2]This issue has been illustrated in Refs. [49–51] for the case of $\pi\pi$ scattering at two loops, and will become clear in NN scattering below.

TABLE I. Short distance van der Waals coefficients for the NNLO chiral potential in singlet $^1S_0$ and the $^3S_1$–$^3D_1$ triplet channels.

Set	Source	c_1 (GeV^{-1})	c_3 (GeV^{-1})	c_4 (GeV^{-1})	MC$_6$ (fm^4)	MC$_{6,+}$ (fm^4)	MC$_{6,-}$ (fm^4)	θ (deg)
Set I	(BM) πN [31]	-0.81 ± 0.15	-4.69 ± 1.34	3.40 ± 0.04	-8.74	-16.96	-5.63	140.8
Set II	(RTdS) NN [11]	-0.76	-5.08	4.70	-10.19	-21.45	-5.58	170.0
Set III	(EMa) NN [20]	-0.81	-3.40	3.40	-6.45	-14.68	-3.35	140.7
Set IV	(EMb) NN [28]	-0.81	-3.20	5.40	-7.28	-20.18	-1.86	182.6

this problem. In Sec. IX, we analyze our results in the light of long distance perturbation theory, reinforcing the usefulness of nonperturbative renormalization due to an undesirable proliferation of counterterms. Finally, in Sec. X, we summarize our conclusions.

For numerical calculations, we take $f_\pi = 92.4$ MeV, $m = 138.03$ MeV, $M = M_p M_n/(M_p + M_n) = 938.918$ MeV, $g_{\pi NN} = 13.083$ in the OPE piece to account for the Goldberger-Treimann discrepancy according to the Nijmegen phase shift analysis NN scattering [52] and $g_A = 1.26$ in the TPE piece of the potential. The values of the coefficients c_1, c_3, and c_4 used in this work are listed in Table I for completeness. The potentials in configuration space used in this paper are exactly those provided in Refs. [7,11,12] but disregarding relativistic corrections, $M/E \to 1$.[3]

II. SHORT DISTANCE INSENSITIVITY CONDITIONS AND RENORMALIZATION

In this section, we elaborate on the essential role played by standard quantum mechanical orthogonality and completeness properties of the wave functions in the rest of this paper. As we have already mentioned, our approach is unconventional from an EFT perspective, and at present it is unclear whether such properties have an EFT justification. At the same time, one should say that many self-denominated EFT calculations do indeed normalize deuteron wave functions to unity and use energy-independent regulators from which orthogonality relations follow automatically.

A. The inner and outer regions

Similar to EFT, our basic assumption is that low energy physics should not depend on short distance fine details. This rather general principle can be made into a precise quantitative statement *in practice* for a quantum mechanical system. For the sake of clarity, let us consider the singlet $^1S_0$ channel for positive energies. If we assume a short distance regulator r_c, above which our long distance (local) potential acts, the reduced Schrödinger equation in the outer region reads

$$-u''_{k,L}(r) + U_L(r)u_{k,L}(r) = k^2 u_{k,L}(r), \qquad r > r_c, \quad (2)$$

where the label L stands for long. Asymptotically, it behaves as

$$u_{k,L}(r) \to A \sin(kr + \delta(k, r_c)), \quad (3)$$

where A is an arbitrary normalization constant and the dependence on the short distance regulator r_c has been explicitly highlighted. In the inner region, the dynamics is *unknown* but we also expect it to be *irrelevant* provided $kr_c \ll 1$, i.e., if we assume the corresponding wavelength to be larger than the short distance scale. The potential can be deduced from perturbation theory in the full amplitude,

$$U(\vec{x}) = C_0\delta(\vec{x}) + C_2\{\nabla^2, \delta(\vec{x})\} + \cdots + U_L(x), \quad (4)$$

where $U_L(x)$ corresponds to the expansion in Eq. (1) [7,11,12]. The distributional contact terms are regularization scheme dependent and correspond to polynomial terms in momentum space. Obviously, they do not contribute to the region $r > r_c$ for $r_c > 0$. The very nature of such a calculation already implies that C_0, C_2, etc., are perturbative corrections to the short-range physics, but they do not include possible nonperturbative effects. As will become clear below (Sec. III), finiteness of the physical phase shift in the limit $r_c \to 0$ implies a highly nonperturbative reinterpretation of the short-range terms, even if the long-range pieces are computed perturbatively.

Following [34,36], it is useful to use a nonlocal and energy-independent potential to describe the short distance dynamics

$$-u''_{k,S}(r) + \int_0^{r_c} U_S(r, r')u_{k,S}(r') = k^2 u_{k,S}(r), \quad r < r_c, \quad (5)$$

where the label S stands for short. This holds provided we are below any inelastic channel such as πNN. Above such threshold, any open channel and hence a genuine energy dependence should be included explicitly. Below the threshold, which is the situation of interest to this paper, there can also be an energy dependence induced by the virtual contribution of inelastic channels. In the present paper, we consider the nucleons to be heavy baryons in which case the threshold at $s_{\pi NN} = (2M + m)^2 = 4(M^2 + k^2)$ corresponds to a c.m. momentum $k = \sqrt{m(M + m/4)} \to \infty$. The nonlocal short distance potential $U_S(r, r')$ encodes, in particular, contact terms (deltas and derivatives of deltas) which appear when the long distance potential $U_L(r)$ is computed in perturbation theory. These terms are in fact ambiguous (and hence unphysical) and depend on the regularization scheme used in the perturbative calculation, but they are not essential since they do not contribute to the absorptive part and hence to the corresponding spectral function [7]. The important point is that these ambiguous distributional terms never contribute to the

[3] In fact, if we do consider relativistic corrections, the changes in observables are negligible. In the case of the deuteron, the changes are one order of magnitude smaller than the provided error, which is deduced from the uncertainty in the D/S ratio η (see Table III), while in the case of the singlet phase shifts the change is about 0.2 degrees at a center-of-mass momentum of 400 MeV, the maximum considered in this work.

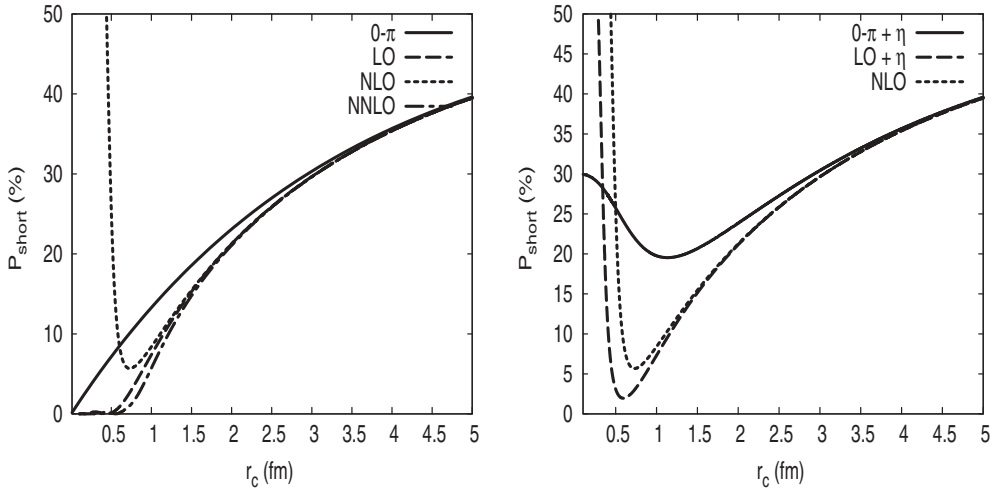

FIG. 1. Probability inside the short distance region as a function of the short distance cutoff radius r_c for the deuteron state for different approximations to the potential. In all cases, the deuteron binding energy is fixed to the experimental value. Left panel: 0-π means a pionless theory in which $\eta = 0.0256$ is also fixed to the experimental number. LO is our previous OPE work [41], where $\eta = 0.02633$ is deduced from the regularity condition of the wave function at the origin. NLO and NNLO (set IV) correspond to the higher terms in Eq. (1) where the experimental η value is also taken. Right panel: Same notation, but fixing $\eta = 0.0256$ as an independent parameter. In these cases, the wave functions in the outer region would diverge at short distances.

long-range part provided $r_c > 0$, since in this case a compact support for distributional terms is guaranteed. This is a clear advantage of the radial cutoff we are using. In fact, our main motivation for carrying out the analysis in coordinate space is this clean separation between short and long distances. Many regulators, mainly those in momentum space, do not fulfill this condition, since the regulator effectively smears these short distance terms and intrudes somewhat into the long distance region.[4]

Finally, we need a matching condition connecting the inner and outer regions,

$$\frac{u'_{k,L}(r_c)}{u_{k,L}(r_c)} = \frac{u'_{k,S}(r_c)}{u_{k,S}(r_c)}. \tag{6}$$

Viewed from the outer region, this relation corresponds to an energy-dependent boundary condition at a given short distance cutoff radius r_c. Because of elastic unitarity, we expect the state to be normalized, so that if we use a box of size a as an infrared regulator, we have

$$\int_0^{r_c} u_{k,S}(r)^2 dr + \int_{r_c}^{a} u_{k,L}(r)^2 dr = 1, \tag{7}$$

with a much larger than the range of the potential. This equation gives a quantitative separation between long distance and known physics and short distance and unknown physics. Obviously, any effective description based on the long-range part should fulfill

$$\int_0^{r_c} u_{k,S}(r)^2 dr \ll 1, \tag{8}$$

which corresponds to the requirement of *a small wave function in the inner unknown region*. This is our basic condition from which most of our results follow. It should be realized that here, long and short distances are intertwined through the matching condition, Eq. (6). In particular, an arbitrarily growing function at the origin cannot fulfill this condition even if a large value of the short distance cutoff is taken.

Let us emphasize that despite the fact that the wave function is not an observable itself and EFT is not naturally formulated in terms of wave functions,[5] in our approach matrix elements do require that wave functions are dominated by the long distances, and in particular short distance insensitivity must be expected. Otherwise, the contribution from short distances would become inadmissibly large. This kind of pathological situation actually occurs when dealing with the deuteron channel in the theory with no explicit pion-exchange potentials and a nonvanishing D/S wave ratio, η [35], with OPE potential [41] and TPE potential at NLO in the Weinberg counting (see Secs. VIII and VIII C below). As an instructive and enlightening example, we illustrate the situation in Fig. 1 in the deuteron state for the dimensionless quantity

$$P(r_c) = \int_0^{r_c} (u(r)^2 + w(r)^2) dr, \tag{9}$$

(for notation see Sec. V) using the pionless, LO, NLO and NNLO potentials, Eq. (1), in the outer region $r > r_c$, and matching to a free particle in the inner region $r < r_c$ (it turns out that the precise form of the wave function inside is not

[4]For instance, the widely used Gaussian regulator in momentum space [4,28,29,42] of a local potential in coordinate space corresponds indeed to a convolution of the original potential smeared over the region of size $1/\Lambda$.

[5]EFT is, however, formulated in terms of regularization scheme and scale-dependent counterterms. So our discussion will parallel in spirit the naturalness arguments on counterterms considered in the standard EFT literature.

essential).[6] In the left panel, we display $P(r_c)$ for the case of a pionless theory where $u(r) = e^{-\gamma r}$ and $w(r) = 0$, in the outer region $r > r_c$ as well as the LO, NLO, and NNLO chiral potentials. For an effective description, one would expect that $P(r_c) \to 0$ as $r_c \to 0$. This is so in all cases except at NLO in the standard Weinberg counting, where the wave function leaks into the short distance region in an uncontrolled way. This is a first and transparent illustration of the fact that the description based on any *preconceived* power counting is not necessarily consistent with the requirement that short distance ambiguities be under control, since the wave function in the inner and unknown region does not become arbitrarily small as the cutoff is removed. As a further example, we also show in the right panel two more problematic cases. Namely, a theory where the asymptotic D/S ratio, η, and the deuteron binding energy are fixed to their experimental values for both the pionless case and the OPE potential. The common feature of these solutions is that the wave functions in the outer region diverge when $r_c \to 0$.

From Fig. 1, it is obvious that in some cases one could instead keep a finite cutoff, perhaps minimizing the inner probability so as to make the approximation as effective as possible. We will analyze this situation in more detail in Sec. VIII C. As we will discuss in Sec. III, tight constraints on the structure of short distance counterterms must be fulfilled if the requirement $P(r_c) \to 0$ as $r_c \to 0^+$ is imposed *a priori*.

B. Wigner bounds on the short distance contributions

To proceed further, we derive Eq. (5) with respect to energy, and we obtain, after some algebra,

$$\frac{d}{dk^2}\left[\frac{u'_{k,S}(r_c)}{u_{k,S}(r_c)}\right] = -\frac{\int_0^{r_c} u_{k,S}(r)^2 dr}{u_{k,S}(r_c)^2} \leqslant 0, \tag{10}$$

whenever r_c is not a zero of the wave function.[7] The short-range theory can be characterized by an *accumulated* phase shift $\delta_S(k, r_c)$, given by the solution of the truncated short-range problem,

$$u_{k,S}(r) = \sin\left(kr + \delta_S(k, r_c)\right), \quad r > r_c, \tag{11}$$

which fulfills, from Eq. (10),

$$\frac{d}{dk^2}\left[k \cot\left(kr_c + \delta_S(k, r_c)\right)\right] \leqslant 0, \tag{12}$$

a condition equivalent to Wigner's causality condition [34]. Using an effective range expansion for the short distance phase shift

$$k \cot \delta_S = -\frac{1}{\alpha_{0,S}} + \frac{1}{2} r_{0,S} k^2 + \cdots, \tag{13}$$

we get the Wigner bound for the effective range

$$r_{0,S} \leqslant 2r_c \left[1 - \frac{r_c}{\alpha_{0,S}} + \frac{r_c^2}{3\alpha_{0,S}}\right], \tag{14}$$

where $\alpha_{0,S}$ and $r_{0,S}$ represent the scattering length and effective range when the short distance potential $U_S(r, r')$ is switched on from the origin up to the scale r_c or equivalently when the long distance potential is switched off from infinity down to r_c (see Refs. [39,40] for more details). In a theory where the long distance potential is absent $U_L(r) = 0$, i.e., a pure short distance description, we have the obvious result that the short distance threshold parameters coincide with the physical parameters $\alpha_{0,S} = \alpha_0$ and $r_{0,S} = r_0$. Thus,

$$r_0 \leqslant 2r_c \left[1 - \frac{r_c}{\alpha_0} + \frac{r_c^2}{3\alpha_0}\right], \quad U_L(r) = 0, \tag{15}$$

which implies that $r_0 \leqslant 0$ for $r_c \to 0$. With the experimental values, one gets the lowest short distance cutoff compatible with causality to be $r_c = 1.4$ fm. For a given long distance potential, we just solve the equations from infinity inward and look for the point where the Wigner condition is first violated. In Fig. 2, we plot the evolution of the Wigner bound on the effective range for the different approximations to the potential according to the expansion (1) as a function of the short distance cutoff radius. As we see, the lower bound on the radius is pushed toward the origin, and in fact *for the NNLO approximation there is no lower bound at all*. Thus, only for the NNLO TPE potential can one build the full strength of the experimental effective range without violation of the Wigner condition. We will see more on this in Sec. IV.

If we change explicitly the short distance radius, $r_c \to r_c + \Delta r_c$, we can use the matching condition, Eq. (6), to evaluate the change seen from the outer region. This results in a variable phase equation which has been analyzed extensively in our previous works [39,40]. If we take the limit $r_c \to 0$, we get that the outer wave function fulfills

$$\frac{d}{dk^2}\left[\frac{u'_k(0^+)}{u_k(0^+)}\right] = 0, \tag{16}$$

where the label L has been suppressed. Thus, the boundary condition becomes *energy independent* when the limit $r_c \to 0^+$ is taken if the inner wave function becomes arbitrarily small. Note that the limit is taken *from above* such that

[6] In a momentum space formulation, this is somewhat equivalent to the cutoff of the Lippmann-Schwinger equation above a given value Λ.

[7] The previous equation holds with respect to the explicit energy dependence. The negativity condition holds also when the potential is implicitly energy dependent but due to integrated out inelastic channels (which move to infinity in the heavy baryon formalism). The simplest way to realize this is to consider the corresponding analog of the familiar optical potential from multichannel scattering theory (see, e.g., [53]); starting from the many-body Lippmann-Schwinger equation $T = V + V(E - H)^{-1}T$, where V is the many-body potential and introducing P_H and P_L, orthogonal self-adjoint projectors, $P_H + P_L = 1$ onto the high energy and low energy complementary subspaces, respectively, and eliminating the high energy degrees of freedom, one gets

$$V_L(E) = P_L V P_L + P_L V P_H (E - H)^{-1} P_H V P_L.$$

Obviously

$$\begin{aligned} V'_L(E) &= -P_L V P_H (E - H)^{-2} P_H V P_L \\ &= -(P_L V P_H (E - H)^{-1})(P_L V P_H (E - H)^{-1})^\dagger \end{aligned}$$

is a negative definite operator since a product of an operator by its adjoint is positive definite, $\langle\psi|AA^\dagger\psi\rangle = \langle A\psi|A\psi\rangle > 0$.

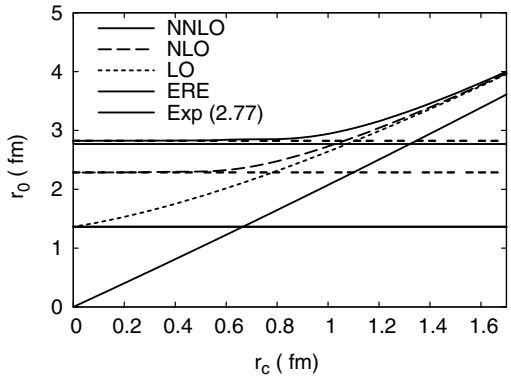

FIG. 2. Wigner bound on the effective range of the short distance interaction [right hand side of Eq. (14)] as a function of the short distance cutoff radius for the contact interaction (ERE), the OPE interaction (LO), the TPE (NLO), and NNLO. We use the conditions $\alpha_0 = -23.74$ fm and $r_0 = 2.77$ fm when $r_c \gg 1/m_\pi$. Causality is violated when the curve crosses the experimental value. Straight horizontal lines correspond to the values obtained for the effective range when the short distance initial condition $r_{0,S}(0^+) = 0$ is assumed.

$r_c > 0$.[8] As we have said already, this justifies not considering contact terms in the potential. A direct consequence is that with the exception of the short distance scattering length $\alpha_{S,0}(0^+)$, which can be fixed by some renormalization condition (see Sec. III), the remaining short distance threshold parameters are also zero in this limit,

$$r_{0,S}(0^+) = 0 \qquad v_{2,S}(0^+) = 0, \cdots. \tag{17}$$

This energy independence of the boundary condition at the origin ensures the orthogonality conditions between different energy states,

$$\int_{0^+}^{\infty} u_k(r) u_{k'}(r) dr = \delta(k - k'). \tag{18}$$

III. SHORT DISTANCE BEHAVIOR OF CHIRAL POTENTIALS, ORTHOGONALITY CONSTRAINTS, AND THE NUMBER OF INDEPENDENT CONSTANTS

As we have said, chiral NN potentials, Eq. (1), although they decay exponentially at large distances, become singular at short distances, where one has

$$U(r) = \frac{\mathrm{MC}_n}{r^n}(1 + a_1 r + a_2 r^2 + \cdots). \tag{19}$$

To avoid any misconception, let us emphasize that the short distance behavior of a long distance potential should be regarded as a long distance feature, i.e., a long wavelength property, since different long distance potentials yield different short distance behaviors. The short distance properties of chiral potentials have nothing to do with short distance properties of the "true" potential, but renormalization and finiteness require a very precise behavior of the wave function when approaching the origin from long distances. In this section, we classify the undetermined constants depending on the attractive or repulsive nature of the corresponding potentials in the single channel case and the eigenvalues of the potential matrix in the coupled channel case. In coordinate space and disregarding relativistic corrections, the potentials in Eq. (1) are local and energy independent.[9] An important condition of the short distance behavior of the wave functions is the orthogonality constraints between states of different energy. For a regular energy-independent potential, these constraints are automatically satisfied, but for singular potentials they generate new relations relevant to the NN interaction. Our approach is not the conventional one of adding short distance counterterms following an *a priori* power counting on the long distance potential. Rather it is the power counting in the potential that uniquely determines the admissible form of the short distance physics if we want to reach a finite limit when the regulator is removed. This can only be achieved by choosing the *regular solution* at the origin, i.e., $u(0) = 0$. In Sec. VIII C, we will show that irregular solutions generate divergent results after renormalization. Although this may look like a potential drawback of removing the cutof, it provides valuable insight into the form of the potential and the validity of the expansion (see Sec. VIII D).

A. One channel case

Let us first review the single channel case in a way that allows the results for the coupled channel situation to be easily stated. The reduced Schrödinger equation for angular momentum l is

$$-u'' + U(r)u + \frac{l(l+1)}{r^2} = k^2 u. \tag{20}$$

For a power law singular potential at the origin of the form $U(r) = \mathrm{MC}_n/r^n = \pm(R/r)^n/R^2$ with $n > 2$ and R the length scale dimension, the de Broglie wavelength is given by $1/k(r) = 1/\sqrt{|U(r)|}$, and the applicability condition for the

[8] To illustrate this point, let us note that for potentials which do not diverge too strongly at the origin $r^2 U(r) \to 0$ such as OPE in the $^1S_0$ channel, there is some irreversibility in the process of integrating from *exactly* $r_c = 0$ out [which requires the regular solution, $u(0) = 0$] or integrating in toward the origin from above $r \to 0^+$ (which generally involves the irregular solution, $u(0) \neq 0$). See the discussion in Ref. [39] and in Sec. III C.

[9] In momentum space and up to NNLO, the long distance part of the potential depends on the momentum transfer q only and not on the total momentum k. Essential nonlocalities, i.e., contributions of the form $V(q, k) = L(q)k^2$ with $L(q)$ a nonpolynomial function, depend weakly on the total momentum and appear first at N^{3}LO [14–18,20] due to relativistic $1/M^2$ one loop contributions. In coordinate space, this weak nonlocality corresponds to a modification of the kinetic energy term in the form of a general self-adjoint Sturm-Liouville operator, $-u''(r) \to -(p(r)u'(r))'$, with a singular $p(r)$ function at the origin and exponentially decaying at long distances. The present formalism can in principle be extended to include these features and will be discussed elsewhere. Nevertheless, according to the results of Sec. VI (see Table IV) on the loss of predictive power already at NNLO there is a lack of phenomenological motivation.

WKB approximation reads $(1/k(r))' \ll 1$, so that for distances $r \ll R(n/2)^{2/(2+n)}$ one has a semiclassical wave function [46–48]. Obviously, since the potential is much larger than the energy, finite energy corrections to the wave function will be suppressed by small relative factors of $k^2/U(r)$. Keeping the leading short distance behavior, one gets for attractive and repulsive singular potentials and any angular momentum the following behavior for the *regular* solutions

$$u_A(r) \to C_A \left(\frac{r}{R}\right)^{n/4} \sin\left[\frac{2}{n-2}\left(\frac{R}{r}\right)^{\frac{n}{2}-1} + \varphi\right], \quad (21)$$

for

$$\text{for} \qquad U_A \to -\frac{1}{R^2}\left(\frac{R}{r}\right)^n, \quad (22)$$

and

$$u_R(r) \to C_R \left(\frac{r}{R}\right)^{n/4} \exp\left[-\frac{2}{n-2}\left(\frac{R}{r}\right)^{\frac{n}{2}-1}\right], \quad (23)$$

for and

$$U_R \to +\frac{1}{R^2}\left(\frac{R}{r}\right)^n, \quad (24)$$

respectively. Here C_A and C_R are normalization constants, and φ an arbitrary short distance phase. In the repulsive case, we have discarded the irregular solution (a similar exponential with a positive sign) which would not allow us to normalize states. For an attractive singular potential, there is a short distance unknown parameter. This phase could, in principle, be energy dependent. Chiral potentials are, however, local and energy independent at NNLO at all distances, and they become nonlocal or energy dependent at N^{3}LO, because of relativistic $1/M^2$ corrections [14–18].[10] Thus, if we require orthogonality of states with different energy (positive or negative), we get[11]

$$\begin{aligned} 0 &= u_k' u_p - u_p u_k'\Big|_0 \\ &= \frac{1}{R}\sin(\varphi(k) - \varphi(p)). \end{aligned} \quad (25)$$

Hence, the phase φ is energy independent and could be fixed by matching the solution to the asymptotic large distance region (we assume a short-range potential), e.g., by requiring a given value of the scattering length α_l at zero energy. In this way, a new and physical scale appears in the problem which is not specified by the potential. This is equivalent to the well-known phenomenon of dimensional transmutation, and in fact it was previously observed in Ref. [48]. Another possibility is to fix φ from a given bound state energy, $E = -B$. The new scale entering the problem is the corresponding wave number, $\gamma = \sqrt{MB}$. Note that although neither α_l nor γ can be predicted from a singular potential, the orthogonality constraint does predict a correlation between them through the potential. Likewise, the phase shifts δ_l can be deduced from either α_l or γ by taking the same short distance phase φ. In the repulsive case, there is no dimensional transmutation since the orthogonality condition follows from regularity at the origin, and the potential fully specifies the wave function. In this case, the scattering length and the spectrum are completely determined from the potential as for standard regular potentials.

B. Coupled channel case

We turn now to the two coupled channel case where the wave functions are denoted by a column vector (u, w) (for some particular cases, see, e.g., Refs. [38,41,48,54]). If we assume that at short distances the reduced potential behaves as

$$U \to M\frac{\boldsymbol{C_n}}{r^n}, \quad (26)$$

where $\mathbf{C}_n$ is a symmetric matrix of van der Waals coefficients, then by diagonalizing the matrix $\boldsymbol{C}_n$ we get

$$\boldsymbol{C}_n = \begin{pmatrix} \cos\theta & \sin\theta \\ -\sin\theta & \cos\theta \end{pmatrix} \begin{pmatrix} C_{n,+} & 0 \\ 0 & C_{n,-} \end{pmatrix} \begin{pmatrix} \cos\theta & -\sin\theta \\ \sin\theta & \cos\theta \end{pmatrix}, \quad (27)$$

where $C_{n,\pm}$ are the corresponding eigenvalues and θ the mixing angle. Thus, at short distances we can decouple the equations to get

$$\begin{pmatrix} u \\ w \end{pmatrix} \to \begin{pmatrix} \cos\theta & \sin\theta \\ -\sin\theta & \cos\theta \end{pmatrix} \begin{pmatrix} u_+ \\ u_- \end{pmatrix}, \quad (28)$$

where (u_+, u_-) are regular solutions as in the single channel case. So, in the two channel situation, we have three possible cases depending upon the sign of the eigenvalues.

(i) Both eigenvalues are negative, i.e., both eigenpotentials are attractive and $\mathrm{MC}_{n,+} = -R_+^{n-2}$ and $\mathrm{MC}_{n,-} = -R_-^{n-2}$ with $R_\pm$ the corresponding scale dimension. In this case, the short distance eigensolutions are oscillatory and there are two undetermined short distance phases, φ_+ and φ_-. Moreover, for two states (u_k, w_k) and (u_p, w_p) with different energies, we get the orthogonality constraint

$$\begin{aligned} 0 &= u_k' u_p - u_p u_k' + w_k' w_p - w_p w_k'\Big|_0 \\ &= \frac{1}{R_+}\sin(\varphi_+(k) - \varphi_+(p)) + \frac{1}{R_-}\sin(\varphi_-(k) - \varphi_-(p)). \end{aligned} \quad (29)$$

(ii) One eigenvalue is negative and the other is positive, $\mathrm{MC}_{n,+} = R_+^{n-2}$ and $\mathrm{MC}_{n,-} = -R_-^{n-2}$. One short distance eigensolution is a decreasing exponential and the other is oscillatory, so we have one short distance phase φ. In this case for two states (u_k, w_k) and (u_p, w_p) with different energies, we get the orthogonality

[10] The subthreshold energy dependence from the virtual pion production channel $NN \to NN\pi$ which is in principle N^{3}LO disappears since in the heavy baryon limit the threshold $s_{\pi NN} = (2M + m)^2 = 4(M^2 + k^2)$ translates into a c.m. momentum $k = \sqrt{m(M + m/4)} \to \infty$.

[11] It should be emphasized that this orthogonality constraint has been obtained from the semiclassical wave function at *finite energy* but very short distances.

constraint

$$0 = u'_k u_p - u_p u'_k + w'_k w_p - w_p w'_k\Big|_0 = \frac{1}{R_+}\sin(\varphi_+(k) - \varphi_+(p)). \quad (30)$$

(iii) Both eigenvalues are positive, $\mathrm{MC}_{n,+} = R_+^{n-2}$ and $\mathrm{MC}_{n,-} = R_-^{n-2}$. Then, both short distance eigensolutions are decreasing exponentials. There are no short distance phases. In this case, the orthogonality relations are automatically satisfied.

This simple argument can be easily generalized to any number of coupled channels. The number of undetermined short distance phases corresponds to the number of attractive eigenpotentials at short distances. Orthogonality of the wave functions requires that all these short distance phases fulfill a generalized condition of the form of Eq. (29).

The orthogonality conditions require the determination of the short distance phases, as we did in Ref. [41] for the OPE case. This requires in general an improvement on the short distance behavior to high orders. An alternative method is to impose the orthogonality constraints in either the single or coupled channel case by integrating in from infinity for a fixed energy, either positive or negative, and then impose the condition at a sufficiently short distance cutoff radius $r = r_c$. In the single channel case, one would get the condition

$$\frac{u'_k(r_c)}{u_k(r_c)} = \frac{u'_0(r_c)}{u_0(r_c)}, \quad (31)$$

if the zero energy state is taken as the reference state. An analogous relation holds for the coupled channel situation, namely,

$$0 = u_k(r_c)u_0(r_c)' - u_k(r_c)'u_0(r_c) + w_k(r_c)w_0(r_c)' - w_k(r_c)'w_0(r_c). \quad (32)$$

Obviously, in this procedure, cutoff independence must be checked. For the TPE chiral potentials analyzed in this paper, we find that $r_c = 0.1$–0.2 fm proves a sufficiently small value of the short distance cutoff.

C. Power counting, counterterms, and short distance parameters

As we see, the number of independent parameters is determined from the potential, although their value can be fixed arbitrarily by some renormalization condition such as fixing scattering lengths to their physical value. This removes the cutoff in a way that causes short distances to become less and less important. Now, if the potential is regular, i.e., $r^2|U(r)| \to 0$, one may *choose* between the regular and irregular solutions.[12] In the first case, the scattering length is predicted, while in the second case, the scattering length becomes an input of the calculation. In either case, the wave function is still normalizable at the origin. Singular potentials at the origin, i.e., fulfilling $r^2|U(r)| \to \infty$, do not allow this choice if one insists on normalizability of the wave function at the origin. If the potential is repulsive, the scattering length is fixed, while for an attractive potential, the scattering length *must* be an input parameter. Furthermore, orthogonality of different energy solutions requires an energy independence of the boundary condition, so that in *all cases* the effective range and higher order threshold parameters cannot be taken as independent parameters, in addition to the scattering lengths.

This can be translated into the language of counterterms quite straightforwardly. In momentum space, fixing α_0 arbitrarily corresponds to taking a constant C_0 cutoff-dependent and energy-independent contribution to the potential $V_0(k', k)$ in the Lippmann-Schwinger equation. Likewise, fixing r_0 can be mapped as adding a term $C_2(k^2 + k'^2)$ to the potential. For higher coupled channel partial waves, in which one fixes the scattering length $\alpha_{l,l'}$, one has instead terms of the form $C_{l',l}k'^{l'}k^l$ in the potential $V_{l',l}(k', k)$.

The OPE potential in the singlet ${}^1S_0$ is regular at the origin and hence one can take α_0 as an independent parameter or not (see Refs. [39,40].) Actually, the smallness of the scattering length for the regular solution suggests using the irregular solution. In Weinberg's counting of the potential, at NLO one has TPE contributions in the potential. At short distances, they behave as an attractive $1/r^5$ potential (see Sec. VIII), and then α_0 *must* be an independent parameter. At NNLO, one has, again, a singular attractive $1/r^6$ potential (see Sec. IV) and thus an adjustable scattering length. This looks quite natural because increasing the order in the potential has a meaning, and we can always compare the effect in the phase shifts of having a higher order potential with the same scattering length (see Sec. VIII). In this construction, if the next term in the expansion were to be more singular and repulsive, the scattering length would be fully predicted from the potential.

The OPE potential in the triplet ${}^3S_1$–${}^3D_1$ coupled channel corresponds to case 2 and hence one has *one* free parameter in addition to the OPE potential parameters. One may choose this parameter to be the deuteron binding energy (or alternatively the triplet S-wave scattering length). Any other bound state or scattering observables are predicted. This case was treated in great detail in our previous work [41].[13] In the NLO TPE potential, we have case 3 because both eigenpotentials present a repulsive $1/r^5$ singularity (see Sec.VIII) and one would predict all observables from the potential parameters. Finally, in the NNLO TPE potential, we have case 1 corresponding to an attractive-attractive (see Sec. V), and two additional parameters need to be specified for a state with a given energy. The orthogonality condition imposes a relation between two states of different energy, so that for all energies in the triplet channel, one has *three* independent parameters. We will take these three parameters to be the deuteron binding energy, the asymptotic D/S ratio and the S-wave scattering length. The trend one observes when going from LO to NNLO is quite natural; as usual in ChPT one has more parameters at any order of the approximation. The NLO approximation poses,

[12] Both cases comply with the normalizability condition at the origin, Eq. (8).

[13] Relevant previous work on this channel was also presented in Refs. [38] and [40], in which the orthogonality conditions were not considered. See the discussion at the end of Sec. V in Ref. [41].

however, a problem since one seems to have more predictive power than at LO (see Sec. VIII for more details on the consequences of using our renormalization ideas literally for the conventional NLO potential).

For the NNLO TPE triplet $^3S_1$–$^3D_1$ channel, we fix the deuteron binding energy, or equivalently γ, and the asymptotic D/S ratio η by their experimental values. This fixes the short distance phases $\varphi_+(\gamma)$ and $\varphi_-(\gamma)$. Next, if we use an α or β (see below for a definition) zero energy scattering state, we have in principle two short distance phases $[\varphi_{\alpha,+}(0), \varphi_{\alpha,-}(0)]$ and $[\varphi_{\beta,+}(0), \varphi_{\beta,-}(0)]$ which can be related to the (α_0, α_{02}) and (α_{02}, α_2) scattering lengths, respectively. Using the orthogonality constraints to the deuteron bound state, one can then eliminate α_{02} and α_2 and treat α_0 as a free parameter. Thus, in the triplet $^3S_1$–$^3D_1$ channel we can treat γ, η, and α_0 as independent parameters. Once these parameters have been fixed, we can actually predict the corresponding phase shifts since any positive energy state must be orthogonal to both the deuteron bound state and the zero energy scattering states. This result is a direct consequence of the singular van der Waals attractive behavior of the TPE potential at the origin. It is remarkable that this same set of independent parameters was also adopted in Ref. [55] within the realistic potential model treatment.

Conflicts between naive dimensional power counting and renormalization have already been reported recently at the LO (OPE) level [42], where it was shown that even the $^3P_0$ partial wave depends strongly on the cutoff in momentum space (a Gaussian regulator is used) if according to the standard Weinberg counting no counterterm is added. The requirement of renormalizability makes the promotion of one counterterm unavoidable for channels that present an attractive singularity. This promotion is the minimal possible one compatible with finiteness, because in a coupled channel problem one could think in general of three counterterms. From this viewpoint, the choice of just one counterterm in triplet channels is a bit mysterious. Our discussion in coordinate space agrees with these authors in the OPE potential, and it actually allows us to identify *a priori* the necessarily promotable counterterms as nontrivial boundary conditions at the origin for singular attractive potentials. Moreover, we also see that the promotion of *only one counterterm* in the triplet channels with an attractive-repulsive singularity invoked in Ref. [42] is also maximal, since any additional counterterm would also produce divergent results (see Sec. VIII C). Thus, we see that although power counting determines the long distance potential, the short distance singular character of the potential does not allow us to fix the counterterms arbitrarily.

To conclude this discussion, let us mention that the short distance phases, whenever they become relevant, play the role of some dimensionless constants which depend exclusively on the form of the potential but not on the potential parameters [41]. For the same reason, they can be taken to be zeroth order in the power counting used to generate the chiral potential in Eq. (1), although they are subjected in general to higher order corrections. In this sense, the form of the short distance interaction is dictated only by the potential and cannot be considered as independent information. (See also Ref. [56] for a similar view on the three-body problem in the absence of long distance potentials.)

IV. THE SINGLET $^1S_0$ CHANNEL

For the singlet $^1S_0$ channel, one has to solve

$$-u''(r) + U_{^1S_0}(r)u(r) = k^2 u(r). \tag{33}$$

At short distances, the NNLO NN chiral potential behaves as [7,11,12]

$$U_{^1S_0}(r) \to \frac{3g^2}{128 f^4 \pi^2 r^6}(-4 + 15g^2 + 24\bar{c}_3 - 8\bar{c}_4) = -\frac{R^4}{r^6}, \tag{34}$$

which is a van der Waals type interaction with typical length scale $R = (-MC_6)^{1/4}$. Here, $\bar{c}_i = Mc_i$. The value of the coefficient is negative for the four parameter sets of Table I, so the solution at short distances is of oscillatory type, Eq. (21) with $n = 6$, and

$$u(r) \to A\left(\frac{r}{R}\right)^{3/2} \sin\left[-\frac{1}{2}\left(\frac{R}{r}\right)^2 + \varphi\right], \tag{35}$$

where there is a undetermined energy-independent phase φ, and A is a normalization constant. Note that the corresponding van der Waals radius is quite sensitive to the choice of chiral parameters.

A. Low energy parameters

For the zero energy state, we use the asymptotic normalization at large distances

$$u_0(r) \to 1 - \frac{r}{\alpha_0}. \tag{36}$$

Then, the effective range is given by

$$r_0 = 2\int_0^\infty dr\left[\left(1 - \frac{r}{\alpha_0}\right)^2 - u_0(r)^2\right]. \tag{37}$$

We can use the superposition principle for boundary conditions

$$u_0(r) = u_{0,c}(r) - \frac{1}{\alpha_0}u_{0,s}(r), \tag{38}$$

where $u_{0,c}(r) \to 1$ and $u_{0,s}(r) \to r$ correspond to cases where the scattering length is either infinity or zero, respectively. Using this decomposition, one gets

$$r_0 = A + \frac{B}{\alpha_0} + \frac{C}{\alpha_0^2}, \tag{39}$$

where

$$A = 2\int_0^\infty dr\left(1 - u_{0,c}^2\right), \tag{40}$$

$$B = -4\int_0^\infty dr(r - u_{0,c}u_{0,s}), \tag{41}$$

$$C = 2\int_0^\infty dr\left(r^2 - u_{0,s}^2\right), \tag{42}$$

depend on the potential parameters only. The interesting thing is that all explicit dependence on the scattering length α_0 is

displayed by Eq. (39). In a sense, this is the nonperturbative universal form of a low energy theorem, which applies to *any* potential regular or singular at the origin which decays faster than a certain power of r at large distances (for an analytical example with the pure van der Waals potential $U = -R^4/r^6$, see Sec. VII). Since the potential is known accurately at long distances, we can visualize Eq. (39) as a long distance correlation between r_0 and α_0. Naturally, if there is scale separation between the different contributions in the potential, Eq. (1), we expect the coefficients A, B, and C to display a converging pattern. This is exactly what happens [see Eqs. (43) and (89) below], although this behavior is not compatible with a naive and perturbative power counting (see Sec. IX).

In the $^1S_0$, the TPE potential becomes singular and attractive at short distances. Nevertheless, already at this point one can see the dramatic difference between attractive and repulsive singular potentials. In the attractive case, the short distance phase allows one to choose the scattering length *independently* of the potential, hence the coefficients A, B, and C are uncorrelated with α_0. For a singular repulsive potential, however, α_0 as well as A, B, and C are determined by the potential. If one assumes A, B, and C to be independent of α_0 in the repulsive case, which can only be possible because of an admixture of both the regular and irregular solutions, the latter will dominate at short distances and the effective range will diverge $r_0 \to -\infty$. This fact will become relevant in Sec. VIII C.

Obviously, for the chiral TPE potential, Eq. (1), the coefficients have to be evaluated by numerical means, and they are finite. We expect that these coefficients scale with the relevant scale of the potential. If long distances dominate, then $A \sim 1/m$, $B \sim 1/m^2$, and $C \sim 1/m^3$ but $r_0 \sim 1/m$. In contrast, if short distances dominate, then $A \sim R$, $B \sim R^2$, and $C \sim R^3$ and $r_0 \sim R$. The real situation is somewhat in between, but it is clear that A is far more sensitive to short distances than C. Actually, for a large scattering length, as is the case in the $^1S_0$ channel, the coefficient A dominates. Note that unlike the standard approaches, where a short distance contribution to the effective range is allowed (in the form of a momentum-dependent counterterm $C_2(k^2 + k'^2)$), we build r_0 *solely* from the potential and the scattering length α_0. This is a direct consequence of the orthogonality relations, which preclude energy-dependent boundary conditions for the local and energy-independent chiral TPE potential.

In Fig. 3, we show the dependence of the effective range as a function of the short distance cutoff radius r_c, i.e., replacing the lower limit of integration in Eq. (37), for values between 2 and 0.1 fm and taking the experimental value of the scattering length $\alpha_0 = -23.74$ fm. As we see, the short distance behavior is well under control and nicely convergent toward the experimental value. This dependence also illustrates that an error estimate based on varying the cutoff between a certain range is only a measure of the size of finite cutoff effects, rather than a measure of the error. The linear behavior observed at small r_c is a consequence of the dominance of the first term in Eq. (37) as compared with the second term where the wave function contribution vanishes as $\sim r_c^4$. Let us remember that in the conventional

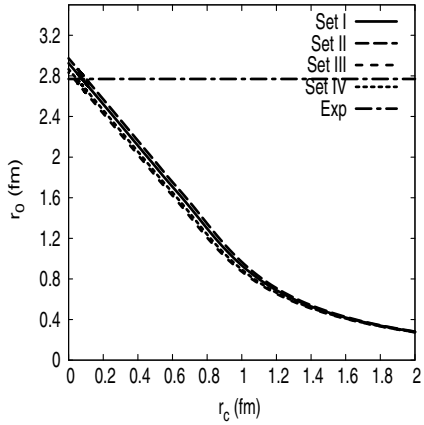

FIG. 3. Effective range for the TPE potential in the singlet $^1S_0$ channel when the lower limit of integration in Eq. (37) is taken to be a short distance cutoff and the experimental value of the scattering length $\alpha_0 = -23.74$ fm is taken. We show sets I–IV (see main text).

treatments, a counterterm C_2 is added to provide a short distance contribution to the effective range parameter, and the result is fitted to experiment so that r_0 becomes an input of the calculation. Obviously one expects C_2 to depend on the regularization scale. As shown in Fig. 3, the size of the counterterm C_2 at $r_c \to 0$ must be numerically small, since the TPE potential provides the bulk of the contribution. This agrees with the orthogonality constraint which requires $C_2 \to 0$ when $r_c \to 0$.

Numerically we find the following renormalized relations in the singlet channel for the OPE and NNLO TPE,

$$
\begin{aligned}
r_0 &= 1.308062 - \frac{4.547741}{\alpha_0} + \frac{5.192606}{\alpha_0^2} \qquad \text{(OPE)},\\
r_0 &= 2.670963 - \frac{5.755234}{\alpha_0} + \frac{6.031119}{\alpha_0^2} \qquad \text{(I)},\\
r_0 &= 2.715075 - \frac{5.847358}{\alpha_0} + \frac{6.093430}{\alpha_0^2} \qquad \text{(II)},\\
r_0 &= 2.586862 - \frac{5.584383}{\alpha_0} + \frac{5.916900}{\alpha_0^2} \qquad \text{(III)},\\
r_0 &= 2.616830 - \frac{5.640921}{\alpha_0} + \frac{5.952694}{\alpha_0^2} \qquad \text{(IV)}
\end{aligned}
\tag{43}
$$

As we see, the C coefficient is not very sensitive to the choice of the coefficients c_1, c_3, c_4, and the OPE potential already provides the bulk of the contribution. On the other hand, the A coefficient changes dramatically when going from OPE to TPE, suggesting that the effect is clearly nonperturbative. A direct inspection of the integrands for the A, B, and C coefficients shows that A picks its main contribution from the short distance region around 1 fm, whereas for B and C the most important contribution is located around 3 fm. One expects that different choices of coefficients c_3 and c_4 influence mostly the A coefficient. We confirm this expectation analytically by only keeping the van der Waals contribution to the full potential in Sec. VII. We emphasize, again, that A, B, and C are intrinsic information on the potential; these

TABLE II. Threshold parameters in the singlet $^1S_0$ channel for the different sets of parameters c_1, c_3, and c_4 given in Table I. We compare our renormalized results given by the cutoff independent universal formula (39) for r_0 and its extension for v_2 to finite cutoff NN calculations using their scattering length as an input. The difference is attributed to finite cutoff effects.

Set	Calculation	$\Lambda = 1/r_c$	α_0 (fm)	r_0 (fm)	v_2 (fm^3)
I	NNLO [10]	0.6–1 GeV	−23.72	2.68	−0.61
I	NNLO [19]	0.5 GeV	−23.75	2.70	–
I	This work	∞	Input	2.92	−0.30
II	NNLO [11]	1/1.4 fm	–	–	–
II	This work	∞	Input	2.97	−0.23
III	NNLO [23]	0.65 GeV	−23.4	2.67	−0.50
III	N^{3}LO [29]	0.7 GeV	−23.6	2.66	−0.50
III	This work	∞	Input	2.83	−0.43
IV	N^{3}LO [28]	0.5 GeV	−23.73	2.73	–
IV	This work	∞	Input	2.87	−0.38
Nijm II	[43,44]	–	−23.73	2.67	−0.48
Reid 93	[43,44]	–	−23.74	2.75	−0.49
Exp.	–	–	−23.74(2)	2.77(5)	–

values for the effective range stem solely from the NNLO chiral potential and the scattering length α_0, without any additional short distance contribution. The closeness of these numbers to the experimental value suggests that there is perhaps no need to make the boundary condition energy dependent if the cutoff is indeed removed, and that the missing 0.1 fm contribution can be clearly attributed to N^{3}LO contributions in the potential.

The results are summarized in Table II. For pn we have the experimental values $\alpha_0 = -23.74(2)$ and $r_0 = 2.77(5)$. The previous formula, Eq. (39), yields $r_0 = 2.92, 2.97, 2.83, 2.87$ for sets I, II, III, and IV, respectively, which values how a systematic discrepancy with the published values in several works (see references in Table II) and also a systematic trend to discrepancy with respect to the experimental value. Our renormalized values are always larger than the finite cutoff results. This seems natural since finite cutoff corrections diminish the integration region. Note also that the size of the discrepancy is *larger* than the experimental uncertainties and hence is statistically significant.

The value of the effective range was not given in the coordinate space calculation of Ref. [11], but the quality of the fit suggests that they obtain a value very close to the experimental one, $r_0 = 2.77(5)$. The contribution to the effective range from the origin to 0.1 fm is about 0.2. In Ref. [11], the cutoff is in coordinate space and an energy-dependent boundary condition is considered. In practice this means cutting off the lower integration in Eq. (37) at $r_c = 1.4$ fm and adding an extra short distance contribution r_S in a way that the experimental value is reproduced. This introduces a new potential-independent parameter. As we have argued, in the limit $r_c \to 0$, the short distance contribution of the effective range should go to zero, as implied by the orthogonality constraints. For finite a, the orthogonality constraint does not imply a vanishing short distance contribution to the effective range.

For set IV, one could reach the upper experimental value by flipping the sign of c_1 and keeping c_3 and c_4 unchanged. For $c_1 = 2.43$ GeV^{-1}, one gets $r_0 = 2.78$ fm. The full experimental range would be covered by letting $0.81 < c_1 < 4.90$ GeV^{-1}. This is in total contradiction to the expectations of πN scattering studies [31]. The insensitivity of our results with respect to the c_1 coefficient has to do with the fact that c_1 only enters in the potential at short distances at order $1/r^4$ which is subleading as compared with the leading van der Waals singularity. This is another confirmation of the short distance dominance in the effective range parameter r_0.

Thus, according to our analysis, for the accepted values of chiral constants of sets I–IV used in previous works, the difference in the value of the $^1S_0$ effective range could only be attributed to three-pion-exchange, relativistic effects and electromagnetic corrections. Another possibility, of course, is to refit the chiral constants to our renormalized, cutoff free results. This will be discussed in Sec. VI.

B. Phase shift

For a finite energy scattering state, we solve for the chiral TPE potential with the normalization

$$u_k(r) \to \frac{\sin(kr + \delta_0)}{\sin \delta_0}. \tag{44}$$

Again, if we use the superposition principle

$$u_k(r) = u_{k,c}(r) + k \cot \delta_0 u_{k,s}(r), \tag{45}$$

with $u_{k,c} \to \cos(kr)$ and $u_{k,s} \to \sin(kr)/k$ and impose the orthogonality constraint with the zero energy state to get

$$\frac{u'_{k,c}(r_c) + k \cot \delta_0 u'_{k,s}(r_c)}{u_{k,c}(r_c) + k \cot \delta_0 u_{k,s}(r_c)} = \frac{-\alpha_0 u'_{0,c}(r_c) + u'_{0,s}(r_c)}{-\alpha_0 u_{0,c}(r_c) + u_{0,s}(r_c)}. \tag{46}$$

Note that the dependence of the phase shift on the scattering length is *explicit*; $\cot \delta_0$ is a bilinear rational mapping of α_0. Taking the limit $r_c \to 0$, we get

$$k \cot \delta_0 = \frac{\alpha_0 \mathcal{A}(k) - \mathcal{B}(k)}{\alpha_0 \mathcal{C}(k) - \mathcal{D}(k)}, \tag{47}$$

whereas the functions $\mathcal{A}$, $\mathcal{B}$, $\mathcal{C}$, and $\mathcal{D}$ are even functions of k which depend only on the potential and are given by

$$\begin{aligned}
\mathcal{A}(k) &= \lim_{a\to 0}(u_{0,c}(r_c)u'_{k,c}(r_c) - u'_{0,c}(r_c)u_{k,c}(r_c)),\\
\mathcal{B}(k) &= \lim_{a\to 0}(u_{k,c}(r_c)u'_{0,s}(r_c) - u_{0,s}(r_c)u'_{k,c}(r_c)),\\
\mathcal{C}(k) &= \lim_{a\to 0}(u'_{0,c}(r_c)u_{k,s}(r_c) - u_{0,c}(r_c)u'_{k,s}(r_c)),\\
\mathcal{D}(k) &= \lim_{a\to 0}(u_{0,s}(r_c)u'_{k,s}(r_c) - u'_{0,s}(r_c)u_{k,s}(r_c)).
\end{aligned} \tag{48}$$

The obvious conditions $\mathcal{A}(0) = \mathcal{D}(0) = 0$ and $\mathcal{B}(0) = \mathcal{C}(0) = 1$ are satisfied. Expanding the expression for small k yields the well-known effective range expansion

$$k \cot \delta = -\frac{1}{\alpha_0} + \frac{1}{2} r_0 k^2 + v_2 k^2 + \cdots, \tag{49}$$

where v_k is a polynomial in $1/\alpha_0$ of degree $k + 1$.

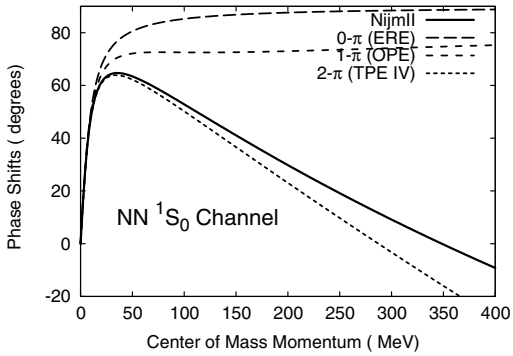

FIG. 4. Renormalized phase shifts for the ERE, OPE and TPE potentials as a function of the c.m. np momentum k in the singlet $^1S_0$ channel compared to the Nijmegen results [43] for different parameter sets. The regular scattering wave functions for finite k are orthogonal to the zero energy wave functions. For the TPE potential, we have taken the chiral couplings of set IV.

The renormalized phase shift is presented in Fig. 4 for set IV. As we see, the trend in the effective range r_0 and the v_2 parameter are reflected in the behavior of the phase shift. [14]

V. THE TRIPLET $^3S_1$–$^3D_1$ CHANNEL

The coupled channel $^3S_1$–$^3D_1$ set of equations read

$$\begin{aligned} -u''(r) + U_{^3S_1}(r)u(r) + U_{E_1}(r)w(r) &= k^2 u(r), \\ -w''(r) + U_{E_1}(r)u(r) + \left[U_{^3D_1}(r) + \frac{6}{r^2}\right] w(r) &= k^2 w(r). \end{aligned} \tag{50}$$

At short distances, the NN chiral NNLO potential behaves as [7,11,12]

$$\begin{aligned} U_{^3S_1}(r) &\to \frac{\mathrm{MC}_{6,^3S_1}}{r^6}, \\ U_{E_1}(r) &\to \frac{\mathrm{MC}_{6,E_1}}{r^6}, \\ U_{^3D_1}(r) &\to \frac{\mathrm{MC}_{6,^3D_1}}{r^6}, \end{aligned} \tag{51}$$

which is a coupled channels van der Waals type interaction, where the coefficients are given by

$$\begin{aligned} \mathrm{MC}_{^3S_1} &= \frac{3g^2}{128 f^4 \pi^2}(4 - 3g^2 + 24\bar{c}_3 - 8\bar{c}_4), \\ \mathrm{MC}_{E_1} &= -\frac{3\sqrt{2}g^2}{128 f^4 \pi^2}(-4 + 3g^2 - 16\bar{c}_4), \\ \mathrm{MC}_{^3D_1} &= \frac{9g^2}{32 f^4 \pi^2}(-1 + 2g^2 + 2\bar{c}_3 - 2\bar{c}_4). \end{aligned} \tag{52}$$

[14] Let us mention that the momentum space calculation of Ref. [42] *does not* reproduce the physical and well-measured scattering length; rather, it tries to fit the phase shifts at certain energies. Hence, there will be some differences between the singlet OPE phase shifts presented here and the corresponding results of Ref. [42].

If we diagonalize the corresponding matrix, we get

$$\begin{pmatrix} C_{6,^3S_1} & C_{6,E_1} \\ C_{6,E_1} & C_{6,^3D_1} \end{pmatrix} = \begin{pmatrix} \cos\theta & \sin\theta \\ -\sin\theta & \cos\theta \end{pmatrix} \begin{pmatrix} C_{6,+} & 0 \\ 0 & C_{6,-} \end{pmatrix} \times \begin{pmatrix} \cos\theta & -\sin\theta \\ \sin\theta & \cos\theta \end{pmatrix}, \tag{53}$$

where $C_{6,\pm}$ are the corresponding eigenvalues and θ the mixing angle. They are listed in Table I for different parameter choices of the chiral couplings c_1, c_3, and c_4. We see that in all cases, both eigenpotentials are attractive at short distances; hence, the short distance behavior of the wave functions is of oscillatory type with $n = 6$. Defining the van der Waals scales as

$$R_\pm = (-\mathrm{MC}_{6,\pm})^{1/4}, \tag{54}$$

the short distance solutions read

$$\begin{pmatrix} u \\ w \end{pmatrix} \to \begin{pmatrix} \cos\theta & \sin\theta \\ -\sin\theta & \cos\theta \end{pmatrix} \begin{pmatrix} \left(\frac{r}{R_+}\right)^{\frac{3}{2}} \sin\left[\frac{1}{2}\left(\frac{R_+}{r}\right)^2 + \varphi_+\right] \\ \left(\frac{r}{R_-}\right)^{\frac{3}{2}} \sin\left[\frac{1}{2}\left(\frac{R_-}{r}\right)^2 + \varphi_-\right] \end{pmatrix}.$$

Thus, we have two arbitrary short distance phases $\varphi_\pm$ for a given fixed energy which cannot be deduced from the potential and hence have to be treated as independent parameters. We will fix them to some physical observables by integrating Eqs. (50) from infinity down to the origin.

A. The deuteron

In the deuteron, $k^2 = -\gamma^2$ and we solve Eq. (50) together with the asymptotic condition at infinity

$$\begin{aligned} u(r) &\to A_S e^{-\gamma r}, \\ w(r) &\to A_D e^{-\gamma r}\left(1 + \frac{3}{\gamma r} + \frac{3}{(\gamma r)^2}\right), \end{aligned} \tag{55}$$

where $\gamma = \sqrt{MB}$ is the deuteron wave number, A_S is the normalization factor and the asymptotic D/S ratio parameter is defined by $\eta = A_D/A_S$. In what follows we use γ and η as *input* parameters, thus fixing the short distance phases $\varphi_\pm$ automatically.

In this paper we compute the matter radius, which reads,

$$r_m^2 = \frac{\langle r^2 \rangle}{4} = \frac{1}{4}\int_0^\infty r^2(u(r)^2 + w(r)^2)dr, \tag{56}$$

the quadrupole moment (without meson exchange currents)

$$Q_d = \frac{1}{20}\int_0^\infty r^2 w(r)(2\sqrt{2}u(r) - w(r))dr, \tag{57}$$

the deuteron inverse radius

$$\langle r^{-1} \rangle = \int_0^\infty dr \frac{u(r)^2 + w(r)^2}{r}, \tag{58}$$

which appears in low energy pion-deuteron scattering, and the D-state probability

$$P_D = \int_0^\infty w(r)^2 dr. \tag{59}$$

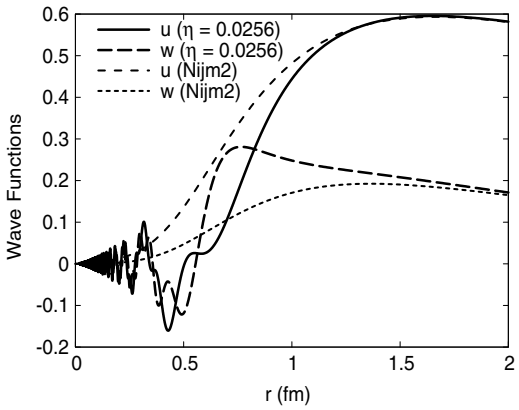

FIG. 5. TPE deuteron wave functions u and w as a function of the distance (in fm) compared to the Nijmegen II wave functions [43,44]. The asymptotic normalization $u \to e^{-\gamma r}$ has been adopted, the asymptotic D/S ratio is $\eta = 0.0256(4)$, and the chiral couplings are from set IV.

Following Ref. [41], we use the superposition principle of boundary conditions and write

$$u(r) = u_S(r) + \eta u_D(r),$$
$$w(r) = w_S(r) + \eta w_D(r), \tag{60}$$

where (u_S, w_S) and (u_D, w_D) correspond to the boundary conditions at infinity, Eq. (55), with $A_S = 1$ and $A_D = 0$ and with $A_S = 0$ and $A_D = 1$, respectively. Obviously, u_S, u_D, w_S, and w_D depend only on the potential and the deuteron binding energy; therefore, the dependence on the asymptotic D/S ratio η can de determined analytically. The value is taken as a free parameter. The resulting deuteron wave functions for set IV are displayed in Fig. 5 and compared with the Nijmegen II results [43,44]. One clearly sees the incommensurable ever-increasing oscillations below $r = 0.6$ fm.

The short distance cutoff dependence of these deuteron properties using the experimental values for the deuteron binding energies and the asymptotic D/S ratio, $\eta = 0.0256$, can be found in Fig. 6. As one sees, the cutoff dependence is well under control, so the infinite cutoff limit can be extracted without difficulty.

Using the superposition principle of boundary conditions, Eq. (60), the asymptotic S-wave ratio depends quadratically on η as follows:

$$\frac{1}{A_S^2} = \int_0^\infty dr\left(u_S^2 + w_S^2\right) + 2\eta \int_0^\infty dr(u_S u_D + w_S w_D) + \eta^2 \int_0^\infty dr\left(u_D^2 + w_D^2\right). \tag{61}$$

The coefficients of this second-order polynomial depends on the potential and the deuteron binding energy. Similar

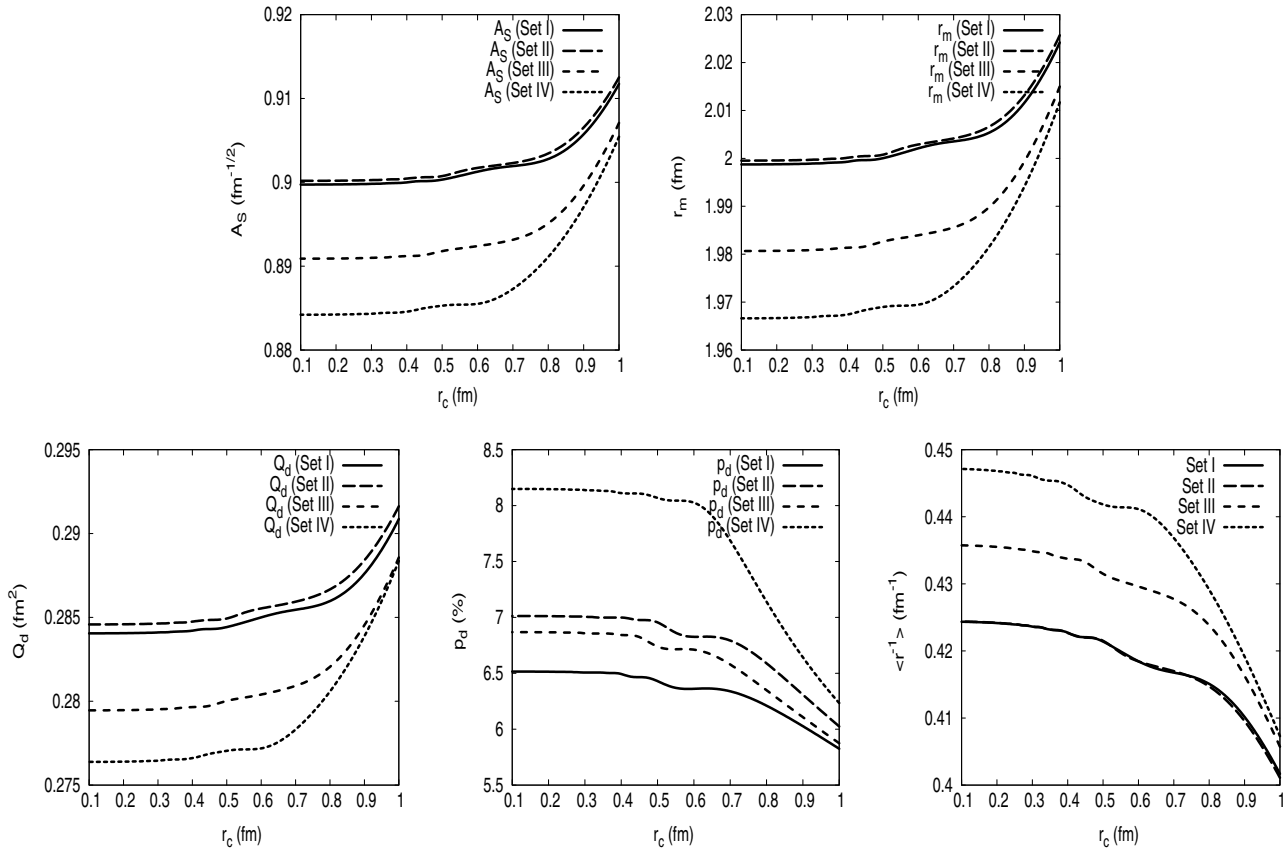

FIG. 6. Dependence of the S-wave normalization A_S, the matter radius r_m, the quadrupole moment Q_d, the D-state probability P_D, and the inverse radius $\langle r^{-1}\rangle$ for the TPE potential on the short distance cutoff r_c for sets I–IV of low energy chiral constants.

TABLE III. Deuteron properties and low energy parameters in the ${}^3S_1$–${}^3D_1$ channel for the pionless theory (Short), the OPE, and the TPE potential. By pionless we mean taking the only normalizable solution with no potential, i.e., $u(r) = e^{-\gamma r}$ and $w(r) = 0$. We use the nonrelativistic relation $\gamma = \sqrt{2\mu_{np}B}$ with $B = 2.224575(9)$. For OPE* we take $g_A = 1.26$ as input instead of $g_{\pi NN} = 13.083$. Errors quoted in the TPE reflect the uncertainty only in the nonpotential parameters γ, η, and α_0. Differences from this work are attributed to finite cutoff effects. Experimental values can be traced from [55].

Set	Ref.	γ	η	A_S	r_m	Q_d	P_D	$\langle r^{-1}\rangle$	α_0	α_{02}	α_2	r_0
Short	—	Input	0	0.6806	1.5265	0	0	∞	4.3177	0	0	0
OPE	[41]	Input	0.02633	0.8681(1)	1.9351(5)	0.2762(1)	7.31(1)%	0.476(3)	5.335(1)	1.673(1)	6.693(1)	1.638(1)
OPE*	[41]	Input	0.02555	0.8625(2)	1.9234(5)	0.2667(1)	7.14(1)%	0.471(3)	5.308(1)	1.612(1)	6.325(1)	1.602(2)
I	N^{2}LO [10]		0.0245	0.884	1.967	0.262	6.11%	—	5.420	—	—	1.753
I	N^{2}LO [19]		0.0256	0.8846	1.9756	0.281	4.17%	—	5.417	—	—	1.753
I	This work	Input	Input	0.900(2)	1.999(4)	0.284(4)	6(1)%	0.424(3)	Input	2.3(2)	3(3)	1.4(4)
II	[11]	—	—	—	—	—	—	—	—	—	—	—
II	This work	Input	Input	0.900(2)	1.999(4)	0.285(4)	7(1)%	0.424(4)	Input	2.22(15)	4(2)	1.46(19)
III	N^{2}LO [23]	—	0.0256	0.873	1.972	0.272	5%	—	5.427	—	—	1.731
III	N^{3}LO [29]	—	0.0254	0.882	1.979	0.266	3%	—	5.417	—	—	1.745
III	This work	Input	Input	0.891(3)	1.981(5)	0.279(4)	7(1)%	0.436(3)	Input	1.88(10)	5.7(16)	1.67(8)
IV	N^{3}LO [28]	—	0.0256	0.8843	1.968	0.275	4.51%	—	5.417	—	—	1.752
IV	This work	Input	Input	0.884(4)	1.967(6)	0.276(3)	8(1)%	0.447(5)	Input	1.67(4)	6.6(4)	1.76(3)
NijmII	[43,44]	0.2316	0.02521	0.8845(8)	1.9675	0.2707	5.635%	0.4502	5.418	1.647	6.505	1.753
Reid93	[43,44]	0.2316	0.02514	0.8845(8)	1.9686	0.2703	5.699%	0.4515	5.422	1.645	6.453	1.755
Exp.	—	0.2316	0.0256(4)	0.8846(9)	1.971(6)	0.2859(3)	—	—	5.419(7)	—	—	1.753(8)

relations hold for other observables. Evaluating the integrals numerically produces the following analytic correlations:

Set I

$$\begin{aligned} 1/A_S^2 &= 3.78888 - 214.675\,\eta + 4489.43\,\eta^2 \\ r_m^2/A_S^2 &= 5.47297 - 54.1956\,\eta + 1295.89\,\eta^2 \\ Q_d/A_S^2 &= -0.342883 + 36.6449\,\eta - 372.841\,\eta^2 \\ P_D/A_S^2 &= 2.10904 - 184.824\,\eta + 4124.37\,\eta^2 \\ \langle r^{-1}\rangle/A_S^2 &= 3.58173 - 252.20\,\eta + 5186.53\,\eta^2 \end{aligned} \tag{62}$$

Set II

$$\begin{aligned} 1/A_S^2 &= 3.01271 - 155.591\,\eta + 3363.94\,\eta^2 \\ r_m^2/A_S^2 &= 5.34737 - 44.8896\,\eta + 1122.59\,\eta^2 \\ Q_d/A_S^2 &= -0.296852 + 33.2406\,\eta - 309.624\,\eta^2 \\ P_D/A_S^2 &= 1.44293 - 132.314\,\eta + 3098.89\,\eta^2 \\ \langle r^{-1}\rangle/A_S^2 &= 2.52815 - 171.36\,\eta + 3635.18\,\eta^2 \end{aligned} \tag{63}$$

Set III

$$\begin{aligned} 1/A_S^2 &= 4.65049 - 283.545\,\eta + 5902.53\,\eta^2 \\ r_m^2/A_S^2 &= 5.58929 - 63.1854\,\eta + 1481.50\,\eta^2 \\ Q_d/A_S^2 &= -0.377779 + 39.2691\,\eta - 420.250\,\eta^2 \\ P_D/A_S^2 &= 2.77521 - 241.491\,\eta + 5330.67\,\eta^2 \\ \langle r^{-1}\rangle/A_S^2 &= 4.87639 - 356.21\,\eta + 7311.77\,\eta^2 \end{aligned} \tag{64}$$

Set IV

$$\begin{aligned} 1/A_S^2 &= 3.40962 - 190.713\,\eta + 4198.86\,\eta^2 \\ r_m^2/A_S^2 &= 5.40066 - 49.2912\,\eta + 1232.81\,\eta^2 \\ Q_d/A_S^2 &= -0.306469 + 33.9354\,\eta - 318.598\,\eta^2 \\ P_D/A_S^2 &= 1.66525 - 155.233\,\eta + 3681.89\,\eta^2 \\ \langle r^{-1}\rangle/A_S^2 &= 3.14658 - 226.20\,\eta + 4907.35\,\eta^2 \end{aligned} \tag{65}$$

The numerical coefficients in these expressions depend on the deuteron binding energy and the TPE potential parameters g, m, f, c_1, c_3, and c_4. The results for the deuteron properties are given in Table III. The uncertainties are due to changing the input γ and η within their experimental uncertainties. We have checked that the short distance cutoffs $a \sim 0.1$–0.2 fm generates much smaller uncertainties. The explicit dependence on η is displayed in Fig. 7. Again, we find a discrepancy in the case of set I with the values quoted in the finite cutoff calculation. Remarkably, our renormalized results in coordinate space agree most with the momentum space calculation of Ref. [19] corresponding to set IV. It is noticeable that this can be done without explicit knowledge of the counterterms used in that work in momentum space. This is precisely one of the points of renormalization; results can be reproduced by just providing physical input data, with no particular reference to the method of solution. Let us remember that c_1, c_3, and c_4 were fixed from the perturbative study of NN peripheral waves where the cutoff sensitivity is rather

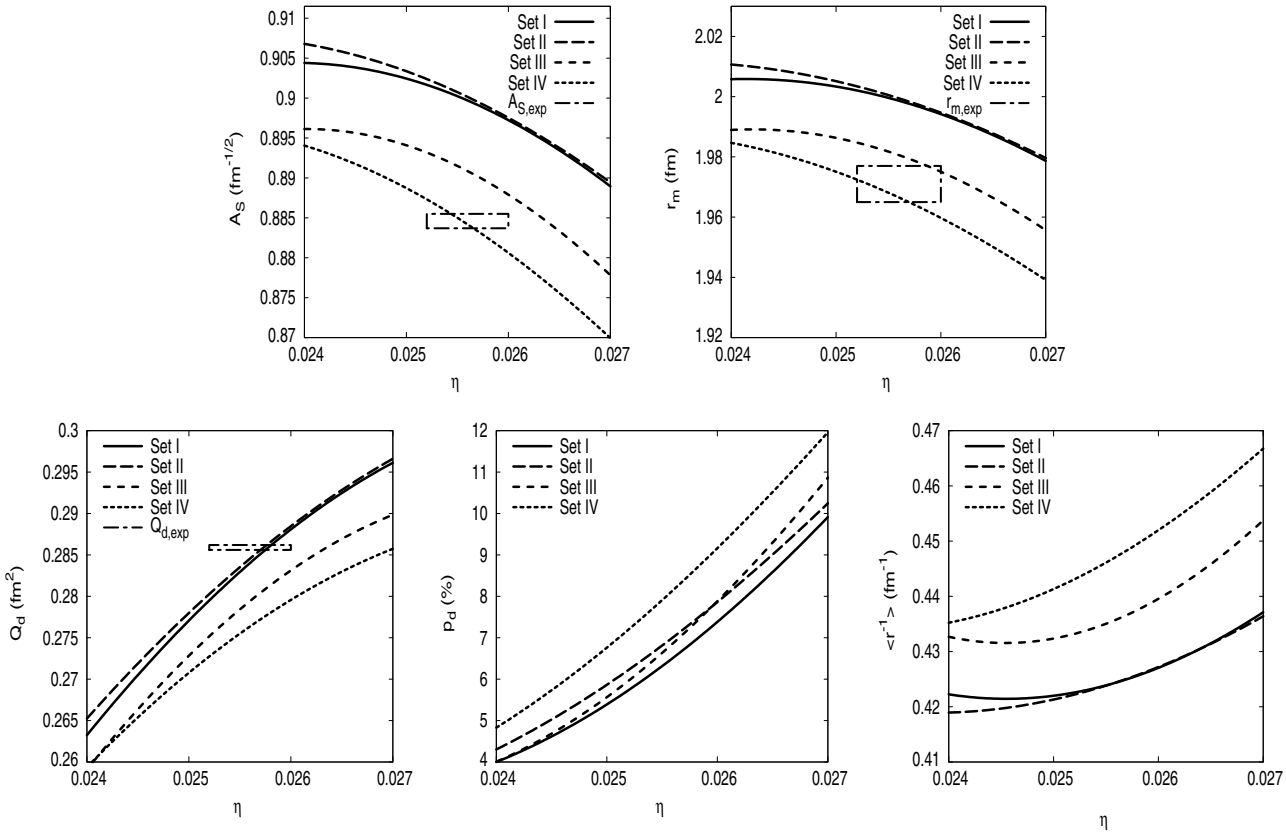

FIG. 7. Dependence of the S-wave normalization A_S, the matter radius r_m, the quadrupole moment Q_d, and the inverse radius $\langle r^{-1}\rangle$ for the TPE potential as a function of the asymptotic D/S ratio η. Boxes represent experimental values. Predicted quadrupole moments as well as the matter radius should be corrected for meson exchange currents (MECs), accounting for adding 0.01 fm^2 and 0.003 fm, respectively, on top of the potential result [57]. We display the four sets of chiral coupling constants.

small. Nevertheless, some significant discrepancies do also occur.

For the parameter set IV [28] obtained by an N^{3}LO fit to NN scattering data, our NNLO calculation reproduces almost exactly the numbers provided in that work. Furthermore, they turn out to be compatible with the experimental numbers at the 1σ level within the uncertainty induced by the asymptotic D/S ratio.[15]

One immediate lesson we learn from inspection of Table III is that regardless of the parameter set, only the experimental uncertainty in the asymptotic D/S ratio for the deuteron generates theoretical uncertainties about an order of magnitude larger than the experimental ones. Furthermore, one also has to take into account other uncertainties, such as the one in $g_{\pi NN}$ and, of course, those induced by c_1, c_3, and c_4, which generally will generate larger uncertainties if all these parameters are regarded as independent (see Sec. VI below). In addition, some systematic errors relate to the accuracy of the expansion in the potential, Eq. (1). In common with nonperturbative finite cutoff calculations [10,11,21–23,28], they are difficult to estimate *a priori* given the nonperturbative nature of our calculation, but they are bound to increase the error (see, however, our discussion in Sec. IX on noninteger power counting). Given the insensitivity of our results to the short distance cutoff, the procedure used in Refs. [22,23] of varying the cutoff becomes unsuitable in our case.

For the deuteron channel, one may conclude that the predictive power of the chiral expansion has reached a limit at NNLO. So, at present, we do not expect to make theoretical predictions in the deuteron to be more accurate than experiment. The inclusion of N^{3}LO and higher orders may provide better central values but is unlikely to improve the situation regarding error estimates since new unknown coefficients in the potential appear and the induced uncertainties will generally increase.

On the other hand, the slopes for A_S and r_m (Fig. 7) suggest that it would be better to take the asymptotic S-wave normalization or the matter radius as input, since generated errors may be comparable or even smaller. For instance, if

[15] One may object to using N^{3}LO parameters in a NNLO calculation, since they are obtained by fitting the same database. However, if there are finite cutoff effects, the situation is not as clear. Finite cutoff effects are minimized in an N^{3}LO calculation as shown in Ref. [29] where the induced uncertainties are drastically reduced when going from NNLO to N^{3}LO. Note that in our calculation, there already are no sizable cutoff-induced uncertainties at NNLO.

the matter radius r_m is taken as input, we get instead $\eta = 0.0253(4)$, a compatible value with similar errors. However, if we take $A_S = 0.8846(9)$ as input for set IV, we obtain $\eta = 0.0255(1)$, a value compatible with the experimental one but with much smaller errors. The reduction of errors is also confirmed in sets I–III, although the central values are a bit off. This result opens up the possibility of making a benchmark determination of the asymptotic D/S deuteron ratio from the chiral effective theory. Obviously, to do so, the chiral constants should be known with rather high accuracy, an illusory expectation at the present moment. In this regard, it would perhaps be profitable to pin down the errors for the chiral constants from peripheral waves. This point will be analyzed elsewhere [58].

Both the loss of predictive power and the very rare possibility of making model-independent theoretical predictions for purely hadronic processes using chiral perturbation theory more accurate than experiment, which we seem to observe in low energy NN scattering, are not new observations. They have already been documented for low energy $\pi\pi$ scattering [49–51] and provide further motivation for using chiral effective approaches.

B. Low energy parameters

The zero energy wave functions are taken asymptotically as [16]

$$\begin{aligned} u_{0,\alpha}(r) &\to 1 - \frac{r}{\alpha_0}, \\ w_{0,\alpha}(r) &\to \frac{3\alpha_{02}}{\alpha_0 r^2}, \\ u_{0,\beta}(r) &\to \frac{r}{\alpha_0}, \\ w_{0,\beta}(r) &\to \left(\frac{\alpha_2}{\alpha_{02}} + \frac{\alpha_{02}}{\alpha_0}\right)\frac{3}{r^2} - \frac{r^3}{15\alpha_{02}}. \end{aligned} \tag{66}$$

Using these zero energy solutions, one can determine the effective range. The $^3S_1$ effective range parameter is given by

$$r_0 = 2\int_0^\infty \left[\left(1 - \frac{r}{\alpha_0}\right)^2 - u_\alpha(r)^2 - w_\alpha(r)^2\right] dr. \tag{67}$$

[16] We correct an error in Eq. (45) of our previous work [41] where α_2 appears. The corrected numerical value is $\alpha_2 = 6.693$ fm^5.

In the zero energy case, the vanishing of the diverging exponentials at the origin imposes a condition on the α and β states which generate a correlation between α_0, α_{02}, and α_2. Using the superposition principle of boundary conditions we may write the solutions in such a way that

$$\begin{aligned} u_{0,\alpha}(r) &= u_1(r) - \frac{1}{\alpha_0}u_2(r) + \frac{3\alpha_{02}}{\alpha_0}u_3(r), \\ w_{0,\alpha}(r) &= w_1(r) - \frac{1}{\alpha_0}w_2(r) + \frac{3\alpha_{02}}{\alpha_0}w_3(r), \\ u_{0,\beta}(r) &= \frac{1}{\alpha_0}u_2(r) + \left(\frac{3\alpha_2}{\alpha_{02}} + \frac{3\alpha_{02}}{\alpha_0}\right)u_3(r) - \frac{1}{15\alpha_{02}}u_4(r), \\ w_{0,\beta}(r) &= \frac{1}{\alpha_0}w_2(r) + \left(\frac{3\alpha_2}{\alpha_{02}} + \frac{3\alpha_{02}}{\alpha_0}\right)w_3(r) - \frac{1}{15\alpha_{02}}w_4(r), \end{aligned} \tag{68}$$

where the functions $u_{1,2,3,4}$ and $w_{1,2,3,4}$ are independent of α_0, α_{02}, and α_2 and fulfill suitable boundary conditions. The orthogonality constraints for the α and β states read in this case

$$\begin{aligned} u_\gamma u'_{0,\alpha} - u'_\gamma u_{0,\alpha} + w_\gamma w'_{0,\alpha} - w'_\gamma u_{0,\alpha}\Big|_{r=r_c} &= 0, \\ u_\gamma u'_{0,\beta} - u'_\gamma u_{0,\beta} + w_\gamma w'_{0,\beta} - w'_\gamma u_{0,\beta}\Big|_{r=r_c} &= 0, \end{aligned} \tag{69}$$

yielding two relations between γ, α_{02}, α_2, η, and α_0, meaning that two of them are not independent. Using the superposition principle decomposition of the bound state, Eq. (60), and for the zero energy states, Eq. (68), we make the orthogonality relation explicit in $\alpha_0, \alpha_{02}, \alpha_2$, and η. If we would use $\alpha_0, \alpha_{02}, \alpha_2$ as input parameters, the orthogonality constraint is actually a nonlinear eigenvalue problem for γ and η. The values of α_{02} and α_2 are not well known, although they have been determined in potential models in our previous work [59]. In contrast, γ, η, and α_0 are well determined experimentally. Thus, in the deuteron scattering channel, we will use γ, η, and α_0 as independent input parameters and α_{02}, α_2 as predictions. This same set of independent parameters was also adopted in Ref. [55] within the high-quality potential model treatment, although the role of the short distance van der Waals singularity was not recognized. Fixing the experimental value of γ, we get the following relations for different parameter choices of c_1, c_3, and c_4:

Set I

$$\begin{aligned} \alpha_{02} &= \frac{2.01763 - 0.456461\,\alpha_0 - 44.8947\,\eta + 11.9351\,\alpha_0\,\eta}{-0.314426 + 13.1555\,\eta} \\ \alpha_2 &= \frac{-0.023522 + 1.04677\,\eta - 11.6459\,\eta^2 + \alpha_0\,(0.008423 - 0.537856\,\eta + 9.39376\,\eta^2)}{\alpha_0\,(-0.023901 + \eta)^2} + \frac{\alpha_{02}^2}{\alpha_0} \end{aligned} \tag{70}$$

Set II

$$\alpha_{02} = \frac{1.71745 - 0.373228\,\alpha_0 - 33.4616\,\eta + 8.76639\,\alpha_0\,\eta}{-0.228075 + 9.865911\,\eta}$$
$$\alpha_2 = \frac{-0.030303 + 1.18083\,\eta - 11.5032\,\eta^2 + \alpha_0\,(0.009559 - 0.566611\,\eta + 9.71850\,\eta^2)}{\alpha_0\,(-0.023118 + \eta)^2} + \frac{\alpha_{02}^2}{\alpha_0} \tag{71}$$

Set III

$$\alpha_{02} = \frac{2.36659 - 0.550871\,\alpha_0 - 59.1666\,\eta + 15.7488\,\alpha_0\,\eta}{-0.414962 + 17.2806\,\eta}$$
$$\alpha_2 = \frac{-0.018755 + 0.937802\,\eta - 11.7229\,\eta^2 + \alpha_0\,(0.007437 - 0.505434\,\eta + 9.09925\,\eta^2)}{\alpha_0\,(-0.024013 + \eta)^2} + \frac{\alpha_{02}^2}{\alpha_0} \tag{72}$$

Set IV

$$\alpha_{02} = \frac{1.89526 - 0.418953\alpha_0 - 41.8369\eta + 10.8526\alpha_0\eta}{-0.279236 + 12.2978\eta}$$
$$\alpha_2 = \frac{-0.023751 + 1.04857\,\eta - 11.5733\,\eta^2 + \alpha_0\,(0.008050 - 0.518604\,\eta + 9.31798\,\eta^2)}{\alpha_0\,(-0.023118 + \eta)^2} + \frac{\alpha_{02}^2}{\alpha_0} \tag{73}$$

The numerical coefficients appearing in these equations depend on the deuteron wave number γ and the TPE parameters g, f, and m and c_1, c_3, and c_4. The dependence on η for fixed values of α_0 within its experimental uncertainty is depicted in Fig. 8. We see that for fixed chiral couplings c_1, c_3, and c_4, the η uncertainty dominates the errors. Numerical values can be seen in Table III. Note the large discrepancy in the effective range r_0 for sets I and II with the experimental number. Finite cutoff effects are observed in set III although the η-induced uncertainty would make the value compatible with that estimate. Good agreement is observed again for set IV, particularly in the E_1 and ${}^3D_1$ scattering lengths and the effective range r_0, but only the latter provides a clear TPE improvement over the OPE. The quantities α_{02} and α_2 are compatible with typical expectations [59] from the high-quality potential models.

C. Phase shifts

For the α and β positive energy scattering states, we choose the asymptotic normalization

$$u_{k,\alpha}(r) \to \frac{\cos\epsilon}{\sin\delta_1}(\hat{j}_0(kr)\cos\delta_1 - \hat{y}_0(kr)\sin\delta_1),$$
$$w_{k,\alpha}(r) \to \frac{\sin\epsilon}{\sin\delta_1}(\hat{j}_2(kr) - \hat{y}_2(kr)\sin\delta_1), \tag{74}$$
$$u_{k,\beta}(r) \to -\frac{1}{\sin\delta_1}(\hat{j}_0(kr)\cos\delta_2 - \hat{y}_0(kr)\sin\delta_2),$$
$$w_{k,\beta}(r) \to \frac{\tan\epsilon}{\sin\delta_1}(\hat{j}_2(kr)\cos\delta_2 - \hat{y}_2(kr)\sin\delta_2), \tag{75}$$

where $\hat{j}_l(x) = x j_l(x)$ and $\hat{y}_l(x) = x y_l(x)$ are the reduced spherical Bessel functions and δ_1 and δ_2 are the eigenphases in the ${}^3S_1$ and ${}^3D_1$ channels, and ϵ is the mixing angle E_1. The use of the superposition principle for boundary conditions as

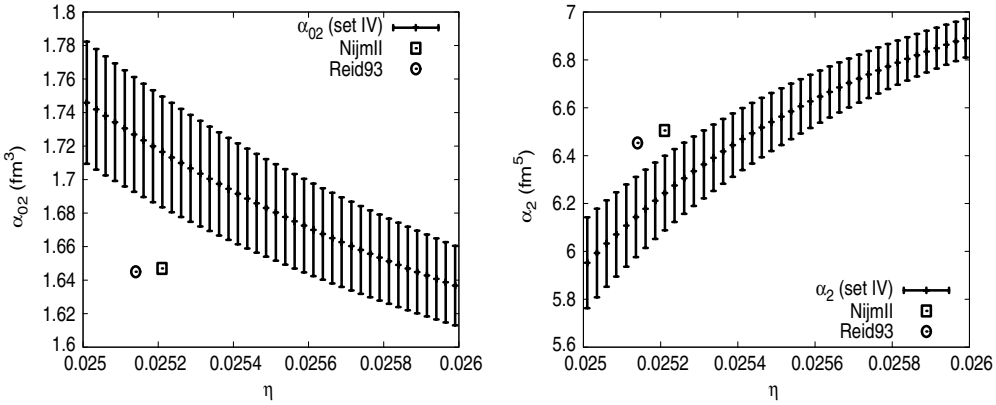

FIG. 8. Dependence of scattering lengths α_{02} (in fm^3) and α_2 (in fm^5) for the TPE potential as a function of η. Boxes represent the Reid93 and Nijm II values determined in Ref. [59]. We used $\alpha_0 = 5.419(7)$ fm to generate the bands, with set IV low energy constants.

well as the orthogonality constraints, yield to

$$\begin{aligned} u_\gamma u'_{k,\alpha} - u'_\gamma u_{k,\alpha} + w_\gamma w'_{k,\alpha} - w'_\gamma u_{k,\alpha}|_{r=r_c} &= 0, \\ u_\gamma u'_{k,\beta} - u'_\gamma u_{k,\beta} + w_\gamma w'_{k,\beta} - w'_\gamma u_{k,\beta}|_{r=r_c} &= 0, \end{aligned} \tag{76}$$

analogous to Eq. (69), to the deuteron wave functions. If orthogonality is applied to the zero energy state, one obtains an explicit relation of δ_1, δ_2, and ϵ with the scattering lengths α_0, α_2, and α_{02} as a direct generalization to the coupled channel case of the one channel singlet case given by Eq. (47). The explicit expressions are rather cumbersome and will not be written down here explicitly. The results are depicted in Fig. 9 for set IV. We observe a clear improvement in the threshold region, in consonance with the low energy parameters of Table III and a moderate improvement over the OPE results in the intermediate energy region. This suggests that finite cutoff effects may also be built into the phase shifts as well as the low energy parameters.

VI. ERROR ANALYSIS AND DETERMINATION OF CHIRAL COUPLINGS FROM LOW ENERGY NN DATA AND THE DEUTERON

A. Propagating experimental errors in c_1, c_3, and c_4.

The results in the previous sections clearly show that deuteron and low energy scattering properties in the $^1S_0$ and $^3S_1$–$^3D_1$ channels are sensitive to finite cutoff effects and also to the values of the chiral constants after removal of the cutoff. We will assume that the values for c_1, c_3, and c_4 are free of uncertainties. Then, set IV provides the best description of triplet data but produces a slightly off value for the effective range in the singlet channel at the 2σ confidence level. Note that in the singlet case, the theoretical prediction for r_0 does not have a large source of error as in the triplet case where uncertainties in η dominate the error. On the contrary, set III provides a compatible value for the effective range in the singlet channel but incompatible values for the triplet channel in A_S and r_0 at the 3–4 σ confidence level on the experimental side. Thus, on this basis we may reject set III and accept set IV.

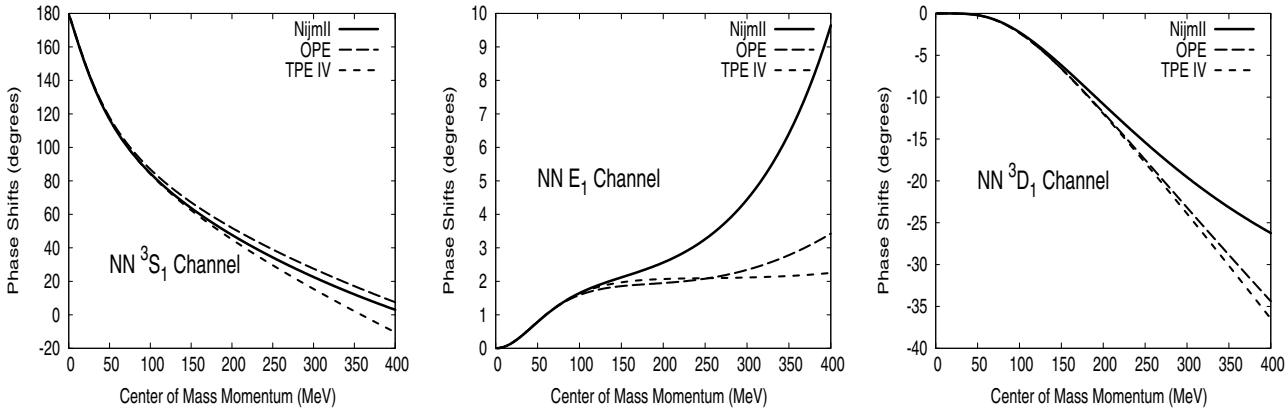

FIG. 9. Renormalized eigenphase shifts for the OPE and TPE potentials as a function of the c.m. np momentum in the triplet $^3S_1$–$^3D_1$ channel compared to the Nijmegen results [43]. The regular scattering wave functions are orthogonal to the regular deuteron bound state wave functions constructed from the OPE with $\gamma = 0.231605$ fm^{-1}, $m = 138.03$ MeV and $g_{\pi NN} = 13.083$ for the OPE contribution to the TPE potential, and $g = 1.26$ for the TPE contribution to the TPE potential. We take set IV (see main text).

To improve on this analysis, let us try to include some errors on the chiral coefficients. The πN analysis of Ref. [31] (set I) and the NN fit of Ref. [11] (set II) yield some errors. Ref. [28] (set IV) does not quote errors, but we will take the educated guess of a 5% error for c_3 and a 30% error for c_4 [60]. We can propagate then by a Monte-Carlo simulation implementing also the errors in $g_{\pi NN} = 13.1 \pm 0.1, \alpha_{0,s} = -23.74 \pm 0.02, \alpha_{0,t} = 5.419 \pm 0.007, \eta = 0.0256 \pm 0.0004$. We assume for simplicity that all these quantities are fully uncorrelated. This will in general enhance the errors, as compared to the case where correlations in c_1, c_3, and c_4 with πN would be taken into account. Perhaps, the best thing would be to consider a simultaneous analysis of both NN and πN low energy data to build in correlations. Obviously, we do not expect good central values for the observables judging from Table III. But there is still the possibility of large error bars.

The outcoming distributions in the low energy and deuteron parameters are somewhat asymmetric. Actually, for a given set of c_1, c_3, and c_4 distributions, we observe the appearance of upper bounds in the ${}^3S_1$ effective range, namely, $r_{0,t} \leqslant 1.79, 1, 75, 1.81$ fm for sets I, II, and IV, respectively, where the outcoming distributions become more dense. The results of the error propagation are summarized in Table IV. Thus, we see that the values of the chiral coefficients deduced from low energy πN [31] are globally inconsistent, at the 1σ level, with the low energy NN threshold parameters after uncertainties are taken into account. The same remark applies to set II [11]. Again, the loss of predictive power becomes manifest for all the sets, although set IV provides the best central values and the smallest errors. The situation for the quadrupole moment is noteworthy since the difference to the potential value is attributed to meson exchange currents (MECs) and relativistic effects, which provide a correction of about 0.01 fm^2 (see Ref. [25] in Ref. [19] and also Ref. [57]). As we see, this is about the size of the error deduced from our analysis. In the case of the deuteron matter radius, the situation is even worse since MEC contributions are much smaller 0.003 fm [57] while our predicted errors are larger. It would be extremely interesting to reanalyze the problem with the present deuteron wave functions [61].

TABLE IV. Singlet ${}^1S_0$ and triplet ${}^3S_1$–${}^3D_1$ scattering and deuteron properties with error estimates using the chiral TPE potential. We make a Monte Carlo calculation of the input parameters $g_{\pi NN} = 13.1 \pm 0.1, \alpha_{0,s} = -23.77 \pm 0.05, \alpha_{0,t} = 5.419 \pm 0.007, \eta = 0.0256 \pm 0.0004$, and the chiral constants c_1, c_3, and c_4. The quoted values span an interval where 68% of the output is contained.

	Set I	Set II	Set IV	Exp.
c_1	$-0.81(15)$	$-0.76(7)$	-0.81	
c_3	$-4.69(1.34)$	$-5.08(24)$	$-3.20(16)$	
c_4	$3.40(4)$	$4.78(10)$	$5.40(1.65)$	
$r_{0,s}$	$2.92^{+0.08}_{-0.04}$	$2.97^{+0.03}_{-0.02}$	$2.86^{+0.04}_{-0.03}$	2.77 ± 0.05
$r_{0,t}$	$1.36^{+0.33}_{-0.75}$	$1.48^{+0.14}_{-0.25}$	$1.76^{+0.03}_{-0.06}$	1.753 ± 0.008
A_s	$0.899^{+0.008}_{-0.009}$	$0.900^{+0.003}_{-0.004}$	$0.884^{+0.005}_{-0.008}$	0.8849 ± 0.0009
Q_d	$0.284^{+0.005}_{-0.007}$	$0.284^{+0.005}_{-0.004}$	$0.276^{+0.004}_{-0.004}$	0.2859 ± 0.0003
r_m	$1.998^{+0.015}_{-0.019}$	$1.998^{+0.007}_{-0.007}$	$1.965^{+0.011}_{-0.014}$	1.971 ± 0.006
P_d	$6.6^{1.0}_{-0.9}$	$7.1^{+0.9}_{-0.9}$	$8.3^{+1.4}_{-1.5}$	—
α_{02}	$2.26^{+0.51}_{-0.39}$	$2.20^{+0.23}_{-0.16}$	$1.67^{+0.13}_{-0.13}$	—
α_2	$3.6^{+3.3}_{-6.9}$	$4.0^{+1.6}_{-2.9}$	$6.71^{+0.48}_{-0.83}$	—

B. Determination of c_1, c_3, and c_4.

Another possibility is to attempt a direct fit to the data. The standard approach is to fit the partial waves to a NN database [43,44]. The problem with such an approach is that, unfortunately, there is no error assignment on the phase shifts, and hence a reliable assessment of errors cannot be made. Actually, besides the work of Ref. [11,21] where a full partial wave analysis was undertaken, other works [23,28,29] assume fixed values for c_1, c_3, and c_4 without attempting any error analysis based on input uncertainties. But even if data for the phase shifts with errors were known, one would expect the quality of the fit to worsen as the energy was increased, because we think that the chiral approach to NN interaction should work best at low energies. If the data were known with uniform uncertainty, one would fit until χ^2/DOF (degrees of freedom) exceeds unity, thus providing an energy window. In such a fit, all points are equally weighted, while we know that the description at low energies, where the theory works best, will be compromised by the highest possible energy within such an energy window.

Along the previous line of reasoning, we propose, instead, to fit directly the low energy threshold parameters for which central values and errors are well known and widely accepted. The basic ingredient is to use purely hadronic information in the process to avoid any contamination due to electromagnetic effects. Specifically, we make a Monte Carlo sampling of the input data assuming that as primary data they are Gaussian distributed and uncorrelated. For any of the samples, we make a χ^2 fit to the values $r_{0,s}, r_{0,t}$, and A_S, i.e., we minimize

$$\chi^2 = \left(\frac{r_{0,s} - r_{0,s}^{\rm exp}}{\Delta r_{0,s}}\right)^2 + \left(\frac{r_{0,t} - r_{0,t}^{\rm exp}}{\Delta r_{0,t}}\right)^2 + \left(\frac{A_S - A_S^{\rm exp}}{\Delta A_S}\right)^2 \tag{77}$$

and then determine the optimal values of c_1, c_3, and c_4. We only accept values where $\chi^2 < 1$, and the resulting distribution of chiral constants c_1, c_3, and c_4 is given in Fig. 10. As we see, there is a very strong, almost linear, correlation between c_3 and c_4. This can be easily understood in terms of the short distance dominance of the singlet effective range, since for the pure van der Waals contribution, and in the limit of large scattering length, $r_{0,s} \sim R = (MC_6)^{1/4}$, with C_6 given in Eq. (34). Deviations from linearity are induced from the larger relative error of $r_{0,s}(1\%)$ as compared to $r_{0,t}$ and A_S (0.1%). This is different from the large scale partial phase-shift analysis obtained in Ref. [21] which found a very small correlation between c_3 and c_4 of about 0.2. We have checked that cutting-off data with decreasing values of χ^2 excludes the points where the distribution is sparse, so that the dense part indeed reflects the uncertainties in the input data. The fact that the three coefficients seem to be on a line is just a consequence

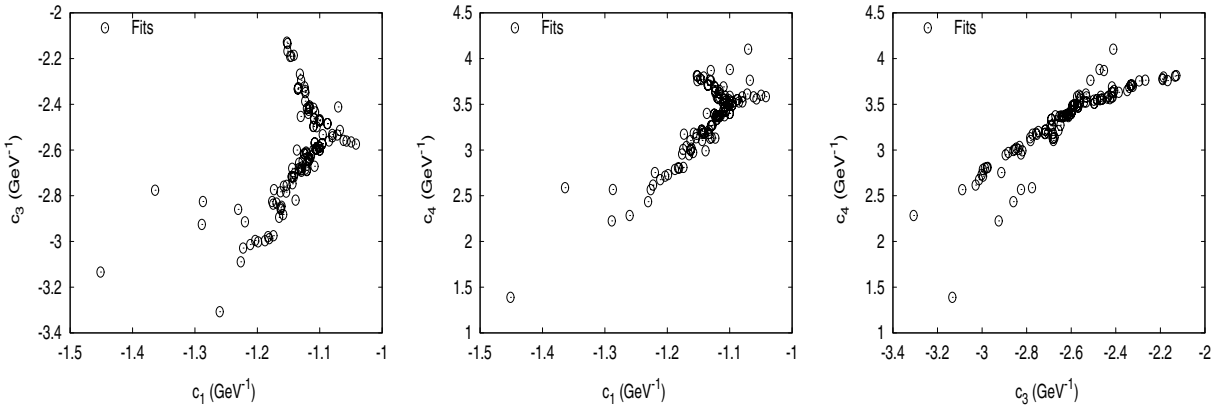

FIG. 10. Correlation plots for the low energy constants c_1, c_3, and c_4 obtained from the renormalized TPE potential by fitting the singlet and triplet effective ranges $r_{0,s} = 2.77 \pm 0.05$ and $r_{0,t} = 1.753 \pm 0.08$ and the deuteron S-wave asymptotic normalization $A_S = 0.8846 \pm 0.0009$. The dispersion in the data reflects the dispersion in all input parameters, $g_{\pi NN} = 13.11 \pm 0.08$, $\alpha_{0,s} = -23.77 \pm 0.05$, $\alpha_{0,t} = 5.419 \pm 0.007$, and $\eta = 0.0256 \pm 0.0004$, which provide $\chi^2 < 1$.

of solving by minimization a system of three equations and three unknowns.

We use $g_{\pi NN} = 13.083$, $\alpha_{0,s} = -23.74 \pm 0.02$, $\alpha_{0,t} = 5.419 \pm 0.007$, $\eta = 0.0256 \pm 0.0004$ and fit c_1, c_3, and c_4 to the values $r_{0,s} = 2.77 \pm 0.05$, $r_{0,t} = 1.753 \pm 0.08$, and $A_S = 0.8846 \pm 0.0009$. Our final result for a sample with 125 points with $\chi^2 < 1$ is

$$\begin{aligned} c_1 &= -1.13^{+0.02}_{-0.04}(\text{stat})\ \text{GeV}^{-1}, \\ c_3 &= -2.60^{+0.18}_{-0.23}(\text{stat})\ \text{GeV}^{-1}, \\ c_4 &= +3.40^{+0.25}_{-0.40}(\text{stat})\ \text{GeV}^{-1}. \end{aligned} \tag{78}$$

The central value is the mean, and the errors were obtained by the standard method of excluding the 16% left and right extreme values of the variables, so as to have a 68% confidence level between the upper and lower values. Cutting-off data with $\chi^2 < 0.5$ does not change significantly the result.

At the 2σ level, our values for c_1, c_3, and c_4 are compatible with the analysis of low energy πN scattering of Ref. [31], $c_1 = -0.81 \pm 0.15$, $c_3 = -4.69 \pm 1.34$, and $c_4 = 3.40 \pm 0.04$, but they are incompatible with the NN full partial wave analyses [11,21] which used an energy-dependent boundary condition at $a = 1.4$ fm. It is difficult to say whether other determinations for the chiral couplings based on NN scattering are incompatible with ours, since no error estimates have been provided.

C. Estimate of the systematic errors

As we have mentioned, any approach based on power counting of the potential cannot make an *a priori* estimate of the accuracy of the calculation. Nevertheless, we can have an idea by simply varying the input parameters.

At LO we may use either $g_A = 1.26$ as input or $g_{\pi NN} = 13.1$, since the difference is the Goldberger-Treiman discrepancy, which should be a higher order correction. The effect can be seen by comparing OPE with OPE* in Table III. When compared to the TPE result, for, e.g., set IV, the error is underestimated this way. At NNLO we use the same procedure in the TPE piece. Again, the difference should be higher orders. Numerically this is equivalent to including $g_{\pi NN} = 13.1 \pm 0.1$ and considering this systematic error as a statistical one, which has already been taken into account.

We can estimate the systematic error in the chiral constants by varying the input used to determine c. To correlate the singlet and triplet channels, we must keep $r_{0,s}$ and $\alpha_{0,s}$. So we can interchange the inputs A_S, $r_{0,t}$ with the outputs r_m, Q_d, α_{02}, and α_2. This yields a total of 15 possible combinations. Another question concerns the assessment of an error to the fitted variables whenever there is no direct experimental quantity, since this choice weights the determination of c. This is the case for α_{02} and α_2, where we make the educated guess of taking the difference between the Reid93 and NijmII values as determined in Ref. [59] as an estimate of the error. The situation with Q_d is a bit special, and we exclude it from the analysis.[17] The results are listed in Table V. We see that this estimate of the systematic error provides a larger fluctuation than the direct propagation of the input errors for c_1. Symmetrizing the errors, we get

$$\begin{aligned} c_1 &= -1.2 \pm 0.2\ (\text{syst})\ \text{GeV}^{-1}, \\ c_3 &= -2.6 \pm 0.1\ (\text{syst})\ \text{GeV}^{-1}, \\ c_4 &= +3.3 \pm 0.1\ (\text{syst})\ \text{GeV}^{-1}. \end{aligned} \tag{79}$$

If we attempt a fit to all observables assigning $\Delta Q_d = 0.01$ fm^2 and $\Delta\alpha_{02} = 0.4$ fm, we get $c_1 = -0.9$, $c_3 = -2.71$, and $c_4 = 3.85$ with a large $\chi^2/\text{DOF} = 3$, basically because of the small errors. Obviously, a more realistic estimate of the errors would be desirable.

[17]The discrepancy of potential models to the experimental value $\sim$0.01 fm^2, attributed to MECs and relativistic effects [57], is about two orders of magnitude larger than the error in the experimental number $\sim$0.0003 fm^2 and the discrepancy between potential models $\sim$0.0004 fm^2. It is not clear whether the discrepancy can be pinned down with similar errors [61].

TABLE V. Central values for the chiral constants c_1, c_3, and c_4 depending on the input. We only include $\chi^2 < 1$.

Fitted	c_1	c_3	c_4	χ^2
$r_{0,s}, A_S, r_{0,t}$	−1.09	−2.61	3.36	0.06
$r_{0,s}, A_S, r_m$	−1.23	−2.57	3.34	0.3
$r_{0,s}, r_{0,t}, r_m$	−1.45	−2.54	3.26	0.2
$r_{0,s}, r_{0,t}, \alpha_2$	−1.09	−2.64	3.17	0.4
$r_{0,s}, r_m, \alpha_2$	−1.03	−2.70	3.26	0.03

VII. THE ROLE OF CHIRAL VAN DER WAALS FORCES

As we have pointed out, our approach is not the conventional one of adding short distance counterterms following a given *a priori* power counting regardless of the approximation in which the long distance potential has been constructed. Instead, the potential power counting dictates the form of the short distance physics by demanding a finite limit when the regulator is removed. In order to stress the differences with previous approaches, it is interesting to see how much of the phase shifts is determined from the short distance chiral potential *without* adding a short-range contribution to the effective range. In the standard approach, this can be achieved by adding a counterterm C_2 in the S-wave channels. In Ref. [41], we showed that both perturbatively and nonperturbatively the orthogonality constraints for the OPE potential imply $C_2 = 0$. Here we will see that the bulk of the S-wave interaction can be explained mainly in terms of the chiral van der Waals force when renormalization is carried out, without any additional short distance contribution or counterterm.

For a pure van der Waals potential of the form

$$U = -\frac{R^4}{r^6}, \tag{80}$$

the zero energy wave function can be analytically computed [47] in terms of Bessel functions $J_\nu(x)$. Normalizing to the asymptotic form $u_0(r) \to 1 - r/\alpha_0$ yields

$$u_0(r) = \Gamma\left(\frac{5}{4}\right)\sqrt{\frac{2r}{R}}J_{\frac{1}{4}}\left(\frac{R^2}{2r^2}\right) - \Gamma\left(\frac{3}{4}\right)\sqrt{\frac{rR}{2}}J_{-\frac{1}{4}}\left(\frac{R^2}{2r^2}\right)\frac{1}{\alpha_0}. \tag{81}$$

The effective range can also be computed analytically [62,63] from Eq. (37) yielding

$$r_0 = \frac{-4R^2}{3\alpha_0} + \frac{4R^3\,\Gamma\left(\frac{3}{4}\right)^2}{3\alpha_0^2\pi} + \frac{16R\,\Gamma\left(\frac{5}{4}\right)^2}{3\pi}, = 1.39473\,R - \frac{1.33333\,R^2}{\alpha_0} + \frac{0.637318\,R^3}{\alpha_0^2}, \tag{82}$$

in agreement with the general low energy theorem of Eq. (39). Taking the values of Table I for $R = (\mathrm{MC}_6)^{1/4}$, one gets in the singlet $^1S_0$ channel

$$\begin{aligned} r_{0,s} &= 2.39811 - \frac{3.9418}{\alpha_{0,s}} + \frac{3.23959}{\alpha_{0,s}^2} \quad \text{(setI)},\\ r_{0,s} &= 2.49192 - \frac{4.25624}{\alpha_{0,s}} + \frac{3.63486}{\alpha_{0,s}^2} \quad \text{(setII)},\\ r_{0,s} &= 2.2227 - \frac{3.8625}{\alpha_{0,s}} + \frac{2.57944}{\alpha_{0,s}^2} \quad \text{(setIII)},\\ r_{0,s} &= 2.29099 - \frac{3.59753}{\alpha_{0,s}} + \frac{2.82459}{\alpha_{0,s}^2} \quad \text{(setIV)}. \end{aligned} \tag{83}$$

The numerical agreement at the 10% level of the $\alpha_{0,s}$ independent term with the full chiral TPE result, Eq. (43), is striking.[18] On the other hand, first-order perturbation theory in the OPE potential yields (see Sec. A of Ref. [41]) in the form of Eq. (39) the result

$$r_{0,s} = \frac{g_{\pi NN}^2}{8M\pi}\left(1 - \frac{8}{3\alpha_{0,s}m} + \frac{2}{\alpha_{0,s}^2m^2}\right), = 1.4369 - \frac{5.4789}{\alpha_{0,s}} + \frac{5.8758}{\alpha_{0,s}^2}. \tag{84}$$

Note that the coefficient in $1/\alpha_{0,s}^2$ is slightly better described by the OPE perturbative value than by the full OPE result [see Eq. (43)], a not unreasonable result since this coefficient is sensitive to the longest range part of the interaction. Likewise, the bulk of the α_0-independent coefficient is given *just* by the most singular contribution to the full chiral potential. As we see, for large scattering lengths, the effective range scales with the van der Waals singlet radius $R_s = (\mathrm{MC}_{6,^1S_0})^{1/4}$ and not with the pion Compton wavelength $1/m$, confirming the dominance of the short distances singularity in the singlet channel.

For the triplet channel, the equation cannot be solved analytically, and the effective range has a correction due to the D-wave [see Eq. (67)]. Moreover, the scattering length is five times smaller than in the singlet case, so that we do not expect in principle such a dramatic agreement. If we neglect the mixing with the D-wave and take the $R_t = (\mathrm{MC}_{6,^3S_1})^{1/4}$ of Eq. (52), we obtain

$$\begin{aligned} r_{0,t} &= 2.50174 - \frac{4.28983}{\alpha_{0,t}} + \frac{3.67797}{\alpha_{0,t}^2} \quad \text{(setI)},\\ r_{0,t} &= 2.58537 - \frac{4.58143}{\alpha_{0,t}} + \frac{4.05928}{\alpha_{0,t}^2} \quad \text{(setII)},\\ r_{0,t} &= 2.35089 - \frac{3.78809}{\alpha_{0,t}} + \frac{3.05196}{\alpha_{0,t}^2} \quad \text{(setIII)},\\ r_{0,t} &= 2.40877 - \frac{3.97691}{\alpha_{0,t}} + \frac{3.28297}{\alpha_{0,t}^2} \quad \text{(setIV)}, \end{aligned} \tag{85}$$

[18]The formula (82) can also be used as a numerical test of the integration method and of the numerical solution of the differential equations. This is a nontrivial condition due to the rapid oscillations of the wave function at the origin. We have checked that it is accurately reproduced.

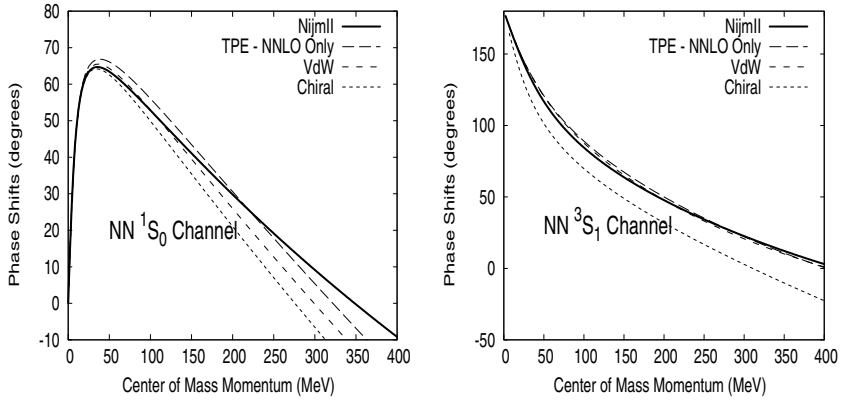

FIG. 11. Renormalized eigenphase shifts in the $^1S_0$ and $^3S_1$–$^3D_1$ channel for the pure chiral van der Waals C_6/r^6 potential (VdW), and the pure NNLO terms compared to the renormalized phase shifts with the same parameters from Table I for set IV. We also show the Nijmegen database [43].

which, using the triplet scattering length value $\alpha_{0,t} = 5.42$, yields $r_{0,t} = 1.83, 1.87, 1.75, 1.78$, respectively, in remarkable agreement with the experimental value. An estimate of the mixing effect can be made by using the largest van der Waals eigenradius $R_+ = (\mathrm{MC}_{6,+})^{\frac{1}{4}}$ obtained by diagonalizing the interaction at short distances. From Table I, Eq. (82), and the experimental value of the scattering length, we get $r_0 = 2.00, 2.07, 1.95, 2.05$ fm for sets I, II, III, and IV, respectively, accounting for about 85% of the full value. Instead, perturbation theory for OPE, Eq. (84), yields $r_0 = 0.62$ fm; and full OPE, $r_0 = 1.64$. Actually, using the relation

$$\mathrm{MC}_{6,^1S_0} - \mathrm{MC}_{6,^3S_1} = R_s^4 - R_t^4 = \frac{3g^2}{64\pi^2 f^4}(4 - 9g^2), \qquad (86)$$

we get an explicit correlation among $\alpha_{0,s}, r_{0,s}, \alpha_{0,t}$, and $r_{0,t}$ regardless of the numerical values of the chiral constants c_3 and c_4. In the range of physical parameters, this looks like a linear correlation (see Fig. 11) between the singlet and triplet effective ranges. For $r_{0,t} = 1.75$, one gets $r_{0,s} = 2.34$.

To check further the dominance of chiral van der Waals interactions, we plot in Fig. 12 the phase shifts for a variety of situations including the pure van der Waals contributions, as well as the contribution of the NNLO only, which reduces to the previous case at short distances but decays exponentially as $\sim e^{-2mr}$ at long distances. The plots confirm, again, our estimations based on the pure van der Waals potential of the effective range for the S waves, and this is the reason why the triplet S wave is better reproduced than the singlet case for set IV. Obviously, by adjusting the effective range and changing the chiral parameters c_3 and c_4 we could obtain a much better description of the data.

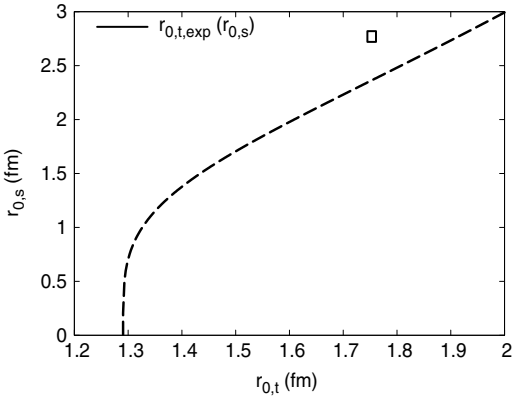

FIG. 12. van der Waals correlation between the singlet and triplet effective ranges using the experimental singlet and triplet scattering lengths. The point represents the experimental values.

The results of this study show that the singularity of the chiral van der Waals force is not a feature that should be avoided, but instead it provides a very simple way to describe the scattering data for the S waves.

Finally, it is interesting to note that central waves based on taking the chiral limit of the potential are less accurately described than the phase shifts obtained from the pure van der Waals contribution. In this limit, the singlet $^1S_0$ channel contains in addition to the van der Waals term a $1/r^5$ contribution stemming from the NLO TPE contribution. The triplet $^3S_1$–$^3D_1$ TPE contribution has a similar structure in addition to the OPE tensor $1/r^3$ singular short distance contribution.

VIII. THE TPE POTENTIAL AT NLO: A MISSING LINK?

In the previous sections, we analyzed the renormalization of the NNLO potential. In this section, we analyze the NLO in the singlet $^1S_0$ and triplet $^3S_1$–$^3D_1$ channels and the problem that arises in the latter. We argue that similar trends are observed in finite cutoff calculations. We also suggest several scenarios of how the problem may be overcome.

A. Convergence in the singlet $^1S_0$ channel

In the singlet $^1S_0$ channel, the potential at short distances behaves as [7,11,12]

$$U_{^1S_0} \to \frac{\mathrm{MC}_{5,^1S_0}}{r^5}, \qquad (87)$$

where

$$\mathrm{MC}_{5,^1S_0} = \frac{M(1 + 10g^2 - 59g^4)}{256\pi^3 f^4}. \qquad (88)$$

The singlet coefficient is negative, and, according to the discussion in Sec. III, one has an undetermined short distance phase which can be fixed by using the scattering length as

TABLE VI. Convergence of threshold parameters of effective range expansion $k\cot\delta = -1/\alpha_0 + r_0k^2/2 + v_2k^4 + v_3k^6 + v_4k^8$ in the singlet $^1S_0$ channel depending on the successive inclusion of terms in the potential $U = U_{\rm LO} + U_{\rm NLO} + U_{\rm NNLO} + \cdots$. LO means LO alone (and taking $g_{\pi NN} = 13.083$ and $g_A = 1.26$), NLO means LO+NLO, and so on. The only input is the scattering length α_0 besides the potential parameters. For the NNLO case, we use set IV for the chiral constants c_1, c_3, and c_4 given in Table I.

$^1S_0$	LO	NLO	NNLO	Exp.	Nijm II
α_0 (fm)	Input	Input	Input	−23.74(2)	−23.73
r_0 (fm)	1.44	2.29	2.86	2.77(5)	2.67
v_2 (fm^3)	−2.11	−1.02	−0.36	–	−0.48
v_3 (fm^5)	9.48	6.09	4.86	–	3.96
v_4 (fm^7)	−51.31	−35.16	−27.64	–	−19.88

input. The effective range in the singlet channel is given by

$$r_0 = 2.122 - \frac{4.889}{\alpha_0} + \frac{5.499}{\alpha_0^2} \qquad \text{(NLO)}, \tag{89}$$

which, compared with the LO and NNLO results in Eq. (43), shows a convergence rate. To show that this trend to convergence is not fortuitous, we display in Table VI the threshold parameters of the effective range expansion $k\cot\delta = -1/\alpha_0 + r_0k^2/2 + v_2k^4 + v_3k^6 + v_4k^8$ depending on the terms kept in the expansion of the potential given by Eq. (1). As we see, there is a clear trend to convergence, although the higher order threshold parameters display a slower convergence rate since they are increasingly sensitive to the shorter range regions. This trend is confirmed in Fig. 13 for the phase shift. Obviously, there is scale separation in the singlet potential; and higher order potentials, although more singular at the origin, yield contributions in the right direction.

B. The problem in the triplet $^3S_1$–$^3D_1$ channel

The triplet $^3S_1$–$^3D_1$ potential at short distances has the behaviour [7,11,12]

$$\begin{aligned} U_{^3S_1}(r) &\to \frac{\mathrm{MC}_{5,^3S_1}}{r^5}, \\ U_{E_1}(r) &\to \frac{\mathrm{MC}_{5,E_1}}{r^5}, \\ U_{^3D_1}(r) &\to \frac{\mathrm{MC}_{5,^3D_1}}{r^5}, \end{aligned} \tag{90}$$

where

$$\begin{aligned} \mathrm{MC}_{5,^3S_1} &= \frac{3M(-1-10g^2+27g^4)}{256\pi^3 f^4}, \\ \mathrm{MC}_{5,E_1} &= -\frac{15Mg^4}{64\sqrt{2}\pi^3 f^4}, \\ \mathrm{MC}_{5,^3D_1} &= \frac{3M(-1-10g^2+37g^4)}{256\pi^3 f^4}, \end{aligned} \tag{91}$$

On the other hand, the diagonalized triplet coefficients are

$$\begin{aligned} \mathrm{MC}_{5,+} &= \frac{3M(-1-10g^2+17g^4)}{256\pi^3 f^4}, \\ \mathrm{MC}_{5,-} &= \frac{3M(-1-10g^2+47g^4)}{256\pi^3 f^4}, \end{aligned} \tag{92}$$

and the mixing angle is given by $\tan\theta = \sqrt{2}$, differing by $-\pi$ from the OPE case [41]. For $0.5356 < g < 0.8217$, one would have an attractive-repulsive situation (see Sec. III), as in the OPE case [41]; and in such a case, one could take either the deuteron binding energy or the $^3S_1$ scattering length. However, for the physical value $g = 1.26$, one has two short distance repulsive eigenchannels, and hence one must take the exponentially decaying regular solutions at the origin. Let us recall that according to Sec. III, *finite renormalized results can only be obtained by precisely choosing the regular solution at the origin*. In this case, there are no short distance phases, and the scattering lengths, as well as the phase shifts, are completely determined from the potential. The (finite) renormalized results are depicted in Fig. 13. As we see, the singlet $^1S_0$ phase shift shows a very reasonable trend, since NLO improves on the LO, and it is improved by the NNLO potential. We recall that in the three cases, the scattering length is exactly the same. However, not completely unexpectedly, the triplet channel results worsen the LO ones. In the next subsection, we show that demanding the standard Weinberg counting requires the irregular solution at the origin, hence yielding to divergent renormalized results.

C. Finite cutoffs and the Weinberg counting

The special status of the NLO calculation as compared with the LO and NNLO ones has been recognized in previous studies in momentum space [10] where regularization was implemented by using a sharp cutoff Λ. As noted by these authors, the allowed cutoff variations at NLO are *smaller* (∼380–600 MeV) than at LO (∼700–800 MeV) or NNLO (∼800–1000), but the reasons have not been made clear. Let us focus on the triplet $^3S_1$–$^3D_1$ channel. Within our coordinate space renormalization scheme, this trend can be easily understood. At LO, one fixes only one parameter, say α_0, and because one has attractive and repulsive potentials at short distances, the system will naturally be driven into the exponential regular solution at the origin. Obviously, if one would fix some other parameter independently, say r_0 (or equivalently using a counterterm C_2), and not the one predicted by the regular solutions, one would be driven instead to the irregular solution and not be allowed to remove the cutoff in practice. In such a situation, one would be forced to keep the cutoff finite at the scale where the repulsive core sets in. However, at LO the Weinberg power counting does not allow one to fix this additional parameter and one can comfortably reach higher cutoff values. On the contrary, at NLO one has two repulsive eigenpotentials, and one cannot fix any low energy parameter arbitrarily. Otherwise, one would be attracted to the irregular solutions at short distances. On the other hand, they are attractive at long distances, so

that one would expect a stability region where the potential becomes flat before turning into a repulsive core in both eigenchannels. This is exactly what one observes in the NLO calculation of Ref. [10]. The occurrence of such a plateau is to some extent fortuitous since it is associated with the critical points of the potential and not with some *a priori* estimate of the validity range of the NLO potential. Finally, in the NNLO calculation, because both eigenpotentials have an attractive character, one can again increase the cutoff since there are no irregular solutions in the problem to which one can be attracted. It is very rewarding that our coordinate space analysis of short distance singularities anticipates when these features can be expected. On the other hand, this does not imply that finite cutoff calculations are necessarily wrong, but simply that the observed features when the cutoff approaches the limit can be understood and, moreover, that the cutoff becomes a crucial parameter if one insists on finiteness.

The previous discussion can be illustrated in our approach by looking at the short distance cutoff dependence of the effective range r_0 (in fm) and the deuteron wave function renormalization A_S (in fm$^{-1/2}$), in the triplet $^3S_1$–$^3D_1$ channel at LO, NLO, and NNLO in the standard Weinberg counting, as presented in Fig. 14. As described in Sec. III C, any counterterms can be mapped into a given renormalization condition. Once these conditions are fixed, we can ask whether other properties are finite. Thus, at LO we fix the deuteron binding energy (one counterterm), at NLO and NNLO we fix the deuteron binding energy, the asymptotic D/S mixing η, and the scattering length α_0 (three counterterms). In all cases, it is clear that by lowering the cutoff at LO and NNLO of the approximation, one nicely approaches the experimental values. This raises immediately the question of whether there is a given value of the cutoff at which NLO improves over LO. As we see, such a region does not exist. In addition, although there is a nice clear trend in both LO and NNLO for distances below 0.5 fm for A_S down to the origin, this is not so at NLO. So, in this case, it is not true that low energy properties are independent of short distance details, in contrast to the standard EFT wisdom. Moreover, Fig. 14 shows explicitly the conflict between the Weinberg counting and the remotion of the cutoff at NLO because r_0 and A_S diverge as a result of the onset of the irregular solution, as anticipated in our study of short distance solutions (see Sec. III). We have checked that this is a general feature on both deuteron and scattering properties. On the contrary, LO and NNLO have a rather smooth limit because in these two cases, Weinberg power counting on the short distance counterterms turns out to be compatible with the choice of the regular solution at the origin. Thus, *in the $^3S_1$–$^3D_1$ channel, the renormalized solution at NLO in the Weinberg counting is divergent, while LO and NNLO are convergent*. In conclusion, the present analysis shows in a somewhat complementary manner as done in Sec. VIII B that indeed the NLO is problematic, at least nonperturbatively. In Sec. IX, we will see that the problem is not solved if the NLO contribution is computed within a perturbative framework using the exact OPE distorted wave basis as a lowest order approximation.

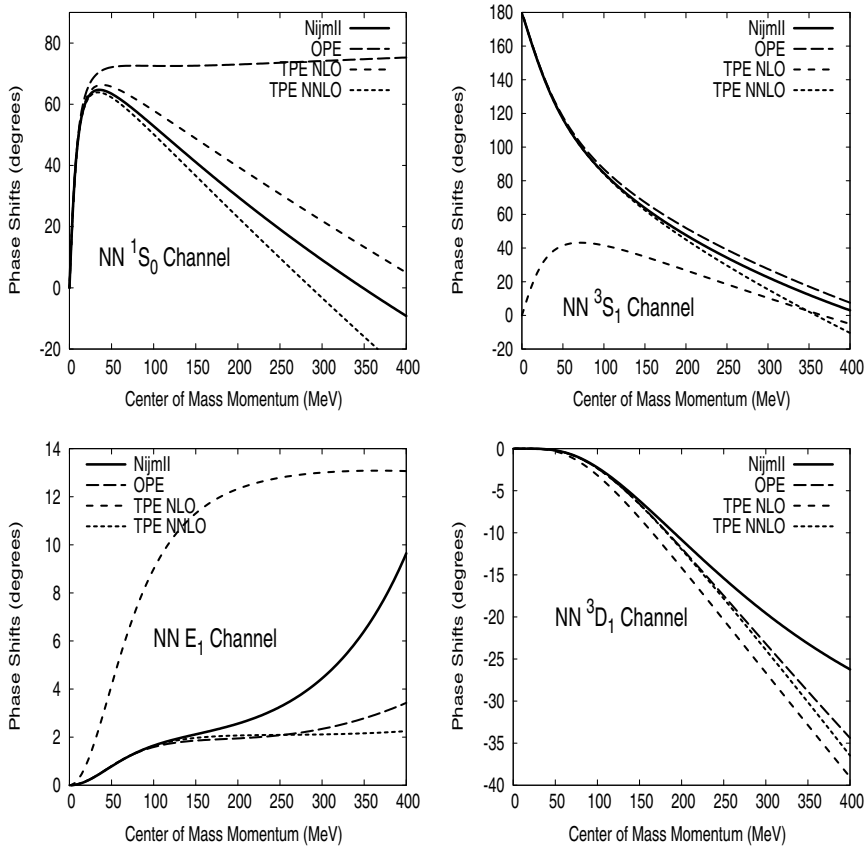

FIG. 13. Renormalized eigenphase shifts at LO, NLO, and NNLO as a function of the c.m. np momentum k in the singlet $^1S_0$ and triplet $^3S_1$–$^3D_1$ channels compared to the Nijmegen results [43] for different parameter sets.

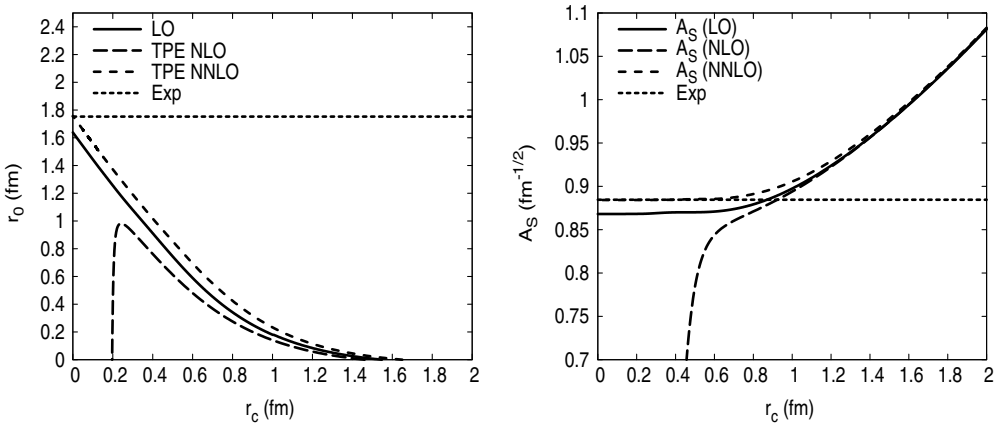

FIG. 14. Cutoff dependence of the effective range r_0 (in fm) and the deuteron wave function renormalization A_S (in fm$^{-1/2}$), in the triplet $^3S_1$–$^3D_1$ channel at LO, NLO, and NNLO in the Weinberg counting. At LO, we fix the deuteron binding energy (one counterterm); at NLO and NNLO, we fix the deuteron binding energy, the asymptotic D/S mixing η, and the scattering length α_0 (three counterterms). We use set IV of chiral coupling constants.

D. The roles of relativity and Δ resonance in the renormalization problem

The requirement of renormalizability may be regarded as a radical step, and renormalized LO calculations demand the violation of dimensional power counting on the counterterms [42] in noncentral waves such as $^3P_0$, because of an attractive $1/r^3$ singularity. To reach a finite limit, the authors of Ref. [42] propose to promote counterterms that are of higher order in Weinberg's power counting. However, it is intriguing that in their proposal they choose to promote just one counterterm in coupled channels, while they could have used a coupled channel counterterm, i.e., three counterterms in total. In the boundary condition approach, we know from the start how many independent parameters must be *exactly* taken to reach a finite and unique limit; the reference to power counting is only specified at the level of the potential. Note that the power counting in the potential fixes its short attractive-repulsive singular character, and this is the origin of the conflict of assuming an *a priori* power counting for the counterterms. Finiteness requires not only that some forbidden counterterms must be allowed (promoted) [42] but also that some allowed counterterms must be forbidden (demoted). In such a framework, our NLO calculations in the $^3S_1$–$^3D_1$ channel lead to finite but nonsensical results thanks to the repulsive-repulsive $1/r^5$ singularity (see Sec. VIII). On the other hand, if one fixes the scattering length as required by the power counting, the limit does not exist because one is driven to the exponentially diverging solution at the origin [for instance, Eq. (67) gives $r_0 \to -\infty$]. How then can we reconcile finiteness with fixing of the parameters?. As we pointed out already, the singular short distance behavior of the chiral potential is in fact a long distance feature which changes dramatically when changing the long distance physics. Actually, one may reverse the argument and use renormalizability as a selective criterion for admissible long distance potentials. In the following, we want to provide at least two possible scenarios for how this might happen, i.e., how modifying the potential at long distances by introducing physically relevant information changes the short distance behavior of the potential.

In the first place, the chiral potential, Eq. (1), was derived in the heavy baryon expansion. The short distance character may change when such a limit is not taken, since the combination Mr does make the order of limits ambiguous. A proper treatment of relativistic effects requires the inclusion of antinucleons in loops, and a satisfactory EFT treatment of relativistic effects remains a challenging open problem because of the nonperturbative divorce of the standard crossing vs unitarity. Further more, one should use a satisfactory relativistic two-body equation, which necessarily makes the problem fully nonlocal in coordinate space. Nevertheless, there exist "relativistic" potentials, where *some* of the terms of higher power in $1/M$ than the TPE obtained in heavy baryon ChPT are kept [25–27], which have $1/r^7$ van der Waals short distance behavior with attractive-repulsive eigenpotentials [64]; this means that as in the OPE case, there is one free parameter. A calculation using these incomplete relativistic potentials will be presented elsewhere [65].

A second scenario is related to the role played by the Δ resonance, [19] which is not included in the present analysis. As pointed out in Ref. [8], the Δ provides the bulk of the chiral constants, yielding $-c_3 = 2c_4 = g_A^2/2\Delta$, with $\Delta = 293$ MeV the nucleon-delta mass splitting, yielding $c_3 = -2.7$ GeV^1 and $c_4 = 1.35$ GeV^{-1}. The difference in the parameters of Ref. [20] may be due to some other resonances. On the other hand, in terms of scales, one has $\Delta \sim 2m_\pi$, which might be regarded as a small parameter. This obviously does not mean that Δ vanishes in the chiral limit. In the standard chiral counting of the potential, Eq. (1), the combinations $\bar{c}_1 = Mc_1, \bar{c}_3 = Mc_3$, and $\bar{c}_4 = Mc_4$ are considered to be zeroth order, but according to the previous argument they could be regarded to be enhanced by one negative power.

[19] We thank D. Phillips for drawing our attention to this point.

Thus, the nominally NNLO terms containing c_3 and c_4 might become NLO contributions, thereby changing the repulsive-repulsive $1/r^5$ singularity into an attractive-attractive $1/r^6$ one. On the other hand, the c_3 and c_4 contributions of the standard NNLO dominate the short distance van der Waals contributions. Actually, much of the NNLO potential is built from these terms all over the range. According to this reasoning, our NNLO calculation may be closer to an NLO one where the $N\Delta$ splitting is regarded as a small parameter. In fact, taking NLO+Δ with $-c_3 = 2c_4 = g_A^2/2\Delta$ and $\eta = 0.0256$, one gets $A_S = 0.8869\,\mathrm{fm}^{-1/2}$, $Q_D = 0.2762\,\mathrm{fm}^2$, $r_m = 1.9726\,\mathrm{fm}$, and $P_d = 0.06$ in overall agreement with Table III. It would be rather interesting to look for further consequences of this Δ counting at higher orders. The importance of the Δ in the NN problem has been stressed already in several works on power counting grounds [3,4,10,66], but the crucial role played in the renormalization problem, i.e., the fact that the cutoff can be completely removed, has not been recognized. Our discussion suggests that the momentum space cutoff could also be comfortably removed in this Δ counting, unlike the Δ-less NLO.

The two possible scenarios outlined above do not prove that the requirement of renormalizability is necessarily right, but they do suggest that looking into the short distance singular behavior of long distance chiral potentials, together with the mathematical requirement of finiteness, may provide a significant physical insight into the NN problem. In the language of Ref. [42], which stressed the promotion of counterterms on the basis of the renormalizability requirement, we are perhaps led also to the demotion of counterterms (as for relativistic potentials), or alternatively to the promotion of terms in the potential (as in the Δ counting described above).

E. Van der Waals forces, the molecular analogy, and the chiral quark model

The previous arguments show that it is possible to change the attractive/repulsive character of the potential at short distances by organizing the calculation of the potential in a different manner, but does not give a clue as to why this actually happens. Remarkably, the analogy with atomic neutral systems subjected to van der Waals forces illustrated in Sec. VII goes farther and provides valuable insight into the problem. In low energy molecular physics where one works in a Born-Oppenheimer approximation, all atomic constituents, electrons, and nuclei interact through the Coulomb force arising from one photon exchange. At long distances between distant electrons, the potential is a dipole-dipole interaction, that is,

$$V_{\mathrm{dip}}(R) = e^2 \sum_{A,B} \left[\frac{\vec{r}_A \cdot \vec{r}_B}{R^3} - 3\frac{(\vec{r}_A \cdot \vec{R})(\vec{r}_B \cdot \vec{R})}{R^5} \right], \quad (93)$$

where the sum runs over electrons belonging to different atoms. In second-order perturbation theory, the atom-atom energy at a separation distance R reads

$$V_{AA} = \langle AA|V_{\mathrm{dip}}|AA\rangle + \sum_{AA \neq A^*A^*} \frac{|\langle AA|V_{\mathrm{dip}}|A^*A^*\rangle|^2}{E_{AA} - E_{A^*A^*}} + \cdots, \quad (94)$$

where $|AA\rangle$ and $|A^*A^*\rangle$ are the electron wave functions corresponding to a pair of separated clusters in their atomic ground state and excited states, respectively. The first-order contribution vanishes for atoms with no permanent dipole moment. The mutual electric polarization causes the van der Waals interaction between the two atoms, C_6/R^6 and, because it is second-order perturbation theory, it is obvious that the C_6 contribution to the potential will always be attractive. However, it is not clear that higher order terms would always be attractive. It is remarkable that the theorem of Thirring and Lieb [67] establishes that the Coulomb force between constituents implies that all terms in the expansion are attractive, without appealing to the dipole approximation. Thus, according to this result, the long distance force will always be singular and attractive at short distances, and that is exactly what one needs. In such a situation, making a long distance expansion of the potential, $U = -R_6^4/r^6 - R_8^6/r^8 + \cdots$ and computing the scattering phase shifts by always fixing the same scattering length, along the lines pursued in this paper, makes much sense. Moreover, one expects the results for the phase shifts to be convergent if there is scale separation between the corresponding van der Waals radii $R_6 \gg R_8 \gg \cdots$. Our experience with several atomic systems confirms these expectations [68].

The argument in the NN system is a straightforward generalization of the molecular system above. It is well known that there are no color hidden states between color neutral systems, so that at long distances one may assume only the exchange of colorless objects. The longest range object will be the pion, and the mutual (chiral) polarizability will cause attraction between the nucleons, exactly in the same way as for atom-atom interactions. If we use as an example the chiral quark model, assuming for simplicity nonrelativistic constituent quarks, one obtains the OPE for quarks. To second-order perturbation theory, we get the NN potential in the Born-Oppenheimer approximation

$$V_{NN} = \langle NN|V_{\mathrm{OPE}}|NN\rangle + \sum_{HH \neq NN} \frac{|\langle NN|V_{\mathrm{OPE}}|HH\rangle|^2}{E_{NN} - E_{HH}} + \cdots, \quad (95)$$

where V_{NN} represents the potential in the NN operator basis. This yields *exactly* when $HH = N\Delta$ the results found in Ref. [3,4,8] and naturally explains why the contribution from one Δ intermediate state is attractive at short distances. Although this analogy with molecular systems is very suggestive, the generalization to all orders along the lines of the Lieb-Thirring theorem within a QCD context remains at present an optimistic speculation.

IX. RENORMALIZED PERTURBATION THEORY VERSUS NONINTEGER POWER COUNTING

A. Perturbations on boundary conditions

In all our calculations, we have taken a long distance potential calculated perturbatively and have computed the scattering amplitudes nonperturbatively by fully iterating a potential computed in perturbation theory, as initially suggested by Weinberg [1]. We will call this form of solution nonperturbative for brevity. This requires a nonperturbative treatment of the renormalization problem, which naturally implies that the short distance renormalization conditions (or counterterms) are determined by the most singular contribution of the long distance potential at the origin. [20] For the NN chiral potential, it turns out that the higher the order the more singular the potential. As a consequence, we have seen in Sec. VIII C that, for instance, Weinberg counting at NLO in the ${}^3S_1$–${}^3D_1$ channel is incompatible with renormalization and finiteness because of the short distance repulsive character of the NLO potential. Although naively this looks counterintuitive, it is important to realize that there are also situations, such as LO and NNLO, where the regularity condition of the wave function conspires against the singularity so that the net effect is well behaved in the scattering amplitudes and deuteron properties. Our results in Secs. IV and V suggest that the pattern obtained when comparing LO and NNLO looks quite converging numerically, although there appears to be no way of making an *a priori* estimate of the corrections.

Perturbative treatments might circumvent this difficulty since they have the indubitable benefit of allowing an *a priori* estimate of the systematic error via dimensional power counting. This causes no problem in the calculation of the long distance potential. However, we anticipate already that singular potentials are indeed singular perturbations, and power counting may not work as one naively expects for the full amplitudes. Kaplan, Savage, and Wise [69,70] suggested such a perturbative scheme some years ago, where the lower order approximation was a contact theory, while OPE and higher order corrections could be computed in perturbation theory. This is equivalent to considering mM/f^2 to be first order and m^2/f^2 second order, so that a calculation involving the chiral constants would be N^{3}LO in that counting. Unfortunately, the expansion turned out to be nonconverging at NNLO [71]. In our coordinate space formulation, this approach corresponds to assuming for the S waves a boundary condition fixing the scattering length α_0 [41] (see Appendix A of that work) and making long distance potential perturbations. In our previous work, we verified that perturbation theory could only account for a contribution to the deuteron and ${}^3S_1$–${}^3D_1$ scattering observables at first order. Unfortunately, the second order was divergent, while nonperturbatively, i.e., exactly solving the Schrödinger equation for the OPE potential, the results were not only finite but also numerically quite close to experiment. This deserves some explanation. In Fig. 15 we show the results in the deuteron channel when we scale the OPE potential $U_{\rm OPE} \to \lambda U_{\rm OPE}$ for the S-wave function normalization $A_S(\lambda)$ and the effective range $r_0(\lambda)$ as a function of the scaling parameter λ by keeping the deuteron binding energy fixed to its experimental value. The nonperturbative result is compared with the first-order perturbation theory used in Ref. [41]. Clearly, perturbation theory fails even for weak coupling. The experimental value for r_0 could be obtained by adding a counterterm C_2 as done by Kaplan, Savage, and Wise [69,70]. A nonvanishing C_2 not only violates the orthogonality of the zero energy and deuteron wave functions for a long distance local potential but also introduces a new parameter, reducing the predictive power. Moreover, the nonperturbative inclusion of this C_2 counterterm with the OPE potential yields divergent results (see the discussion in Sec. VIII C). In fact, much of the strength of C_2 is naturally provided by the short distance $1/r^3$ singularity of the OPE potential.

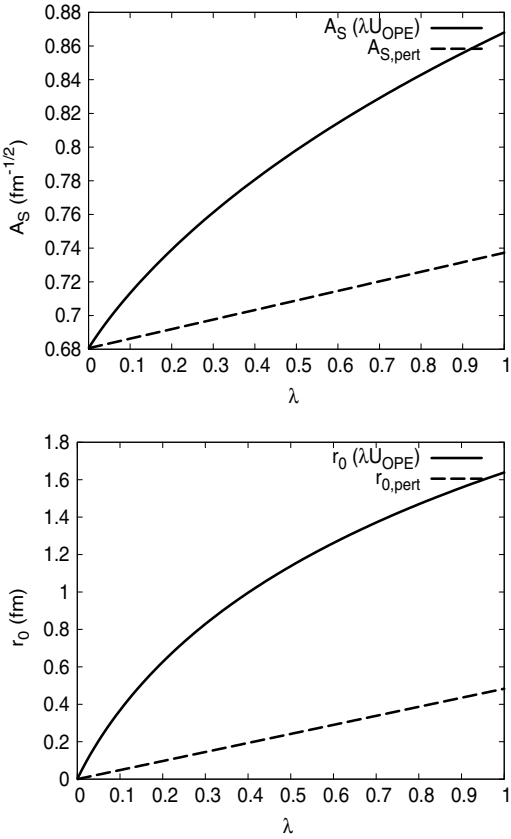

FIG. 15. Dependence of the S-wave function normalization $A_S(\lambda)$ in the deuteron and the effective range $r_0(\lambda)$ in the ${}^3S_1$–${}^3D_1$ channel when one scales the OPE potential $U_{\rm LO} \to \lambda U_{\rm LO}$. In all cases, we fix the deuteron binding energy to its experimental value.

B. Perturbations of the OPE potential

Recently, Nogga, Timmermans, and van Kolck (NTvK) [42] suggested treating the OPE effects nonperturbatively, i.e., to all orders, while TPE and higher as well as Δ contributions should be computed in perturbation theory (see also Refs. [56,72,73] for related ideas). In this section, we analyze

[20] It should be stressed here that we are using nonorthodox renormalization techniques, which do not find an obvious translation with the standard EFT.

such a proposal disregarding the Δ. Our main conclusions will not change, although numbers could be modified. In such a situation, the perturbative expansion is equivalent to considering the $mM/(4\pi f^2)$ to be zeroth order while $m^2/(4\pi f)^2$ is taken to be second order and m/M is first order, so that the potential can be written as

$$\begin{aligned} U^{(0)} &= U^{(0)}_{1\pi}, \\ U^{(2)} &= U^{(2)}_{1\pi} + U^{(2)}_{2\pi}, \\ U^{(3)} &= U^{(3)}_{1\pi} + U^{(3)}_{2\pi}. \end{aligned} \tag{96}$$

Nonperturbatively, $U_{1\pi} = U^{(0)}_{1\pi} + U^{(0)}_{2\pi} + U^{(0)}_{3\pi} + \cdots$ amounts to taking $g_{\pi NN} = 13.1$ in the OPE piece, hence accounting for the Goldberger-Treiman discrepancy. In perturbation theory, we must take $U^{(0)}_{1\pi}$ with $g_A = 1.26$ and include OPE corrections to higher order. Note that the missing first order implies substantial simplification in the perturbative treatment. Indeed, NNLO can be done within first-order perturbation theory since going to second-order perturbation theory considers $U^{(2)^2}$ which is N^{3}LO. In the remainder of this section, we analyze some aspects of such proposal by scaling the strength of the perturbation and show that the appearance of nonanalytical behavior is intrinsic to singular potentials, yielding to perturbative divergences. As we will see, finite perturbative calculations, including chiral TPE to NNLO, would require four counterterms for the singlet $^1S_0$ and six counterterms for the triplet $^3S_1$–$^3D_1$ channel. Our nonperturbative results, i.e., fully iterated NNLO potentials, are based on just one and three counterterms, respectively.

C. Singlet $^1S_0$ channel in distorted OPE waves

Let us examine first the $^1S_0$ channel and consider the effect of the NLO and NNLO TPE potentials on top of the LO OPE potential in long distance perturbation theory. The fact that they are taken second and third order, respectively, means that the effect will be additive at NNLO in the scattering properties. For the total potential in Eq. (96), we write the wave function as

$$u_k(r) = u^{(0)}_k(r) + u^{(2)}_k(r) + u^{(3)}_k(r) + \cdots, \tag{97}$$

and the phase shift becomes

$$\delta_0 = \delta^{(0)}_0 + \delta^{(2)}_0 + \delta^{(3)}_0 + \cdots. \tag{98}$$

At LO, the scattering length $\alpha^{(0)}_0$ is a free parameter which we fix to the physical value, $\alpha^{(0)}_0 = \alpha_0$. As we did in our nonperturbative treatment in Sec. VIII A, we will keep the scattering length fixed to its experimental value at any order of the approximation, so that differences may be only attributable to the potential. In the normalization of Eq. (44), the correction to the phase shift is just given by

$$\delta^{(2)}_0 = -k \sin^2 \delta^{(0)}_0 \int_{r_c}^{\infty} U^{(2)}(r) u^{(0)}_k(r)^2 dr, \tag{99}$$

and a similar expression for $\delta^{(3)}_0$ which can be deduced by the standard Lagrange identity. Here, a short distance cutoff r_c has been assumed because at short distances the NLO potential diverges as $U_{\rm NLO} \sim 1/r^5$. The previous formula yields a change also in the scattering length, so that we may eliminate the cutoff radius by subtracting off the zero energy contribution by fixing $\alpha^{(2)}_0 = 0$. It is convenient to recast the result in the form of an effective range expansion in the OPE distorted wave basis,

$$\begin{aligned} k \cot \delta_0 + \frac{1}{\alpha_0} = k \cot \delta^{(0)}_0 + \frac{1}{\alpha^{(0)}_0} \\ + \int_{r_c}^{\infty} dr U^{(2)}(r) \left[u^{(0)}_k(r)^2 - u^{(0)}_0(r)^2 \right] \\ + \int_{r_c}^{\infty} dr U^{(3)}(r) \left[u^{(0)}_k(r)^2 - u^{(0)}_0(r)^2 \right], \end{aligned} \tag{100}$$

which guarantees $\alpha^{(2)}_0 = \alpha^{(3)}_0 = 0$, due to the one subtraction. If we expand in powers of the energy the LO wave function we get

$$u^{(0)}_k(r) = u^{(0)}_0(r) + k^2 u^{(0)}_2(r) + k^4 u^{(0)}_4(r) + \cdots. \tag{101}$$

where

$$\begin{aligned} -u^{(0)\prime\prime}_0(r) + U(r) u^{(0)}_0(r) &= 0, \\ -u^{(0)\prime\prime}_2(r) + U(r) u^{(0)}_2(r) &= u^{(0)}_0(r), \\ -u^{(0)\prime\prime}_4(r) + U(r) u^{(0)}_4(r) &= u^{(0)}_2(r), \end{aligned} \tag{102}$$

and so on. These equations can be solved recursively. Thus, the NLO correction to the effective range is given by

$$r^{(2)}_0 = 4 \int_{r_c}^{\infty} U^{(2)}(r) u^{(0)}_2(r) u^{(0)}_0(r) dr. \tag{103}$$

To estimate the short distance contribution, we use the OPE exchange potential in the form $U_{\rm LO} = -e^{-mr}/(R_s r)$, with $R_s = 16 f^2 \pi / g^2 m^2 M$ the characteristic length $^1S_0$-channel scale. Note that the OPE potential in the $^1S_0$ channel is Coulomb-like at short distances for which the complete regular plus irregular solution is known. One could then use a short distance expansion of the general analytical Coulomb solution. This facilitates guessing the solution at short distances for the zeroth energy wave function. The higher energy wave functions can be computed straightforwardly, yielding for $r \to 0$

$$\begin{aligned} u^{(0)}_0(r) &\sim c_0 \left[1 + mr - \frac{3r}{2R_s} - \frac{r}{R_s} \log\left(\frac{r}{R_s} \right) \right] + c_1 r, \\ u^{(0)}_2(r) &\sim -c_0 r R_s + \mathcal{O}(r^3), \\ u^{(0)}_4(r) &\sim \frac{1}{3!} c_0 r^3 R_s + \mathcal{O}(r^5), \\ u^{(0)}_6(r) &\sim -\frac{1}{5!} c_0 r^5 R_s + \mathcal{O}(r^7), \\ u^{(0)}_8(r) &\sim \frac{1}{7!} c_0 r^7 R_s + \mathcal{O}(r^9), \end{aligned} \tag{104}$$

as can be readily checked by solving the Schrödinger equation in powers of energy, Eq. (102). The coefficients c_1 and c_0 correspond to the linearly independent regular and irregular solutions, respectively, and are determined by matching to the integrated in asymptotic condition $u^{(0)}_0(r) \to 1 - r/\alpha_0$ at large

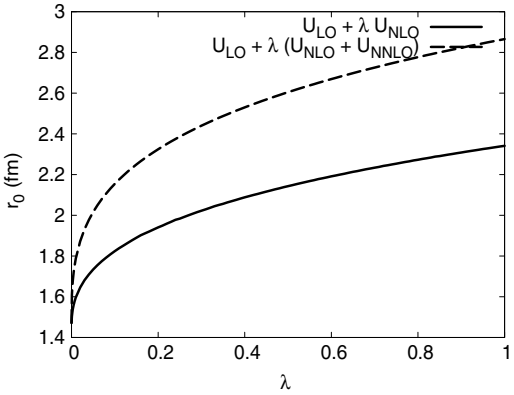

FIG. 16. Dependence of the effective range $r_0(\lambda)$ in the $^1S_0$ channel when the scaled potentials $U = U_{\rm LO} + \lambda U_{\rm NLO}$ and $U = U_{\rm LO} + \lambda(U_{\rm NLO} + U_{\rm NNLO})$ are considered. In all cases, we fix the scattering length to its experimental value.

distances and at zero energy. Obviously, the irregular solution contributes, $c_0 \neq 0$, because α_0 is taken to be independent of the potential, and hence terms proportional to the coefficient c_1 are subleading. Thus, we get

$$r_0^{(2)} \sim 4 \int_{r_c} dr \frac{\mathrm{MC}_5}{r^5}(-c_0^2 R_s) r. \tag{105}$$

Thus, we conclude that the first-order perturbative result is badly divergent. This is very puzzling, since the nonperturbative calculation in Sec. VIII A yields a finite number [see Eq. (89)], and suggests nonanalytical dependence on the coupling constant. To enlighten the situation, let us scale the NLO potential by a factor λ, $U_{\rm NLO} \to \lambda U_{\rm NLO}$, and compute nonperturbatively the effective range as a function of the scaling parameters, $r_0(\lambda)$, with the obvious conditions $r_0(0) = r_0^{(0)}$ and $r_0(1) = r_0^{\rm NLO}$. The result is presented in Fig. 16. The infinite slope at the origin can be clearly seen. Numerically, we find that for small $\lambda \ll 0.1$, the correction to the effective range behaves as $r_0 - r_0^{(0)} \sim \sqrt{\lambda}$; whereas for $\lambda \sim 1$, it behaves as $r_0 - r_0^{(0)} \sim \lambda^{\frac{1}{3}}$. This fractional power counting λ^α, with $0 < \alpha < 1$, is evident from the universal low energy theorem (39) for a potential with a *single* scale, $U(r) = F(r/R)/R^2$, and appears when the short distance regulator is removed.[21] An explicit example is provided by Eq. (82), when a pure van der Waals potential acts as a perturbation to a boundary condition (a contact theory with only α_0), since the strength of the potential is $\lambda \mathrm{MC}_6 = R^4$, but r_0 contains $R \sim \lambda^{1/4}$, $R^2 \sim \lambda^{1/2}$, and $R^3 \sim \lambda^{3/4}$. It would be interesting to predict *a priori* this nonperturbative noninteger power counting analytically for potentials with multiple scales, as we have done here numerically [68]. [22]

Obviously, to prevent the perturbative divergence, one could subtract an energy-dependent contribution and provide the effective range as an input parameter. [23] Then one would obtain

$$k \cot\delta = k\cot\delta^{(0)} + \frac{1}{2}\left(r_0 - r_0^{(0)}\right)k^2 + \int_{r_c}^{\infty} dr[U^{(2)}(r) + U^{(3)}(r)] \times \left[u_k^{(0)}(r)^2 - u_0^{(0)}(r)^2 - 2k^2 u_0^{(0)}(r) u_2^{(0)}(r)^2\right]. \tag{106}$$

Note that this equation requires that we assume $r_0 - r_0^{(0)} = \mathcal{O}(\lambda)$, while nonperturbatively we find $r_0 - r_0^{(0)} = \mathcal{O}(\lambda^{\frac{1}{2}})$. Now the NLO and NNLO corrections to the v_2 parameter would come as a prediction, that is,

$$v_2^{(2)} + v_2^{(3)} = \int_{r_c}^{\infty} dr[U^{(2)}(r) + U^{(3)}(r)] \times \left[2u_4^{(0)}(r)u_0^{(0)}(r) + u_2^{(0)}(r)^2\right], \tag{107}$$

which is also divergent since the leading behavior of the integrand is $\sim 1/r^3$ at NLO and $\sim 1/r^4$ at NNLO for small r, see Eq. (104). Thus, a further subtraction would be needed, predicting the correction to v_3 as

$$v_3^{(2)} + v_3^{(3)} = \int_{r_c}^{\infty} dr[U^{(2)}(r) + U^{(3)}(r)] \times \left[2u_6^{(0)}(r)u_0^{(0)}(r) + 2u_2^{(0)}(r)u_4^{(0)}(r)\right], \tag{108}$$

which is logarithmically divergent because of Eq. (104). Finally, if a fourth subtraction is implemented, a convergent prediction is obtained for v_4 at NLO and NNLO,

$$v_4^{(2)} + v_4^{(3)} = \int_{r_c}^{\infty} dr[U^{(2)}(r) + U^{(3)}(r)] \times \left[2u_8^{(0)}(r)u_0^{(0)}(r) + 2u_2^{(0)}(r)u_4^{(0)}(r) + u_4^{(0)}(r)^2\right]. \tag{109}$$

These four subtractions, needed to make a renormalized *perturbative* prediction of the $^1S_0$ phase shift at NNLO , actually correspond to having four counterterms, i.e., fixing α_0, r_0, v_2, and v_3. This result disagrees with the standard Weinberg counting (two counterterms at NLO and NNLO in the $^1S_0$ channel). Moreover, besides the loss of predictive power as compared to the nonperturbative result where only one counterterm is needed, the deduced renormalized value for v_4 is worsened in perturbation theory, since $v_4^{(0)} = -50.74$ fm^7, $v_4^{(2)} = -10.45$ fm^7, and $v_4^{(3)} = -2.88$ fm^7. The situation is summarized in Table VII, where we show our numerical results obtained in perturbation theory as explained above and compare them with the NijmII and Reid93 potential model calculations (see, e.g., Ref. [59]). Although these are not directly experimental data, it is noteworthy that they differ by a few percent while the perturbative calculation is about a factor of 3 larger. The integrals for v_4 are rather well converging, and

[21] In Ref. [48], a potential well was used as a short distance regulator which was not removed; hence, the nonanalyticity was not seen.

[22] Fractional power counting has also been reported to occur in the EFT analysis of the three-body problem for the pionless theory [56, 73].

[23] This is equivalent to using a short distance energy-dependent boundary condition in the solution and hence to violating the orthogonality conditions discussed in Sec. III.

TABLE VII. Threshold parameters of the effective range expansion $k\cot\delta = -1/\alpha_0 + r_0k^2/2 + v_2k^4 + v_3k^6 + v_4k^8$ in the singlet $^1S_0$ channel in OPE distorted wave perturbation theory. We take $U^{(0)} = U^{(0)}_{1\pi}$ with $g_A = 1.26$. For the NNLO case, we use set IV for the chiral constants c_1, c_3, and c_4 given in Table I.

$^1S_0$	LO	NLO_{pert}	$\text{N}^2\text{LO}_{\text{pert}}$	Exp.	Nijm II	Reid93
α_0 (fm)	Input	Input	Input	−23.74(2)	−23.73	−23.74
r_0 (fm)	1.383	Input	Input	2.77(5)	2.67	2.75
v_2 (fm^3)	−2.053	Input	Input	–	−0.48	−0.49
v_3 (fm^5)	9.484	Input	Input	–	3.96	3.65
v_4 (fm^7)	−50.74	−61.19	−64.07	–	−19.88	−18.30

the matching between the numerical solution and the short distance solutions, Eq. (104), is quite stable in the region around $r \sim 0.1$ fm.

Thus, in this particular example of the $^1S_0$ channel, one sees that our nonperturbative approach based on the choice of the regular solutions at the origin predicts the phase shift and hence all low energy parameters from α_0 and the potential as displayed in Table VI. A perturbative treatment of the amplitude based on OPE distorted waves requires us to fix α_0, r_0, v_2, and v_3 at NNLO. The phenomenological success and converging pattern observed when the potential considered at LO, NLO, and NNLO is solved nonperturbatively is very encouraging. The price to pay is to face nonanalytical behavior which implies a noninteger power counting. The trend observed here can be generalized to other channels. A more thorough discussion of this issue will be presented elsewhere [68].

D. Triplet $^3S_1$–$^3D_1$ channel in distorted OPE waves

We turn now to the triplet $^3S_1$–$^3D_1$ channel. The reasoning is a straightforward, although tedious, coupled channel generalization of the $^1S_0$ case, with the additional feature that the short distance behavior is dominated by a $1/r^3$ singularity (instead of $1/r$); therefore, the short distance behavior is different. It is convenient to introduce the potential matrix as

$$\mathbf{U}(r) = \begin{pmatrix} U_{^3S_1}(r) & U_{E_1}(r) \\ U_{E_1}(r) & U_{^3D_1}(r) \end{pmatrix}, \tag{110}$$

and the matrix wave function,

$$\mathbf{u}_k(r) = \mathbf{A}\begin{pmatrix} u_{k,\alpha}(r) & u_{k,\beta}(r) \\ w_{k,\alpha}(r) & w_{k,\beta}(r) \end{pmatrix}, \tag{111}$$

with $\mathbf{A}$ a constant energy-dependent matrix, subject to a slightly different normalization than Eq. (75),

$$\mathbf{u}_k(r) \to \frac{1}{k}\hat{\mathbf{j}}(kr)\mathbf{D}^{-1}\hat{\mathbf{M}} - \hat{\mathbf{y}}(kr)\mathbf{D}. \tag{112}$$

Here, $\hat{\mathbf{M}}$ is the effective range matrix defined by its relation to the unitary $\mathbf{S}$ matrix,

$$\mathbf{DSD}^{-1} = (\hat{\mathbf{M}} + \mathrm{i}k\mathbf{D}^2)(\hat{\mathbf{M}} - \mathrm{i}k\mathbf{D}^2)^{-1}, \tag{113}$$

and $\mathbf{D} = \text{diag}(1, k^2)$. The reduced Bessel functions matrices are given by $\hat{\mathbf{j}} = \text{diag}(\hat{j}_0, \hat{j}_2)$ and $\hat{\mathbf{y}} = \text{diag}(\hat{y}_0, \hat{y}_2)$ with $\hat{j}_l(x) = xj_l(x)$ and $\hat{y}_l(x) = xy_l(x)$. At low energies, one has the effective range expansion(see, e.g., [59] and references therein),

$$\hat{\mathbf{M}} = -(\mathbf{a})^{-1} + \tfrac{1}{2}\mathbf{r}k^2 + \mathbf{v}k^4 + \cdots. \tag{114}$$

Here, we have introduced the scattering length matrix

$$\mathbf{a} = \begin{pmatrix} \alpha_0 & \alpha_{02} \\ \alpha_{02} & \alpha_2 \end{pmatrix}, \tag{115}$$

the effective range matrix

$$\mathbf{r} = \begin{pmatrix} r_0 & r_{02} \\ r_{02} & r_2 \end{pmatrix}, \tag{116}$$

and so on. These parameters have been determined in [59] from the potentials of Ref. [44]. Proceeding similarly as in the one channel case, one gets, after one subtraction at zero energy the effective range function in perturbation theory,

$$\hat{\mathbf{M}} + (\mathbf{a})^{-1} = \hat{\mathbf{M}}^{(0)} + (\mathbf{a}^{(0)})^{-1} + \int_{r_c}^{\infty} dr\left[\mathbf{u}_k^{(0)\dagger}\mathbf{U}^{(2)}\mathbf{u}_k^{(0)} - \mathbf{u}_0^{(0)\dagger}\mathbf{U}^{(2)}\mathbf{u}_0^{(0)}\right] \tag{117}$$

The condition $\alpha_0^{(0)} = \alpha_0$ must be imposed, since $\alpha_{02}^{(0)}$ and $\alpha_2^{(0)}$ are predicted from $\alpha_0^{(0)}$ (at LO one only needs one counterterm). This formula implies that one introduces two new conditions to fix now α_{02} and α_2 to their experimental value.Along similar lines as done before, we analyze the finiteness of the previous expression by computing the effective range matrix. To this end we expand the coupled channel wave function in powers of momentum

$$\mathbf{u}_k^{(0)}(r) = \mathbf{u}_0^{(0)}(r) + k^2\mathbf{u}_2^{(0)}(r) + k^4\mathbf{u}_4^{(0)}(r) + \ldots \tag{118}$$

to get

$$\mathbf{r}^{(2)} = \int_{r_c}^{\infty} dr\left[\mathbf{u}_2^{(0)\dagger}\mathbf{U}^{(2)}\mathbf{u}_0^{(0)} + \mathbf{u}_0^{(0)\dagger}\mathbf{U}^{(2)}\mathbf{u}_2^{(0)}\right] \tag{119}$$

The LO OPE short distance behavior of the triplet wave functions has been worked out in our previous work [41]. It is convenient to define the triplet length scale as

$$R_t = \frac{3g_A^2M}{32\pi f_\pi^2}, \tag{120}$$

for which $R_t = 1.07764$ fm. One has the general structure

$$\begin{aligned} u(r) &= \frac{1}{\sqrt{3}}\left(\frac{r}{R_t}\right)^{3/4}\Big[- C_{1R} f_{1R}(r) e^{+4\sqrt{2}\sqrt{\frac{R_t}{r}}} \\ &\quad - C_{2R} f_{2R}(r) e^{-4\sqrt{2}\sqrt{\frac{R_t}{r}}} + \sqrt{2} C_{1A} f_{1A}(r) e^{-4i\sqrt{\frac{R_t}{r}}} \\ &\quad + \sqrt{2} C_{2A} f_{2A}(r) e^{4i\sqrt{\frac{R_t}{r}}}\Big], \\ w(r) &= \frac{1}{\sqrt{3}}\left(\frac{r}{R_t}\right)^{3/4}\Big[\sqrt{2} C_{1R} g_{1R}(r) e^{+4\sqrt{2}\sqrt{\frac{R_t}{r}}} \\ &\quad + \sqrt{2} C_{2R} g_{2R}(r) e^{-4\sqrt{2}\sqrt{\frac{R_t}{r}}} + C_{1A} g_{1A}(r) e^{-4i\sqrt{\frac{R_t}{r}}} \\ &\quad + C_{2A} g_{2A}(r) e^{4i\sqrt{\frac{R_t}{r}}}\Big], \end{aligned} \tag{121}$$

where the constants C_{1R}, C_{2R}, C_{1A}, and C_{2A} depend on the energy and the OPE potential parameters. The regular solution is selected when one takes $C_{1R} = 0$. The functions appearing in this formula are of the form

$$\begin{aligned} f(r) &= \sum_{n=0}^{\infty} a_n \left(\frac{r}{R_t}\right)^{n/2}, \\ g(r) &= \sum_{n=0}^{\infty} b_n \left(\frac{r}{R_t}\right)^{n/2}. \end{aligned} \tag{122}$$

For the present calculation we only need the power behavior (see Appendix B of Ref. [41])

$$\begin{aligned} \mathbf{u}_0^{(0)}(r) &\sim r^{3/4}, \\ \mathbf{u}_2^{(0)}(r) &\sim r^{3/4+5/2}, \\ \mathbf{u}_4^{(0)}(r) &\sim r^{3/4+5}, \end{aligned} \tag{123}$$

which shows that, again, the first-order correction to the effective range matrix is logarithmically divergent because the NLO potential diverges as $1/r^5$ and $\mathbf{U}^{(2)}\mathbf{u}_0\mathbf{u}_2 \sim 1/r$.[24] As previously, the situation could be amended by adding three new counterterms to fix the effective range matrix $\mathbf{r}$, and then $\mathbf{v}$ would come as a prediction. So, at NLO in perturbation theory, one needs a total of six counterterms to generate a coupled channel finite amplitude. When adding the NNLO contribution, this number of counterterms remains the same since $\mathbf{U}^{(3)}\mathbf{u}_0^{(0)}\mathbf{u}_4^{(0)} \sim r^{1/2}$ and $\mathbf{U}^{(3)}[\mathbf{u}_2^{(0)}]^2 \sim r^{1/2}$.

An illustration of nonanalytical nonperturbative behavior in the ${}^3S_1$–${}^3D_1$ channel is given in Fig. 17. There, we see the behavior of the S-wave function normalization $A_S(\lambda)$ in the deuteron and the effective range $r_0(\lambda)$ in the ${}^3S_1$–${}^3D_1$ channel when the TPE potential is scaled as $U = U_{\rm LO} + \lambda(U_{\rm NLO} + U_{\rm NNLO})$ and the deuteron binding energy, the asymptotic D/S ratio η, and the S-wave scattering length α_0 are fixed to their experimental values.

[24]There is a subtlety here. The terms containing the regular exponential at the origin are convergent, regardless of the power of r in the denominator. Naively, logarithmically divergent integrals would become convergent when combined with oscillating functions. However, these functions appear *squared* so that the logarithmic divergence prevails.

E. The deuteron in distorted OPE waves

To conclude our analysis of perturbation theory we study now the deuteron bound state. According to Fig. 17, some tiny nonanalyticity appears for very small couplings in the asymptotic S-wave normalization A_S. Note that there is an apparent linear behavior, with the exception of the very small λ region, making one suspect that the result might be obtained in perturbation theory. We will see below by an explicit perturbative calculation that *this is not so*. We have checked that this trend also occurs for other quantities such as the quadrupole moment Q_d, the matter radius r_m, and the D-state probability P_D. Here, we show, as it has been done above for the scattering problem, that this can be traced to a first-order divergent renormalized result.

We define the two-component deuteron state as

$$\mathbf{u}_\gamma(r) = \begin{pmatrix} u_\gamma(r) \\ w_\gamma(r) \end{pmatrix}. \tag{124}$$

In perturbation theory, we expand the potential

$$\mathbf{U}(r) = \mathbf{U}^{(0)}(r) + \mathbf{U}^{(2)}(r) + \mathbf{U}^{(3)}(r) + \cdots, \tag{125}$$

and thus the deuteron wave function for fixed energy (or γ) becomes

$$\mathbf{u}_\gamma(r) = \mathbf{u}_\gamma^{(0)}(r) + \mathbf{u}_\gamma^{(2)}(r) + \mathbf{u}_\gamma^{(3)}(r) + \cdots, \tag{126}$$

where $[u_\gamma^{(0)}(r), w_\gamma^{(0)}(r)]$ correspond to the lowest order solutions of the problem and $[u_\gamma^{(2)}(r), w_\gamma^{(2)}(r)]$ and $[u_\gamma^{(3)}(r), w_\gamma^{(3)}(r)]$ satisfy

$$\begin{aligned} &-\mathbf{u}_\gamma^{(0)}(r) + [\mathbf{U}^{(0)}(r) + \gamma^2]\,\mathbf{u}_\gamma^{(0)}(r) = 0, \\ &-\mathbf{u}_\gamma^{(2)}(r) + [\mathbf{U}^{(0)}(r) + \gamma^2]\,\mathbf{u}_\gamma^{(2)}(r) = -\mathbf{U}^{(2)}(r)\mathbf{u}_\gamma^{(0)}(r), \\ &-\mathbf{u}_\gamma^{(3)}(r) + [\mathbf{U}^{(0)}(r) + \gamma^2]\,\mathbf{u}_\gamma^{(3)}(r) = -\mathbf{U}^{(3)}(r)\mathbf{u}_\gamma^{(0)}(r). \end{aligned} \tag{127}$$

We look for normalized solutions, so that perturbatively

$$\begin{aligned} 1 &= \int_0^\infty dr\, \mathbf{u}_\gamma^{(0)\dagger}(r)\mathbf{u}_\gamma^{(0)}(r), \\ 0 &= \int_0^\infty dr \left(\mathbf{u}_\gamma^{(2)\dagger}(r)\mathbf{u}_\gamma^{(0)}(r) + \mathbf{u}_\gamma^{(0)\dagger}(r)\mathbf{u}_\gamma^{(2)}(r)\right), \\ 0 &= \int_0^\infty dr \left(\mathbf{u}_\gamma^{(3)\dagger}(r)\mathbf{u}_\gamma^{(0)}(r) + \mathbf{u}_\gamma^{(0)\dagger}(r)\mathbf{u}_\gamma^{(3)}(r)\right). \end{aligned} \tag{128}$$

The zeroth-order equation was solved in our previous work [41], which showed that γ was a free parameter; therefore, $\gamma^{(0)} = \gamma$, and the regular solution at the origin was selected [see Eq. (121)] to ensure normalizability at the origin. We will always keep the same fixed value at any order of the approximation, so that $\gamma^{(2)} = \gamma^{(3)} = 0$. To analyze the NLO and NNLO problem analytically, we proceed by the variable coefficients method. The zeroth-order equation is a homogenous linear system with four linearly independent solutions,

$$\mathbf{u}_i^{(0)}(r) = \begin{pmatrix} u_i(r) \\ w_i(r) \end{pmatrix}, \qquad i = 1, 2, 3, 4. \tag{129}$$

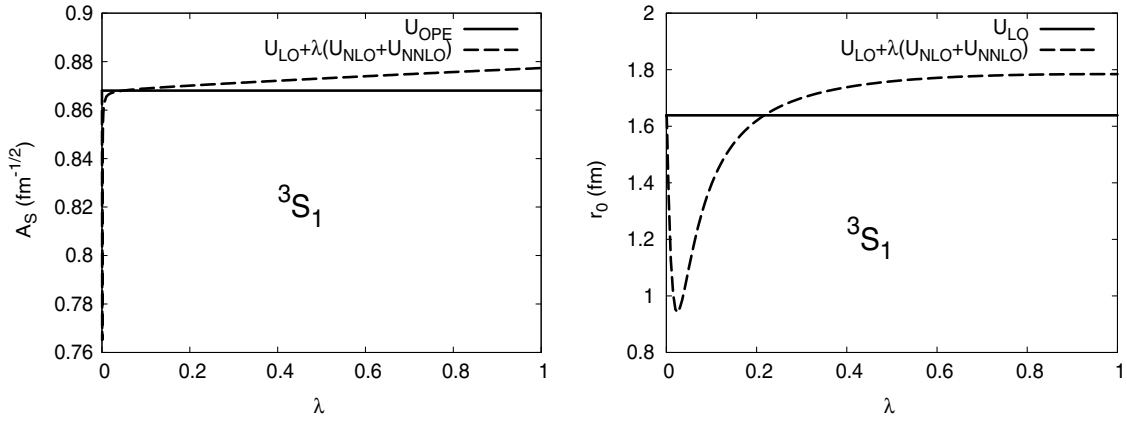

FIG. 17. Dependence of the S-wave function normalization $A_S(\lambda)$ in the deuteron and the effective range $r_0(\lambda)$ in the $^3S_1$–$^3D_1$ channel when one scales the TPE potential $U = U_{\rm LO} + \lambda(U_{\rm NLO} + U_{\rm NNLO})$. In all cases, we fix the deuteron binding energy, the asymptotic D/S ratio η, and the S-wave scattering length α_0 to their experimental values.

The first-order equation is an inhomogeneous linear system, which solution can be written as

$$\begin{aligned} u_\gamma^{(2)}(r) + u_\gamma^{(3)}(r) &= \sum_{i=1}^{4} c_i(r) u_i(r), \\ w_\gamma^{(2)}(r) + w_\gamma^{(3)}(r) &= \sum_{i=1}^{4} c_i(r) w_i(r). \end{aligned} \tag{130}$$

The variable coefficients satisfy

$$\begin{aligned} \sum_{i=1}^{4} c_i'(r) u_i(r) &= 0, \\ \sum_{i=1}^{4} c_i'(r) w_i(r) &= 0, \\ \sum_{i=1}^{4} c_i'(r) u_i'(r) &= F_u(r), \\ \sum_{i=1}^{4} c_i'(r) w_i'(r) &= F_w(r), \end{aligned} \tag{131}$$

where we have defined the driving term

$$\begin{aligned} \mathbf{F}(r) &= \begin{pmatrix} F_u(r) \\ F_w(r) \end{pmatrix} \\ &= -\mathbf{U}^{(2)}(r)\mathbf{u}_\gamma^{(0)}(r) - \mathbf{U}^{(3)}(r)\mathbf{u}_\gamma^{(0)}(r), \end{aligned} \tag{132}$$

which at short distances behaves as

$$\mathbf{F}(r) \sim r^{3/4} C_5 r^{-5} + r^{3/4} C_6 r^{-6}. \tag{133}$$

Whereas at large distances, one has

$$\mathbf{F}(r) \sim e^{-\gamma r} e^{-mr}. \tag{134}$$

To proceed further, we choose the following linearly independent solutions fulfilling the asymptotic boundary condition at infinity

$$\begin{aligned} u_1(r) &\to e^{-\gamma r}, \\ w_1(r) &\to 0, \\ u_2(r) &\to 0, \\ w_2(r) &\to e^{-\gamma r}\left(1 + \frac{3}{\gamma r} + \frac{3}{(\gamma r)^2}\right), \\ u_3(r) &\to e^{\gamma r}, \\ w_3(r) &\to 0, \\ u_4(r) &\to 0, \\ w_4(r) &\to e^{\gamma r}\left(1 - \frac{3}{\gamma r} + \frac{3}{(\gamma r)^2}\right). \end{aligned} \tag{135}$$

Any of these solutions has a short distance behavior of the general form given in Eq. (121). Therefore, *all these solutions are necessarily singular* at the origin. Using Krammer's rule, the solutions to the linear differential system, Eq. (131), which are regular at infinity read

$$c_1(r) = \frac{1}{W}\int_0^r dr' \begin{vmatrix} 0 & u_2 & u_3 & u_4 \\ 0 & w_2 & w_3 & w_4 \\ F_u & u_2' & u_3' & u_4' \\ F_w & w_2' & w_3' & w_4' \end{vmatrix}, \tag{136}$$

$$c_2(r) = \frac{1}{W}\int_0^r dr \begin{vmatrix} u_1 & 0 & u_3 & u_4 \\ w_1 & 0 & w_3 & w_4 \\ u_1' & F_u & u_3' & u_4' \\ w_1' & F_w' & w_3' & w_4' \end{vmatrix}, \tag{137}$$

$$c_3(r) = -\frac{1}{W}\int_r^\infty dr' \begin{vmatrix} u_1 & u_2 & 0 & u_4 \\ w_1 & w_2 & 0 & w_4 \\ u_1' & u_2' & F_u & u_4' \\ w_1' & w_2' & F_w & w_4' \end{vmatrix}, \tag{138}$$

$$c_4(r) = -\frac{1}{W}\int_r^\infty dr' \begin{vmatrix} u_1 & u_2 & u_3 & 0 \\ w_1 & w_2 & w_3 & 0 \\ u_1' & u_2' & u_3' & F_u \\ w_1' & w_2' & w_3' & F_w \end{vmatrix}, \tag{139}$$

where W is the Wronskian

$$W = \begin{vmatrix} u_1 & u_2 & u_3 & u_4 \\ w_1 & w_2 & w_3 & w_4 \\ u_1' & u_2' & u_3' & u_4' \\ w_1' & w_2' & w_3' & w_4' \end{vmatrix} = -4\gamma^2. \tag{140}$$

At asymptotically large distances, we have

$$\begin{aligned} u^{(2)}(r) &\to c_S^{(2)} e^{-\gamma r}, \\ w^{(2)}(r) &\to c_D^{(2)} \eta^{(0)} e^{-\gamma r} \left(1 + \frac{3}{\gamma r} + \frac{3}{(\gamma r)^2}\right), \end{aligned} \tag{141}$$

and similarly for the N^{2}LO correction. Note that the normalization condition, Eq. (128), implies a linear relation between $c_S^{(2)}$ and $c_D^{(2)}$ as well as $c_S^{(3)}$ and $c_D^{(3)}$. The total D/S ratio obtained by including the zeroth-order contribution is given by

$$\eta = \eta^{(0)} \frac{1 + c_D^{(2)} + c_D^{(3)}}{1 + c_S^{(2)} + c_S^{(3)}}. \tag{142}$$

If we fix η, we get a relation between c_S and c_D. The coefficients $c_S^{(2)}$ and $c_D^{(2)}$ are given by

$$\begin{aligned} c_S^{(2)} + c_S^{(3)} &= c_1(\infty), \\ \eta^{(0)}\left(c_D^{(2)} + c_D^{(3)}\right) &= c_2(\infty). \end{aligned} \tag{143}$$

The long distance behavior of the integrands is well behaved since, up to inessential powers in r, one has

$$\begin{aligned} c_1'(r) &\sim e^{-2mr}, \\ c_2'(r) &\sim e^{-2mr}, \\ c_3'(r) &\sim e^{-(2m+2\gamma)r}, \\ c_4'(r) &\sim e^{-(2m+2\gamma)r}. \end{aligned} \tag{144}$$

However, the leading short distance behavior of the integrand is given as

$$c_i'(r) \sim r^{3/4} (e^{4\sqrt{2R/r}})^2 \left(\frac{C_5}{r^5} + \frac{C_6}{r^6}\right) r^{3/4} e^{\pm i 4\sqrt{R/r}}. \tag{145}$$

So, we expect the coefficients c_S and c_D to diverge if the short distance cutoff is removed, $r_c \to 0$. It is unclear how this divergence might be avoided. Unlike the scattering problem in perturbation theory, where energy-dependent (and hence orthogonality-violating) subtractions are needed, it would be difficult to accept a bound state not normalized to unity unless one includes, besides pn, other Fock state components such as $pn\pi$. This short distance analysis holds also when the $1/r^6$ Δ contributions are taken into account perturbatively.

Thus, perturbation theory on the distorted OPE basis for the deuteron makes sense only as a finite cutoff theory. In the Appendix, we develop further such an approach to NLO, where η is an input, and to NNLO, where *both* A_S and η should be fixed. We also show that in the cutoff theory, the NLO yields tiny corrections to deuteron properties whereas the NNLO dominates. This proves that, at least perturbatively and in the absence of the Δ, the (integer) power counting to NNLO in deuteron properties is obviously not convergent. To some extent, this result resembles qualitatively the findings of Ref. [71] based on the idea that OPE and TPE can be included perturbatively [69]. Of course, an amelioration of the convergence in the cutoff theory when Δ's are included is not precluded and deserves further investigation. However, the very need of a finite cutoff will still hold, as our analytical study shows.

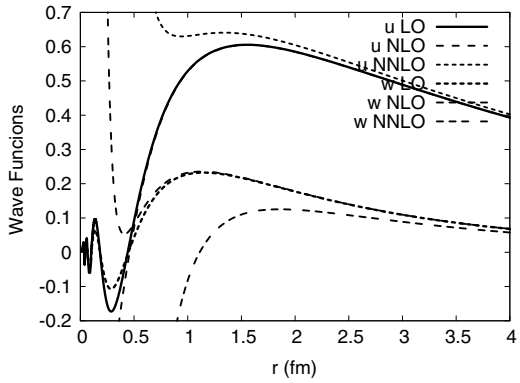

FIG. 18. Deuteron wave functions at LO, NLO, and NNLO in perturbation theory when a short distance cutoff $r_c = 0.5$ fm is considered for the perturbative corrections. At LO we fix γ, at NLO we fix γ and η, and at NNLO we fix γ, η, and A_S. Solutions are perturbatively normalized. The LO wave functions are normalized by taking $A_S = 1$.

In Fig. 18, we show LO, NLO, and NNLO order wave functions when a finite short distance cutoff $r_c = 0.5$ fm is considered. The strong divergence of the wave function at the origin can be clearly seen.

X. CONCLUSIONS

In the present work, we have extended to the TPE potential the coordinate space renormalization of central waves in NN interaction discussed in our previous work [41] for the OPE potential. As we have stressed throughout the paper, the main advantage of such a framework is that the (renormalized) potential is finite everywhere except at the origin where a van der Waals attractive singularity takes place. This suggests using a radial cutoff which provides a compact support for the short-range part of the potential, thus making scheme-dependent contact interactions innocuous for the long-range solution. As a result, model-independent long-range correlations between NN observables can be deduced if the renormalized potential is iterated to all orders. Although the regularization and renormalization techniques employed along this work are somewhat unconventional from the standard EFT viewpoint, it is rewarding to know that renormalized EFT OPE calculations do not significantly differ from our results. It remains to be seen if the TPE extension of Ref. [42] confirms this plausible equivalence.

Important constraints can be deduced from the requirement of a small wave function in the unknown short distance region. As a consequence, the boundary condition for the wave function at short distances becomes energy independent if the long-range contribution to the potential is also energy independent. We stress here that such requirements, although

quite natural from a physical viewpoint, may not appear obvious within the EFT framework so far, and it would be very interesting to provide further arguments within EFT itself supporting our unconventional framework [58]. Actually, we find that the singularity structure of the potential at short distances determines uniquely how many parameters must be regarded as unknown, nonpredictable information. This is done in terms of short distance phases or equivalently via suitable mixed boundary conditions at the origin. Moreover, for an energy-independent potential, the orthogonality of wave functions precludes a possible energy dependence of the boundary conditions. In the particular cases studied in this paper, namely, $^1S_0$ and $^3S_1$–$^3D_1$ channels, we have found that besides the NNLO TPE potential parameters, one can use the S-wave scattering lengths in both channels as well as the deuteron binding energy and the asymptotic D/S ratio of the deuteron wave functions as independent input information. The remaining scattering or bound state properties in the triplet channel are then predicted unambiguously. This reduction of parameters contradicts EFT counting arguments on the structure of short distance interactions, but amazingly TPE potentials do saturate the bulk of finite-range observables rather accurately. Based on the superposition principle of boundary conditions, we have found analytical and simple universal rational relations that clearly exhibit these features. These universal relations would be very difficult to deduce in momentum space and, moreover, they are free from uncertainties attributable to finite cutoff effects. So, the cutoff has been effectively eliminated. On a numerical level, the fact that our problem is an initial value problem for the Schrödinger equation starting at infinity makes it possible to obtain any solution by competitive algorithms with adaptable integration steps with any prescribed accuracy. This allows one to faithfully describe the short distance oscillations of the wave function. This is in contrast to the standard Lippmann-Schwinger treatments, where matrix inversion methods may eventually run into computer space limitations with a natural loss of space resolution as a side effect. The nontrivial oscillating structure of the wave functions with ever-decreasing periods of the wave functions close to the origin would actually be very difficult to reproduce within a momentum space framework.

According to our analysis, there are finite cutoff effects in previous works dealing also with TPE potentials in both coordinate and momentum space. The induced corrections are larger than the experimental uncertainty of the computed observables; so in some cases, agreement with data may be clearly attributed to the choice of a finite cutoff. In our energy-independent boundary condition treatment, we found short distance cutoffs of about $r_c = 0.1$–0.2 fm to be rather innocuous. Within a Wilsonian viewpoint of renormalization, changes in the cutoff should correspond to decimation, i.e., halving, and not to linear changes in the scale. If we associate this coordinate space cutoff with a momentum space ultraviolet cutoff of $\Lambda = \pi/2r_c$ [74], then we are dealing with an equivalent momentum scale of about 1.5–3 GeV, which is much larger than the scales below 1 GeV usually employed in momentum space calculations where only linear sensitivity to changes of the cutoff is implemented. Nevertheless, it is fair to say that the calculations based on sets III and IV provide discrepancies that are not too large.

As one naturally expects in a renormalized theory, errors are dominated by uncertainties in the input data and not by cutoff uncertainties. Indeed, we seem to reach a limit in the accuracy of the predictions, paralleling the findings in ChPT for mesons at the two loop level. At the OPE level, one can predict bound state and scattering properties in the singlet $^1S_0$ and triplet $^3S_1$–$^3D_1$ channels solely from the deuteron energy and the $^1S_0$ scattering length. At the TPE level, one needs not only the additional chiral constants c_1, c_3, and c_4 but also the triplet S-wave scattering length and the asymptotic D/S ratio. Although the TPE central value predictions improve, the induced TPE errors turn out to be *larger* than the OPE uncertainties. In fact, because of these large uncertainties, the TPE calculation, within errors, becomes compatible with experimental data at the 1σ level. This suggests that in order to evaluate in a statistically significant sense other effects, such as electromagnetic, relativistic, and three-pion effects, one must first improve on the input data. Otherwise, predictive power is lost. Nevertheless, given the finite cutoff effects detected in previous works, the role of these corrections beyond TPE should be reanalyzed within the present approach.

One of the important consequences of our treatment is that the chiral constants c_1, c_3, and c_4 can be determined from *low energy data* and *deuteron properties*. Specifically, we have used the singlet and triplet effective ranges as well as the asymptotic S-wave deuteron wave function to c_1, c_3, and c_4 *with errors* varying all input data within their experimental uncertainties. The decision on what set of data should be used to pin down the chiral coefficients is not entirely trivial, because it should become clear which hypothesis we want to verify or to refute. The absence of cutoff effects makes this test cleaner; we just check whether the TPE potential holds from zero to infinity. Obviously, this cannot be literally true, but one expects that at low energies, other short-range effects can be considered negligible. Let us remember that error analysis within NN calculations was only carried out in a large-scale partial wave analysis of data in Ref. [11]. The determinations of chiral constants based on a fit to NN databases [43–45] for phase shifts lack any error estimates because the databases themselves are treated as errorless. The determination of chiral constants from peripheral waves has similar drawbacks. From the chiral theory point of view, we see that it is possible to determine these parameters precisely in the regime where we trust the theory most, namely, in the description of low energy NN data. A fit becomes possible, and the values it yields only differ by 2σ with the determination from πN data. We do not exclude that our values for the chiral constants may eventually spoil the successful overall fit of phase shifts in all channels presented in the past, after all renormalization has been carried out. If so, the situation on the effectiveness of the effective field theory would be in a less optimistic shape than assumed hitherto. A preliminary analysis of the problem shows what van der Waals coefficients in the TPE potential correspond to attractive short-range interactions and, hence, what phase shifts are completely determined in terms of coupled channel scattering lengths. This issue is very relevant and would require a detailed channel-by-channel

analysis and renormalization, taking as input the scattering lengths documented in our previous work [59] and integrating in from large distances along the lines of the present approach. Full details are reported elsewhere [75].

Nevertheless, despite the good convergence in the $^1S_0$ channel for LO, NLO, and NNLO calculations, we have noted a difficulty for the triplet $^3S_1$–$^3D_1$ channel at NLO of the potential. In contrast to dimensional power counting expectations, one cannot use the scattering length α_0, the effective range r_0, and α_{02} as arbitrary input parameters at NLO in the potential (one could equally take γ, η, and α_0), but they are entirely predicted from the potential as required by finiteness of the phase shifts. Otherwise, the scattering amplitude diverges, as we have shown. We have also seen that even if one assumes a finite value of the cutoff the NLO is worse than the LO, suggesting that the problem may indeed be related to the power counting on the long distance potential. Remarkably, these parameters must be fixed at NNLO where, according to the standard approach, no further low energy parameters should be fixed. This mismatch in orders can be understood if one considers the $N\Delta$ splitting to be a small parameter, making much of the NNLO contributions to the potential NLO ones, because c_3 and c_4 would be order of -1. In such a case, our interpretation goes hand in hand with the standard approach; one needs three independent low energy parameters at NLO in this counting. The consequences of this Δ counting to higher orders within the context of renormalization will be explored elsewhere. Of course, we should point out that despite the rather tantalizing description achieved at NNLO, the existence of a consistent power counting guaranteeing the success of the present approach to all orders remains to be proved. A key ingredient of such a power counting would be the correct incorporation of all long-range physics. Apparently, within Weinberg's power counting, the NLO in the deuteron channel misses important contributions.

Finally, we have analyzed the consequences of a perturbative expansion of TPE effects taking the OPE results as a zeroth-order approximation as suggested recently [42]. Our nonperturbative calculations based on iterating a perturbative potential to all orders exhibit unequivocal nonanalytic dependence on the expansion parameter, due to the singular character of the chiral potentials at the origin. This is equivalent to a noninteger enhancement of the power counting λ^α with $0 < \alpha < 1$ in the potential strength λ, and it would be interesting to know the general rules of such a counting *a priori* [68]. Thus, perturbation theory based on standard power counting becomes divergent and can only yield finite results at the expense of introducing more perturbative counterterms than are needed in a nonperturbative treatment. This is just a manifestation of the fact that singular potentials require infinite counterterms in perturbation theory, while only a few are needed nonperturbatively. Specifically, our analysis shows that it would be necessary to include at least four counterterms for the singlet $^1S_0$ and six for the triplet $^3S_1$–$^3D_1$ channel at NNLO. This proliferation of counterterms is expected to occur also in other partial waves because the singularity of the potential dominates over the centrifugal barrier at short distances. In the $^1S_0$ channel, we have seen that adding more counterterms in fact worsens the results for the effective range expansion parameters. In contrast, our nonperturbative calculations are based on just one and three counterterms, respectively. The good quality of our results suggests that our choice of fewer counterterms cannot be refuted on the basis of phenomenology. In the deuteron case, we have made a calculation to NNLO in perturbation theory. Our analysis shows that such a perturbative approach only makes sense if a finite cutoff is introduced. In any case, the cutoff theory has less predictive power, does not provide a better phenomenological description of the deuteron than our nonperturbative renormalized results, and is nonconvergent since NNLO corrections are numerically *much larger* (two or three orders of magnitude) than NLO ones, despite being parametrically small. In our view, this is a perturbative manifestation of the short distance dominance which has been unveiled nonperturbatively. In addition, the difficulties faced by a perturbative treatment are simply absent in the nonperturbative approach.

One of the main goals of nuclear physics is the determination of the nucleon-nucleon interaction. From a theoretical viewpoint, the disentanglement of such an interaction in terms of pion exchanges based on chiral symmetry requires dealing with nontrivial and, to some extent, unconventional nonperturbative renormalization issues in the continuum, but it is crucial because it shows our quantitative understanding of the underlying theory of quarks and gluons in the chirally symmetric broken phase. Our results also show that the singular chiral van der Waals forces are not necessarily spurious and inconvenient features of the chiral potential. Instead, as we have shown, the singularities alone in conjunction with renormalization ideas explain much of the observed S-wave phase shifts with natural values of the chiral constants, and provide an appealing physical picture. In this regard, it is interesting to realize that based on the analogy with molecular systems, which also exhibit a long-range van der Waals force, the liquid drop model was formulated more than 60 years ago. Chiral dynamics may provide not only a closer analogy and perhaps more quantitative insights into the hydrodynamic and thermodynamic properties of nuclei but also a theoretical justification from the underlying theory of strong interactions.

ACKNOWLEDGMENTS

One of us (E.R.A.) thanks M. Rentmeester, R. Machleidt, E. Epelbaum, N. Kaiser, and G. Colangelo for useful correspondence. We also thank them and R. Higa and A. Nogga for discussions and D. Phillips for stressing the role of the Δ. We thank J. Nieves for reading an early version of the manuscript. This work is supported in part by funds provided by the Spanish DGI with Grant No. FIS2005-00810, Junta de Andalucía Grant No. FM-225, and EURIDICE Grant No. HPRN-CT-2003-00311.

APPENDIX A: THE DEUTERON IN OPE-DISTORTED PERTURBATION THEORY WITH A CUTOFF TO NNLO

In this Appendix, we illustrate the situation discussed in Sec. IX by solving numerically the set of perturbative

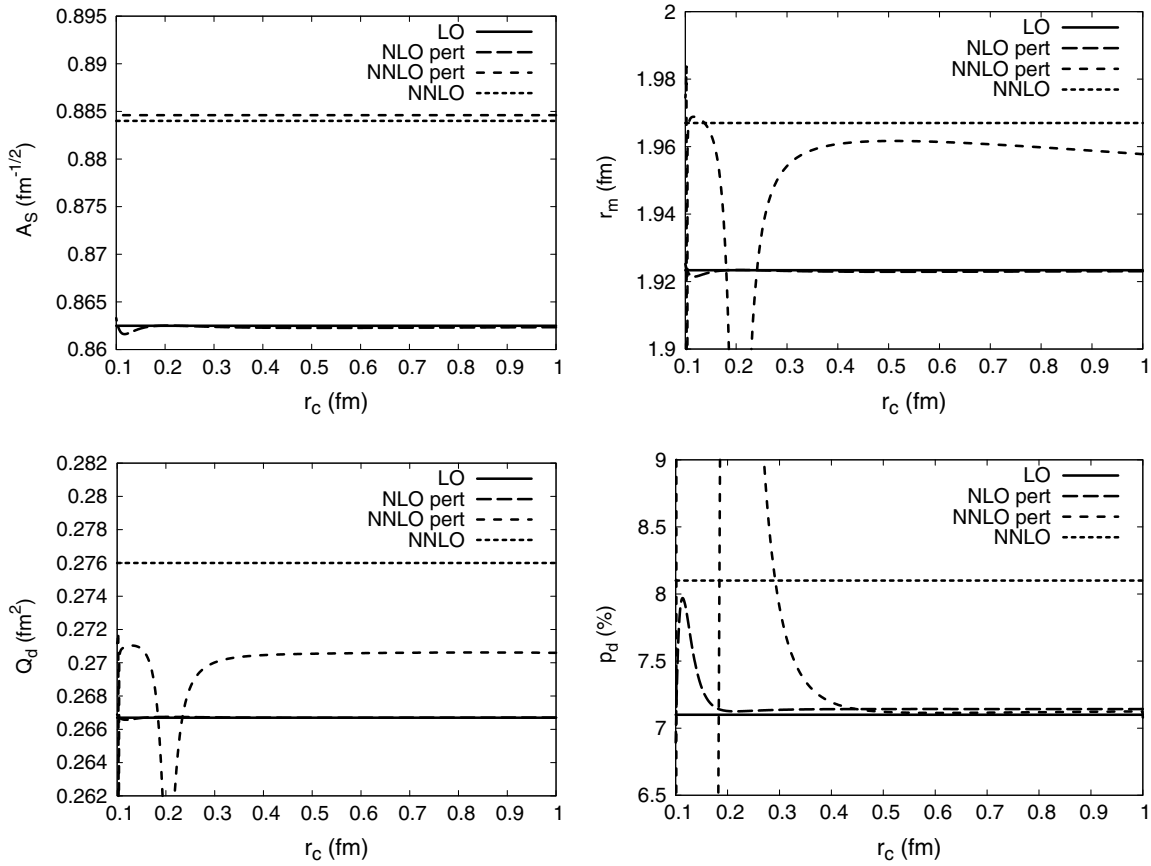

FIG. 19. Dependence of the S-wave function normalization $A_S(r_c)$, matter radius $r_m(r_c)$, quadrupole moment $Q_d(r_c)$, and D-wave probability $P_D(r_c)$ in the deuteron in perturbation theory to NLO and NNLO on the short distance cutoff. We use set IV for the NNLO. In each case, the first-order solution is fixed to be normalized and to reproduce the asymptotic D/S ratio η. We compare with the experimental value and the OPE result.

Eqs. (127). As we have mentioned, such a calculation only makes sense within a finite cutoff scheme.

In practice, we integrate from large distances ($\sim$25 fm) with the conditions specified by Eq. (141) with some prescribed values of c_S and c_D.[25] This can be advantageously done using the superposition principle of boundary conditions, Eq. (60), yielding in perturbation theory

$$\begin{aligned} u_\gamma(r) &= u_\gamma^{(0)}(r) + u_\gamma^{(2)}(r) + u_\gamma^{(3)}(r) + \cdots, \\ w_\gamma(r) &= u_\gamma^{(0)}(r) + u_\gamma^{(2)}(r) + u_\gamma^{(3)}(r) + \cdots. \end{aligned} \tag{A1}$$

At LO, the wave function can be written as

$$\begin{aligned} u_\gamma^{(0)}(r) &= u_S^{(0)}(r) + \eta^{(0)} u_D^{(0)}(r), \\ w_\gamma^{(0)}(r) &= w_S^{(0)}(r) + \eta^{(0)} w_D^{(0)}(r), \end{aligned} \tag{A2}$$

and $\eta^{(0)}$ is determined from the regularity condition at the origin [41]. At LO, the normalization factor is

$$\frac{1}{\left(A_S^{(0)}\right)^2} = \int_0^\infty dr \left(u_\gamma^{(0)}(r)^2 + w_\gamma^{(0)}(r)^2\right). \tag{A3}$$

[25]This is a numerically more efficient and stable procedure than the direct use of the explicit expressions in Eq. (143) involving determinants.

The NLO and NNLO contributions are

$$\begin{aligned} u_\gamma^{(2)}(r) &= c_S^{(2)} u_S^{(2)}(r) + \eta^{(0)} c_D^{(2)} u_D^{(2)}(r), \\ w_\gamma^{(2)}(r) &= c_S^{(2)} w_S^{(2)}(r) + \eta^{(0)} c_D^{(2)} w_D^{(2)}(r), \\ u_\gamma^{(3)}(r) &= c_S^{(3)} u_S^{(3)}(r) + \eta^{(0)} c_D^{(3)} u_D^{(3)}(r), \\ w_\gamma^{(3)}(r) &= c_S^{(3)} w_S^{(3)}(r) + \eta^{(0)} c_D^{(3)} w_D^{(3)}(r). \end{aligned} \tag{A4}$$

The advantage is that the functions appearing here only depend on the potential and the deuteron binding energy, whereas the coefficients must be determined by some additional conditions. In the first place, normalization to NLO and NNLO requires orthogonality of the wave functions to the LO solution,

$$\begin{aligned} 0 &= \int_0^\infty dr (u^{(0)}(r) u^{(2)}(r) + w^{(0)}(r) w^{(2)}(r)), \\ 0 &= \int_0^\infty dr (u^{(0)}(r) u^{(3)}(r) + w^{(0)}(r) w^{(3)}(r)). \end{aligned} \tag{A5}$$

TABLE VIII. Comparison of finite cutoff perturbation theory, $r_c = 0.5$ fm, with renormalized nonperturbative results for the deuteron properties. We use the nonrelativistic relation $\gamma = \sqrt{2\mu_{np}B}$ with $B = 2.224575(9)$. The errors quoted in the perturbative calculations reflect the uncertainty in the input parameters γ, η, and A_S. Similarly, the errors quoted in the TPE reflect the uncertainty in the nonpotential parameters γ and η. We use set IV of low energy constants c_1, c_3, and c_4.

	r_c	γ (fm^{-1})	η	A_S (fm$^{-1/2}$)	r_m (fm)	Q_d (fm^2)	P_D	$\langle r^{-1}\rangle$ (fm^{-1})
Nonperturbative:								
$U_{1\pi}$	0	Input	0.02633	0.8681(1)	1.9351(5)	0.2762(1)	7.31(1)%	0.476(3)
$U_{1\pi} + U_{2\pi}$	0	Input	Input	0.884(4)	1.967(6)	0.276(3)	8(1)%	0.447(5)
Perturbative:								
$U_{1\pi}^{(0)}$	0	Input	0.02555	0.8625(2)	1.9233(5)	0.2667(1)	7.14(1)%	0.484(3)
$U_{1\pi}^{(2)} + U_{2\pi}^{(2)}$	0.5 fm	Input	Input	0.862(2)	1.923(4)	0.2667(3)	7.14(1)%	0.484(3)
$U_{1\pi}^{(3)} + U_{2\pi}^{(3)}$	0.5 fm	Input	Input	Input	1.962(2)	0.2705(2)	7.12(1)%	0.484(3)
Potentials:								
NijmII	—	0.231605	0.02521	0.8845(8)	1.9675	0.2707	5.635%	0.4502
Reid93	—	0.231605	0.02514	0.8845(8)	1.9686	0.2703	5.699%	0.4515
Exp.	—	0.231605	0.0256(4)	0.8846(9)	1.971(6)	0.2859(3)	—	—

This implies the couple of linear relations [26]

$$
\begin{aligned}
-\eta^{(0)}\frac{c_D^{(2)}}{c_S^{(2)}} &= \frac{\int_0^\infty dr\left(u^{(0)}(r)u_S^{(2)}(r) + w^{(0)}(r)w_S^{(2)}(r)\right)}{\int_0^\infty dr\left(u^{(0)}(r)u_D^{(2)}(r) + w^{(0)}(r)w_D^{(2)}(r)\right)}, \\
-\eta^{(0)}\frac{c_D^{(3)}}{c_S^{(3)}} &= \frac{\int_0^\infty dr\left(u^{(0)}(r)u_S^{(3)}(r) + w^{(0)}(r)w_S^{(3)}(r)\right)}{\int_0^\infty dr\left(u^{(0)}(r)u_D^{(3)}(r) + w^{(0)}(r)w_D^{(3)}(r)\right)}.
\end{aligned}
\tag{A6}
$$

Further relations can be obtained by imposing renormalization conditions. Note that the required number of conditions increases with the order. This is similar in spirit to the procedure of adding more counterterms for the scattering problem discussed in Sec. IX. For instance, using the perturbative expansion for A_S and A_D

$$
\begin{aligned}
A_S &= A_S^{(0)}\left(1 + c_S^{(2)} + c_S^{(3)} + \cdots\right), \\
A_D &= A_D^{(0)}\eta^{(0)}\left(1 + c_D^{(2)} + c_D^{(3)} + \cdots\right) = \eta A_S.
\end{aligned}
\tag{A7}
$$

In practice, we use a short distance cutoff r_c for the NLO and NNLO contributions only. Deuteron properties can be written to NNLO as follows

$$
\begin{aligned}
r_m &= r_m^{(0)} + c_S^{(2)} r_m^{(2,S)} + \eta^{(0)} c_D^{(2)} r_m^{(2,D)} \\
&\quad + c_S^{(3)} r_m^{(3,S)} + \eta^{(0)} c_D^{(3)} r_m^{(3,D)} + \cdots,
\end{aligned}
\tag{A8}
$$

$$
\begin{aligned}
Q_d &= Q_d^{(0)} + c_S^{(2)} Q_d^{(2,S)} + \eta^{(0)} c_D^{(2)} Q_d^{(2,D)} \\
&\quad + c_S^{(3)} Q_d^{(3,S)} + \eta^{(0)} c_D^{(3)} Q_d^{(3,D)} + \cdots,
\end{aligned}
\tag{A9}
$$

where the potential contributions have explicitly been factored out. The numerical solution requires some care, due to the short distance instabilities and oscillations. This requires using an adaptive grid to optimize the convergence. Since solutions of different orders must be mixed in the evaluation of the orthogonality conditions, Eq. (A6), and observables, Eq. (A9), we solve simultaneously all LO, NLO, and NNLO equations to provide all functions on the same grid.

[26] For instance, at $r_c = 0.5$ fm, we get $c_D^{(2)} = -5.865 c_S^{(2)}$ and $c_D^{(3)} = -5.545 c_S^{(3)}$.

At NLO and fixing $r = r_c$, we demand the experimental value of η, from Eq. (142) and Eq. (A6). This way, a solution which we denote by $(c_S^{(2)}|_{\rm NLO}, c_D^{(2)}|_{\rm NLO})$ can be obtained. From there, we can obtain deuteron properties to NLO, as a function of the perturbative cutoff r_c. In Fig. 19, we show the dependence of A_S, r_m, Q_d, and p_d on r_c. As we see, the NLO correction is tiny and stable for $r_c > 0.2$ fm. At NNLO, we fix η and A_S. The solution is now $(c_S^{(2)}|_{\rm NNLO}, c_D^{(2)}|_{\rm NNLO})$ and $(c_S^{(3)}|_{\rm NNLO}, c_D^{(3)}|_{\rm NNLO})$. Note that in general the NLO coefficients $c_S^{(2)}$ and $c_D^{(2)}$ must be readjusted. In this case, the correction is much larger than the NLO case (see Fig. 19), and the cutoff dependence is stronger thanks to the the $1/r^6$ singularity of the NNLO potential. As a curiosity, we mention that at short distances worrisome negative D-wave probabilities show up below $r_c = 0.17$ fm at NNLO, a spurious feature which can only take place in perturbation theory and sets a unitarity bound on the short distance perturbative cutoff. Numerical results are provided in Table VIII for set IV. Typically, we find that results do not depend dramatically on the chosen chiral couplings. We take $r_c = 0.5$ fm as a standard choice. As we see, finite cutoff perturbation theory does not work better than our nonperturbative results of Sec. V, and in fact requires one more counterterm. Actually, this is a perturbative indication that NNLO is more important than NLO, casting doubt on the convergence of the approach.

Finally, we have checked that taking the LO to be the *full* OPE potential $\mathbf{U}_{1\pi}$ and the perturbation to be $\mathbf{U}_{2\pi}^{(2)} + \mathbf{U}_{2\pi}^{(3)}$ as a whole and keeping the cutoff $r_c > 0.1$ fm does not change the results significantly. Actually, the perturbative result does not account for the value obtained nonperturbatively, despite the apparent linear behavior observed when changing numerically the scaling parameter λ in the region $\lambda \gg 0.1$ (see Fig. 17). This supports our conclusion that perturbation theory does not compute the slope of $A_S(\lambda)$ at the origin. In addition, even if we disregard the divergence by introducing a cutoff, the perturbative calculation does not account for the nonperturbative renormalized result.

[1] S. Weinberg, Phys. Lett. **B251**, 288 (1990).
[2] C. Ordonez and U. van Kolck, Phys. Lett. **B291**, 459 (1992).
[3] U. L. Van Kolck, UMI-94-01021, 1993 (unpublished).
[4] C. Ordonez, L. Ray, and U. van Kolck, Phys. Rev. C **53**, 2086 (1996).
[5] P. F. Bedaque and U. van Kolck, Annu. Rev. Nucl. Part. Sci. **52**, 339 (2002).
[6] T. A. Rijken and V. G. J. Stoks, Phys. Rev. C **54**, 2851 (1996).
[7] N. Kaiser, R. Brockmann, and W. Weise, Nucl. Phys. **A625**, 758 (1997).
[8] N. Kaiser, S. Gerstendorfer, and W. Weise, Nucl. Phys. **A637**, 395 (1998).
[9] E. Epelbaum, W. Gloeckle, and U.-G. Meissner, Nucl. Phys. **A637**, 107 (1998).
[10] E. Epelbaum, W. Gloeckle, and U.-G. Meissner, Nucl. Phys. **A671**, 295 (2000).
[11] M. C. M. Rentmeester, R. G. E. Timmermans, J. L. Friar, and J. J. de Swart, Phys. Rev. Lett. **82**, 4992 (1999).
[12] J. L. Friar, Phys. Rev. C **60**, 034002 (1999).
[13] K. G. Richardson, Ph.D. thesis, University of Manchester (1999); hep-ph/0008118.
[14] N. Kaiser, Phys. Rev. C **61**, 014003 (2000).
[15] N. Kaiser, Phys. Rev. C **62**, 024001 (2000).
[16] N. Kaiser, Phys. Rev. C **65**, 017001 (2002).
[17] N. Kaiser, Phys. Rev. C **64**, 057001 (2001).
[18] N. Kaiser, Phys. Rev. C **63**, 044010 (2001).
[19] D. R. Entem and R. Machleidt, Phys. Lett. **B524**, 93 (2002).
[20] D. R. Entem and R. Machleidt, Phys. Rev. C **66**, 014002 (2002).
[21] M. C. M. Rentmeester, R. G. E. Timmermans, and J. J. de Swart, Phys. Rev. C **67**, 044001 (2003).
[22] E. Epelbaum, W. Gloeckle, and U.-G. Meissner, Eur. Phys. J. A **19**, 125 (2004).
[23] E. Epelbaum, W. Gloeckle, and U.-G. Meissner, Eur. Phys. J. A **19**, 401 (2004).
[24] D. R. Entem and R. Machleidt (2003), nucl-th/0303017.
[25] R. Higa and M. R. Robilotta, Phys. Rev. C **68**, 024004 (2003).
[26] R. Higa, M. R. Robilotta, and C. A. da Rocha, Phys. Rev. C **69**, 034009 (2004).
[27] R. Higa (2004), nucl-th/0411046.
[28] D. R. Entem and R. Machleidt, Phys. Rev. C **68**, 041001(R) (2003).
[29] E. Epelbaum, W. Glockle, and U.-G. Meissner, Nucl. Phys. **A747**, 362 (2005).
[30] N. Fettes, U.-G. Meissner, and S. Steininger, Nucl. Phys. **A640**, 199 (1998).
[31] P. Buettiker and U.-G. Meissner, Nucl. Phys. **A668**, 97 (2000).
[32] A. Gomez Nicola, J. Nieves, J. R. Pelaez, and E. Ruiz Arriola, Phys. Lett. **B486**, 77 (2000).
[33] A. Gomez Nicola, J. Nieves, J. R. Pelaez, and E. Ruiz Arriola, Phys. Rev. D **69**, 076007 (2004).
[34] D. R. Phillips and T. D. Cohen, Phys. Lett. **B390**, 7 (1997).
[35] D. R. Phillips and T. D. Cohen, Nucl. Phys. **A668**, 45 (2000).
[36] K. A. Scaldeferri, D. R. Phillips, C. W. Kao, and T. D. Cohen, Phys. Rev. C **56**, 679 (1997).
[37] T. Frederico, V. S. Timoteo, and L. Tomio, Nucl. Phys. **A653**, 209 (1999).
[38] S. R. Beane, P. F. Bedaque, M. J. Savage, and U. van Kolck, Nucl. Phys. **A700**, 377 (2002).
[39] M. Pavon Valderrama and E. Ruiz Arriola, Phys. Lett. **B580**, 149 (2004).
[40] M. P. Valderrama and E. R. Arriola, Phys. Rev. C **70**, 044006 (2004).
[41] M. P. Valderrama and E. R. Arriola, Phys. Rev. C **72**, 054002 (2005).
[42] A. Nogga, R. G. E. Timmermans, and U. van Kolck, Phys. Rev. C **72**, 054006 (2005).
[43] V. G. J. Stoks, R. A. M. Klomp, M. C. M. Rentmeester, and J. J. de Swart, Phys. Rev. C **48**, 792 (1993).
[44] V. G. J. Stoks, R. A. M. Klomp, C. P. F. Terheggen, and J. J. de Swart, Phys. Rev. C **49**, 2950 (1994).
[45] R. A. Arndt, I. I. Strakovsky, and R. L. Workman, Phys. Rev. C **50**, 2731 (1994), nucl-th/9407035.
[46] K. M. Case, Phys. Rev. **80**, 797 (1950).
[47] W. M. Frank, D. J. Land, and R. M. Spector, Rev. Mod. Phys. **43**, 36 (1971).
[48] S. R. Beane, P. F. Bedaque, L. Childress, A. Kryjevski, J. McGuire, and U. vanKolck, Phys. Rev. A **64**, 042103 (2001).
[49] J. Nieves and E. Ruiz Arriola, Eur. Phys. J. A **8**, 377 (2000).
[50] G. Colangelo, J. Gasser, and H. Leutwyler, Phys. Lett. **B488**, 261 (2000).
[51] G. Colangelo, J. Gasser, and H. Leutwyler, Nucl. Phys. **B603**, 125 (2001).
[52] J. J. de Swart, M. C. M. Rentmeester, and R. G. E. Timmermans, PiN Newslett. **13**, 96 (1997).
[53] A. M. Lane and R. G. Thomas, Rev. Mod. Phys. **30**, 257 (1958).
[54] D. W. L. Sprung, W. van Dijk, E. Wang, D. C. Zheng, P. Sarriguren, and J. Martorell, Phys. Rev. C **49**, 2942 (1994).
[55] J. J. de Swart, C. P. F. Terheggen, and V. G. J. Stoks (1995), nucl-th/9509032.
[56] H. W. Griesshammer, Nucl. Phys. **A760**, 110 (2005).
[57] D. R. Phillips, Phys. Lett. **B567**, 12 (2003).
[58] M. Pavon Valderrama and E. Ruiz Arriola (in progress).
[59] M. Pavon Valderrama and E. Ruiz Arriola, Phys. Rev. C **72**, 044007 (2005).
[60] R. Machleidt (private communication).
[61] A. Nogga, M. Pavon Valderrama, D. R. Phillips, and E. Ruiz Arriola (in preparation).
[62] B. Gao, Phys. Rev. A **58**, 4222 (1998).
[63] V. V. Flambaum, G. F. Gribakin, and C. Harabati, Phys. Rev. A **59**, 1998 (1999).
[64] R. Higa (private communication).
[65] R. Higa, M. Pavon Valderrama, and E. Ruiz Arriola (in preparation).
[66] V. R. Pandharipande, D. R. Phillips, and U. van Kolck, Phys. Rev. C **71**, 064002 (2005).
[67] E. H. Lieb and W. E. Thirring, Phys. Rev. A **34**, 40 (1986).
[68] A. Calle Cordón, M. Pavon Valderrama, and E. Ruiz Arriola (in preparation).
[69] D. B. Kaplan, M. J. Savage, and M. B. Wise, Nucl. Phys. **B534**, 329 (1998).
[70] D. B. Kaplan, M. J. Savage, and M. B. Wise, Phys. Rev. C **59**, 617 (1999).
[71] S. Fleming, T. Mehen, and I. W. Stewart, Nucl. Phys. **A677**, 313 (2000).
[72] M. C. Birse, Phys. Rev. C **74**, 014003 (2006).
[73] M. C. Birse, J. Phys. A **39**, L49 (2006).
[74] M. Pavon Valderrama and E. Ruiz Arriola, in *Proceedings of Workshop on the Physics of Excited Nucleons, NSTAR 2004, Grenoble, France (2004),* nucl-th/0410020.
[75] M. Pavon Valderrama and E. Ruiz Arriola (2005), nucl-th/0507075.